Geological Survey of Canada
Commission géologique du Canada

PAPER 86-16

THE UPPER TRIASSIC KUTCHO FORMATION CASSIAR MOUNTAINS, NORTH-CENTRAL BRITISH COLUMBIA

L.E. Thorstad
H. Gabrielse

1986

Canada

Geological Survey of Canada
Paper 86-16

THE UPPER TRIASSIC KUTCHO FORMATION CASSIAR MOUNTAINS, NORTH-CENTRAL BRITISH COLUMBIA

L.E. Thorstad
H. Gabrielse

1986

Available in Canada through

authorized bookstore agents
and other bookstores

or by mail from

Canadian Government Publishing Centre
Supply and Services Canada
Ottawa, Canada K1A 0S9

and from

Geological Survey of Canada offices:

601 Booth Street
Ottawa, Canada K1A 0E8

3303-33rd Street N.W.,
Calgary, Alberta T2L 2A7

100 West Pender Street
Vancouver, British Columbia V6B 1R8
(mainly B.C. and Yukon)

A deposit copy of this publication is also available
for reference in public libraries across Canada

Cat. No. M44-86/16E	Canada: $5.00
ISBN 0-660-12197-2	Other countries: $6.00

Price subject to change without notice

Cover
Conglomerate in the upper part of the Kutcho Formation in the type area containing clasts of quartz-feldspar porphyry. GSC 204462

Critical Reader
R.G. Anderson

Original manuscript received 1985-06-04
Final version approved for publication 1986-03-17

CONTENTS

Tables

Appendices

Figures

Frontispiece. View northwestward to rocks of the King Salmon Assemblage in the hanging wall of the King Salmon Fault which lies directly beneath the light weathering limestone of the Sinwa Formation.

THE UPPER TRIASSIC KUTCHO FORMATION CASSIAR MOUNTAINS, NORTH-CENTRAL BRITISH COLUMBIA

Abstract

The Kutcho Formation is an Upper Triassic volcano-sedimentary rock sequence overlain by Upper Triassic Sinwa and Lower Jurassic Inklin formations. These three units form the King Salmon Assemblage which lies within a southwestward transported, faultbounded allochthon whose basement is the Cache Creek Group. The volcanics comprise a distinctive bimodal suite of calc-alkaline basalt or basaltic andesite and rhyodacite or rhyolite.

A Rb-Sr whole-rock isochron of 210 ± 10 Ma, with $^{87}Sr/^{86}Sr$ initial ratio of 0.7042, dates Kutcho volcanism as Late Triassic.

The King Salmon Assemblage was isoclinally folded, metamorphosed (greenschist facies) and thrust southwestward along the King Salmon Fault in Toarcian to Middle Bajocian time. A penetrative axial planar cleavage subparallel with the sole of the King Salmon thrust fault is typical.

The Kutcho Formation hosts the Kutcho Creek massive sulphide deposit within the feldspar quartz-eye sericite schist. Mineralization (80-85% sulphides, 15-20% gangue) in the stratabound deposit consists of pyrite, chalcopyrite, sphalerite with minor bornite, chalcocite, pyrrhotite and trace tetrahedrite-tennantite, digenite and galena. Alteration around the deposit involves Na_2O depletion and K_2O, SiO_2, MgO and CaO enrichment. The deposit is similar to syngenetic, volcanogenic Kuroko-type deposits.

The Kutcho Formation and other coeval Triassic volcanic sequences, were probably formed within an extensive island arc environment related to subduction beneath the terranes of Stikinia, Cache Creek and Quesnellia. The southwest vergence of faults bounding the King Salmon Assemblage resulted from late Middle Jurassic emplacement and underthrusting of the arc and related subduction sequences by the Stikine Terrane.

Résumé

La formation de Kutcho du Trias supérieur est constituée d'une séquence de roches volcano-sédimentaires recouvertes par les formations de Sinwa du Trias supérieur et d'Inklin du Jurassique inférieur. Ces trois unités forment l'assemblage de King Salmon qui se trouve dans un allochtone limité par une faille, transporté vers le sud-ouest et dont le substratum est le groupe de Cache Creek. Les vulcanites se composent d'une série bimodale de basalte calco-alcalin ou d'andésite basaltique et de rhyodacite ou de rhyolite.

L'isochrone de 210 ± 10 Ma de la roche totale déterminé au moyen de la méthode Rb/Sr, dont le rapport initial ($^{87}Sr/^{86}Sr$) est de 0,7042, a permis de situer l'épisode de volcanisme de Kutcho au Trias supérieur.

L'assemblage de King Salmon présente des plis isoclinaux, se compose de roches métamorphiques (faciès des schistes verts) et avance vers le sud-ouest, le long de la faille de chevauchement de King Salmon, du Toarcien au Bajocien moyen. Un profond clivage axio-planaire, subparallèle à la base du chevauchement de King Salmon caractérise cet assemblage.

Le gisement de sulfures massifs de Kutcho Creek se trouve dans les séricitoschistes à feldspath et quartz oeillé de la formation de Kutcho.

La minéralisation (80 à 85 % de sulfures, 15 à 20 % de gangue) dans le gisement stratiforme comprend de la pyrite, de la chalcopyrite, de la sphalérite ainsi qu'un peu de bornite, de chalcocite, de pyrhotite et des traces de tétraédrite et tennantite, de digénite et de galène. L'altération autour du gisement se manifeste par l'épuisement du Na_2O et par l'enrichissement en K_2O, SiO_2, MgO et CaO. Le gisement ressemble aux gisements-types de Kuroko de nature syngénétique et volcanogénique.

La formation de Kutcho et d'autres séquences contemporaines volcaniques du Trias, ont probablement été formées au sein d'un arc insulaire étendu, associé à la subduction sous les terrains de Stikinia, de Cache Creek et de Quesnellia. La vergence vers le sud-ouest des failles bordant l'assemblage de King Salmon a comme origine la mise en place et l'avancée en profondeur, à la fin du Jurassique moyen, de l'arc insulaire, et des phases de subduction connexes associées au terrain exotique de Stikinia.

SUMMARY

The Upper Triassic Kutcho Formation is an unusual volcanic assemblage comprising a bimodal suite of calc-alkaline basaltic andesite or basalt and rhyodacite or rhyolite. Unlike most other Upper Triassic volcanic rocks of the Intermontane Belt the formation is closely associated with, and appears to have been emplaced upon, an oceanic terrane (Cache Creek Terrane). Truncation of the Kutcho Formation and its associated strata (King Salmon Assemblage; Late Triassic to Early Jurassic) by the Kutcho Fault and the presence of similar rocks (Sitlika Assemblage) between the Takla and Vital faults in the Takla Lake area of central British Columbia suggest the possibility that the two assemblages were offset from one another by dextral faults in post Early Jurassic time.

Strata overlying the volcanic members of the Kutcho Formation, and tentatively included in the formation, are not equivocally dated. It has been assumed that limestone bodies of the Upper Triassic Sinwa Formation overlie the polymictic conglomerate which, with argillite and tuff, cap the Kutcho volcanics. Many clasts and large blocks of limestone occur in conglomerate elsewhere assigned to the Lower Jurassic Inklin Formation, however, and the limestone bodies in the type area of the Kutcho Formation may be olistoliths. In this case the formational name should be restricted to the volcanic sequence.

The volcanogenic, exhalative, stratabound, massive sulphide (Cu-Zn-Ag) deposit in the Kutcho volcanic rocks is moderately north-dipping, pinches and swells along an easterly length of 3.5 km., and is similar in many aspects to Kuroko deposits hosted in Cenozoic rocks of Japan. Whatever its origin the mineralization further demonstrates the importance of Upper Triassic volcanic rocks in the exploration for mineral deposits in the Intermontane Belt.

A pronounced alteration halo envelops the sulphides. It is characterized by a loss of Na_2O and an enrichment of K_2O, MgO and CaO. Silica content is anomalously high.

The Kutcho rocks, including the sulphide deposits, were regionally metamorphosed in the greenschist facies (300-450°C) coincident with regional deformation of rocks in the King Salmon Allochthon. The metamorphism resulted in the development of sericite and chlorite on pervasive foliation planes and imparts a characteristic sheen to the rocks which contrasts to those south of the King Salmon Fault. Also formed during metamorphism are tremolite-actinolite, carbonate, epidote, albite, biotite and quartz.

Strong foliation in the King Salmon Assemblage is axial planar to tight folds near the King Salmon Fault and to open folds farther away from the fault. Clasts in conglomerate in the hanging wall near the trace of the King Salmon Fault have been intensely flattened in the

SOMMAIRE

La formation de Kutcho du Trias supérieur est constituée d'un assemblabe inhabituel, de roches volcaniques, composé d'une série bimodale d'andésite basaltique ou de basalte calco-alcalin et de rhyodacite ou de rhyolite. Contrairement à la plupart des roches volcaniques du Trias supérieur de la zone des entremonts, cette formation est étroitement liée à un terrain océanique (terrain de Cache Creek) et semble recouvrir ce dernier. La troncature de la formation de Kutcho et des strates qui lui sont associées (assemblage de King Salmon dont la mise en place date du Trias supérieur au Jurassique inférieur) par la faille de Kutcho et la présence des mêmes types de roches (assemblage de Sitlika) entre les failles de Takla et de Vital dans la région du lac Takla, au centre de la Colombie-Britannique, semblent indiquer que ces deux assemblages ont été déplacés l'un par rapport à l'autre par des failles dextres, au cours d'une période postérieure au Jurassique inférieur.

Les strates susjacentes aux membres volcaniques de la formation de Kutcho, strates d'ailleurs provisoirement incluses dans cette formation, sont datées sans ambiguité. Il semble que les massifs de calcaire de la formation de Sinwa du Trias supérieur reposent sur les conglomérats polygéniques qui, avec l'argilite et le tuf, coiffent les roches volcaniques de Kutcho. Cependant, un grand nombre de fragments et de grands blocs de calcaire se manifestant ailleurs dans le conglomérat, ont été classés dans la formation d'Inklin du Jurassique inférieur, et par conséquent, les massifs de calcaire dans la région type de la formation de Kutcho peuvent représenter des olistolites. Dans ce cas, le nom de la formation devrait être réservé à la seule séquence volcanique.

Le gisement de sulfures massifs (Cu-Zn-Ag) de nature volcanogénique, exhalative et stratiforme, qui se trouve dans les roches volcaniques de Kutcho, a un pendage nord modéré, forme un boudinage sur 3,5 km suivant une direction est et ressemble en de nombreux aspects aux gisements de Kuroko logés dans des roches cénozoïques du Japon. Quelle que soit son origine, la minéralisation confirme l'importance des roches volcaniques du Trais supérieur dans l'exploration des gisements minéraux de la zone des entremonts.

Une auréole d'altération marquée entoure les sulfures; elle se caractérise par une diminution de Na_2O et un enrichissement en K_2O, MgO et CaO. La teneur en silice est anormalement élevée.

Les roches de Kutcho, y compris les gisements de sulfures, ont subi un métamorphisme régional et ont atteint le faciès des schistes verts (300 à 450°C), le tout coïncidant avec la déformation régionale des roches de l'allochtone de King Salmon. Le métamorphisme a donné nassance à de la séricite et à de la chlorite que l'on retrouve sur des plans de foliation pénétrants et a communiqué un reflet caractéristique aux roches qui contrastent avec les roches du sud de la faille de King Salmon. Pendant le métamorphisme, il y a eu formation de trémolite et actinolite, de carbonate, d'épidote, d'albite, de biotite et de quartz.

La foliation marquée de l'assemblage de King Salmon passe d'axio-planaire à des plis serrés à proximité de la faille et à des plis ouverts lorsqu'on s'éloigne de la faille. Les fragments des conglomérats de la lèvre supérieure à proximité de la ligne de faille du chevanchement de King Salmon ont été très aplatis dans le sens du plan de foliation; ils sont allongés et s'orientent parallèles à la

plane of foliation and stretched parallel with the direction of thrusting. Where folds are more open clasts have been much less strained. Locally, in areas where the west-northwest trending structures are fairly open, an earlier north trending set of fold axes can be recognized. The relationship of those fold axes to the earlier northerly trending folds in the Cache Creek Group is unknown.

Regional relationships involving deformation, emplacement of crosscutting granitic rocks, and the age of northerly derived sediments in the Bowser Basin to the south constrain the time of deformation and metamorphism to between late Early Jurassic and late Middle Jurassic. Judging from sedimentation in the Bowser Basin rocks of the King Salmon Allochthon continued to be strongly uplifted throughout the Late Jurassic.

Taken as a whole the geology of the Cache Creek and King Salmon rocks in the Cry Lake map area documents the evolution from oceanic to volcanic island arc to interarc(?) sedimentary environments during Mississippian through Early Jurassic time. The succeeding deformation resulted from collision and continued intraplate deformation of Stikine and Cache Creek terranes.

direction du charriage. Là où les plis sont plus ouverts, les fragments ont été beaucoup moins déformés. À certains endroits, où les structures de direction ouest-nord-ouest se remarquent à leur aspect assez ouvert, il est possible d'observer un ensemble plus ancien d'axes de plis de direction nord. La relation entre les premiers axes de plis et les plis plus anciens de direction nord, dans le groupe de Cache Creek, est inconnue.

Les relations régionales entre la déformation, la mise en place de roches granitiques transversales et l'âge des sédiments dérivés, de direction nord, du bassin de Bowser au sud, témoignent du fait que la déformation et le métamorphisme se sont produits entre la fin du Jurassique inférieur et la fin du Jurassique moyen. L'étude de la sédimentation dans le bassin de Bowser montre que les roches de l'allochtone de King Salmon ont continué à se soulever d'une façon importante pendant tout le Jurassique supérieur.

Dans son ensemble, la géologie des roches de Cache Creek et de King Salmon dans la région cartographique de Cry Lake montre bien l'évolution d'un milieu sédimentaire océanique, à un milieu d'arc insulaire volcanique, à un milieu d'interarc(?), allant du Mississipien jusqu'à la fin du Jurassique inférieur. La déformation subséquente a été causée par lis mouvements de collision et de déformation continus au sein d'une même plaque dans les terrains de Stikinia et de Cache Creek.

INTRODUCTION

The "Kutcho sequence" was described by Monger and Thorstad (1978) as the lowest division of the King Salmon Assemblage. This study defines the Upper Triassic volcanic and volcaniclastic Kutcho Formation, its physical and chemical Allochthon and other rocks of the Cry Lake map area. Its contact relations with the Cache Creek Group bear on inferences of Permian to Mesozoic tectonic events. The important Kutcho Creek sulphide deposit is described within the tectonic setting, stratigraphy, structure, composition and metamorphism of the host Kutcho Formation.

Location and access

The Cry Lake map area (104I; 58°-59°N latitude and 128°-130°W longitude) is adjacent Dease Lake, map area to the west and about 120 km south of Watson Lake, Yukon Territory (Fig. 1). The Cassiar Mountains of north-central British Columbia underlie most of the map area.

Access is largely by aircraft or winter cat trails. The Cassiar-Stewart Highway runs along the western margin of the Cry Lake map area and a winter cat trail runs from Dease Lake to near the headwaters of Tucho River (see Fig. 4). Air charters are available at Dease Lake and Watson Lake. A helicopter is also commonly available at Eddontenajon Lake, 20 km southwest of the map area (Fig. 1). Supplies and accommodation are available at Watson Lake and to a limited degree at Dease Lake and Eddontenajon Lake.

Physiographic setting

The Cassiar Mountains in the Cry Lake map area consist predominantly of ridges and alpine valleys with elevations ranging from 1215 to 2300 m and maximum relief of 1070 m. Treeline at about 1525 m elevation permits alpine exposure of 30 per cent of the map area.

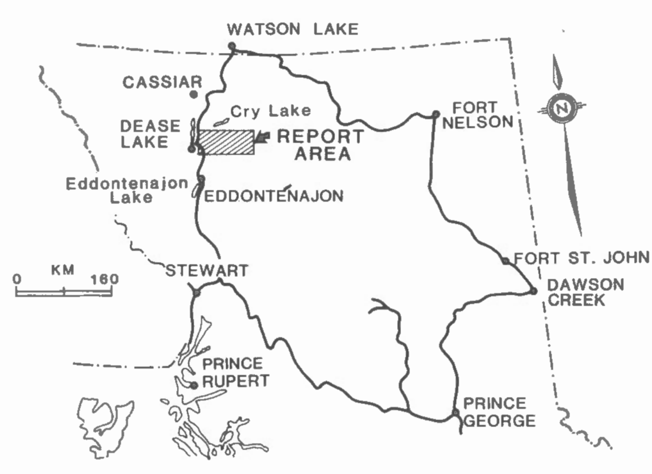

Figure 1. Location of report area, north-central British Columbia.

Extensive glaciation has sculptured the terrain leaving U-shaped valleys, cirques, moraines, lateral channels and till deposits ranging from 3 to 15 m thick. Glacial movement was from south to north. Poor drainage with abundant swamps is typical of low lying areas.

The field season extends from June to late September. Summer weather is variable with frequent precipitation and occasional snow above 1500 m.

Previous work

The Cry Lake map area was first mapped by the Geological Survey of Canada in 1956 as part of Operation Stikine with further local investigations in 1957, 1960 and 1961 (Gabrielse, 1962).

Rocks of the Kutcho Formation attracted the attention of exploration geologists in the early 1970s when a massive sulphide Cu-Zn(Ag;Pb)deposit was discovered as a result of regional geochemical sampling. A massive sulphide float boulder was located in 1973 providing the first visual evidence of a massive body of sulphide mineralization. Silt sampling programs have indicated high copper and zinc values and soil geochemistry indicated anomalous results only at or near the massive sulphide outcrop area. Both charged potential and induced potential have been used successfully to delineate mineralization. Extensive drilling and mapping programs have been carried out by two companies to determine the extent and grade of the ore body. Following the initial staking of the property in 1972 by Sumac Mines Limited and by Imperial Oil Limited, work from 1972 to 1977 was largely restricted to the area of discovery in the eastern part of the King Salmon Allochthon. A. Panteleyev and D. Pearson of the British Columbia Ministry of Energy, Mines and Petroleum Resources worked intermittently on the local geology of the deposit from 1974 to 1977 (Panteleyev, 1974; Panteleyev and Pearson, 1977; Pearson and Panteleyev, 1975).

The geology of the Cry Lake map area was re-examined by the Geological Survey of Canada during the 1977, 1978 and 1979 field seasons (Anderson, 1978, 1979, 1980; Gabrielse, 1978; Monger and Thorstad, 1978; Thorstad, 1979; Tipper, 1978). During this period the senior author's (Thorstad's) studies concentrated on Upper Paleozoic and Mesozoic rock sequences, with special emphasis on the Kutcho Formation.

Acknowledgments

The Geological Survey of Canada provided logistical support during field work from 1977 to 1979 and subsequent laboratory and drafting services to Thorstad. Special appreciation is extended to J.W.H. Monger for his invaluable help. The writers acknowledge C.I. Godwin and R.L. Armstrong for their advice during the preparation of the paper which forms part of a M.Sc thesis at the University of British Columbia by Thorstad. Sumac Mines Ltd. and Esso Minerals, Canada in particular C. Scott and D. Bridge, provided logistical support, access to the Kutcho Creek property and much information. C.A. Aird of Esso Resources Canada, Ltd. critically reviewed the section on Economic Geology and provided many helpful suggestions. Appreciation is also extended to A. Panteleyev of the British Columbia Mines and Petroleum Resources Branch for stimulating discussions and for data that have been included in this report. R.G. Anderson provided many helpful suggestions concerning chemical analyses, age dating and organization of the report.

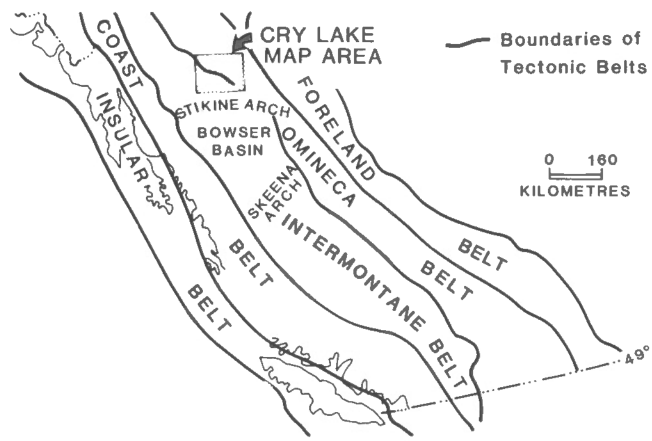

Figure 2. Location of Cry Lake map area and tectonic belts of the Canadian Cordillera.

REGIONAL GEOLOGY

Introduction

Five structural and lithological belts make up the Canadian Cordillera, from east to west: the Foreland, Omineca, Intermontane, Coast and Insular belts (Fig. 2; Monger et al., 1972; Wheeler and Gabrielse, 1972; Sutherland Brown et al., 1971). The distribution and character of the belts represent a summation of all geological processes that have affected the Cordillera.

The easternmost belt (Foreland) is composed of miogeoclinal and foredeep sediments. The Omineca Belt, which straddles the miogeocline-eugeocline boundary, is marked by Mesozoic plutonism and regional metamorphism mainly of distal miogeoclinal sediments. The Intermontane Belt comprises a sequence of Upper Paleozoic island arc and oceanic rocks (Monger, 1977a) and lower Mesozoic island arc volcanic and inter-arc sedimentary rocks including the Kutcho Formation and stratigraphically related rocks of the King Salmon Assemblage (Monger and Thorstad, 1978) overlain by Mesozoic to Cenozoic successor basin sediments and volcanics. The Coast and Insular belts consist of a Mesozoic plutonic-metamorphic terrane and an Upper Paleozoic to Mesozoic volcano-sedimentary sequence, respectively.

Within the belts are terranes (Coney et al., 1980; Monger and Berg, 1984) underlain by distinctive rock assemblages, commonly fault-bounded, whose relationship to one another at time of deposition is unknown, or suspect.

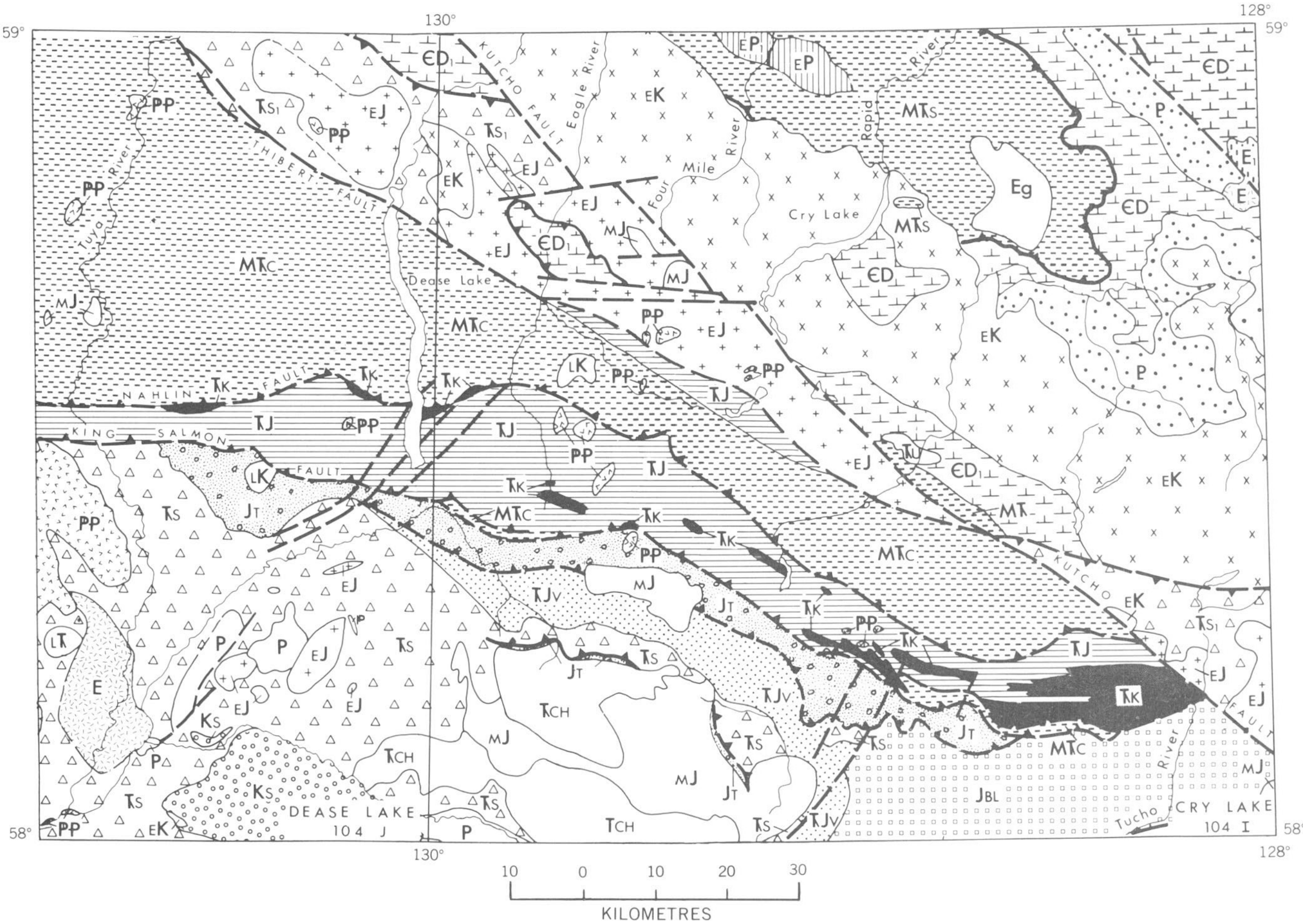

CENOZOIC

PLIOCENE AND PLEISTOCENE

PP	basaltic flows, ash

EOCENE

Eg	granite, locally miarolitic
E	conglomerate, shale, siltstone, coal; E₁ rhyolite

MESOZOIC

CRETACEOUS

uK	granite

LOWER AND MIDDLE CRETACEOUS

Ks	SUSTUT GROUP: sandstone, shale, conglomerate; nonmarine
LK	granite

JURASSIC

MIDDLE JURASSIC

JBL	BOWSER LAKE GROUP: pebble conglomerate, sandstone, shale; in part nonmarine; includes andesitic volcanic rocks in eastern part
MJ	granodiorite, monzodiorite, monzonite

LOWER JURASSIC

JT	TAKWAHONI FORMATION: greywacke, shale, conglomerate; minor sandstone, limestone
LJ	granodiorite, diorite, monzodiorite

TRIASSIC AND JURASSIC

UPPER TRIASSIC AND LOWER JURASSIC

ŦJ	SINWA AND INKLIN FORMATIONS: Sinwa limestone; Inklin greywacke, phyllitic slate, conglomerate
ŦJv	andesitic volcanics, flows, breccia

TRIASSIC

UPPER TRIASSIC

ŦK	KUTCHO FORMATION: basaltic to rhyolitic schists (flows, breccia, crystal tuff); fine grained volcanic sediments, basic schist; conglomerate, may be basal Inklin Formation, in part

(ŦJ, ŦJv, ŦK: King Salmon Assemblage)

LŦ	monzodiorite, granodiorite

MIDDLE AND UPPER TRIASSIC

Ŧs	STUHINI GROUP AND UNNAMED ROCKS: andesite, tuff, breccia, volcanic sandstone; Ŧu ; peridotite, dunite, pyroxenite; Ŧs₁ , includes Upper Triassic limestone and Lower Jurassic shale, greywacke, conglomerate

PALEOZOIC AND MESOZOIC

MISSISSIPPIAN TO TRIASSIC

MŦ	greenstone, rhyolite, chlorite phyllite, tuff; age uncertain
MŦs | MŦc	MŦs , SYLVESTER GROUP: chert, argillite, basalt, limestone, ultramafic rocks, tonalite, diorite; MŦc , CACHE CREEK GROUP: chert, argillite, ultramafic rocks, gabbro, basalt, limestone

PALEOZOIC

PERMIAN

P	limestone, greenstone, phyllite, chert
LP	diorite, grandiorite; LP₁, granite; age uncertain

CAMBRIAN TO UPPER DEVONIAN

ЄD | ЄD₁	ATAN, KECHIKA, SANDPILE AND McDAME GROUPS: sandstone, siltstone, shale, limestone, dolomite; ЄD mainly shelf and platform facies; ЄD₁ , mainly off-shelf facies

PROTEROZOIC

UPPER PROTEROZOIC

P	INGENIKA GROUP: metamorphosed siltstone, sandstone, shale; limestone, dolomite

Figure 3. Regional geology of Cry Lake and part of Dease Lake map areas.

The Cry Lake map area embraces parts of five terranes separated by regional faults (Fig. 3, 4). The area northeast of the Kutcho and Thibert faults is underlain by miogeoclinal sediments, unmetamorphosed to strongly metamorphosed and intruded by granitic rocks of sialic crustal affinity, all assigned to ancestral North America. Overlying the cratonal rocks are two allochthonous terranes: the Slide Mountain Terrane (upper Paleozoic to lower Mesozoic Sylvester Group oceanic rocks) and the Quesnellia Terrane (arc type volcanic and associated granitic rocks and sediments of late Paleozoic(?) to early Jurassic age). The King Salmon Assemblage is part of the Cache Creek Terrane (Monger, 1974, 1977c) a composite unit of oceanic aspect in the lower part succeeded by island arc rocks in the upper part. The Cache Creek Terrane has been thrust southward along the King Salmon Fault onto Mesozoic island-arc and plutonic rocks and associated clastics of Stikinia, the largest terrane of the Intermontane Belt (see Frontispiece).

Stratigraphy

Pre-Mesozoic rocks, which occur only north of the Kutcho and Thibert faults, are predominantly Proterozoic and Paleozoic platform and slope lithologies. These include, in stratigraphic order, Proterozoic carbonate and shale (Ingenika Group), Lower Cambrian Atan Group limestone and quartzite, Cambro-Ordovician Kechika Group shale, slate and wavy banded limestone, and Silurian to Mississippian Sandpile Group and McDame Group carbonate and clastics (Gabrielse et al., 1979). The Sylvester Allochthon, a klippe of Paleozoic to Triassic chert, slate, limestone, basic volcanic and ultramafic rocks (the Sylvester Group), rests on the Middle Paleozoic clastics. Two small areas of Mesozoic rocks lie north of the Kutcho and Thibert faults. One consists of Upper Triassic augite porphyry and possibly older strata and the other a linear belt of Kutcho Formation rocks underlying limestone in the Eaglehead Lakes area (Fig. 3). The Cache

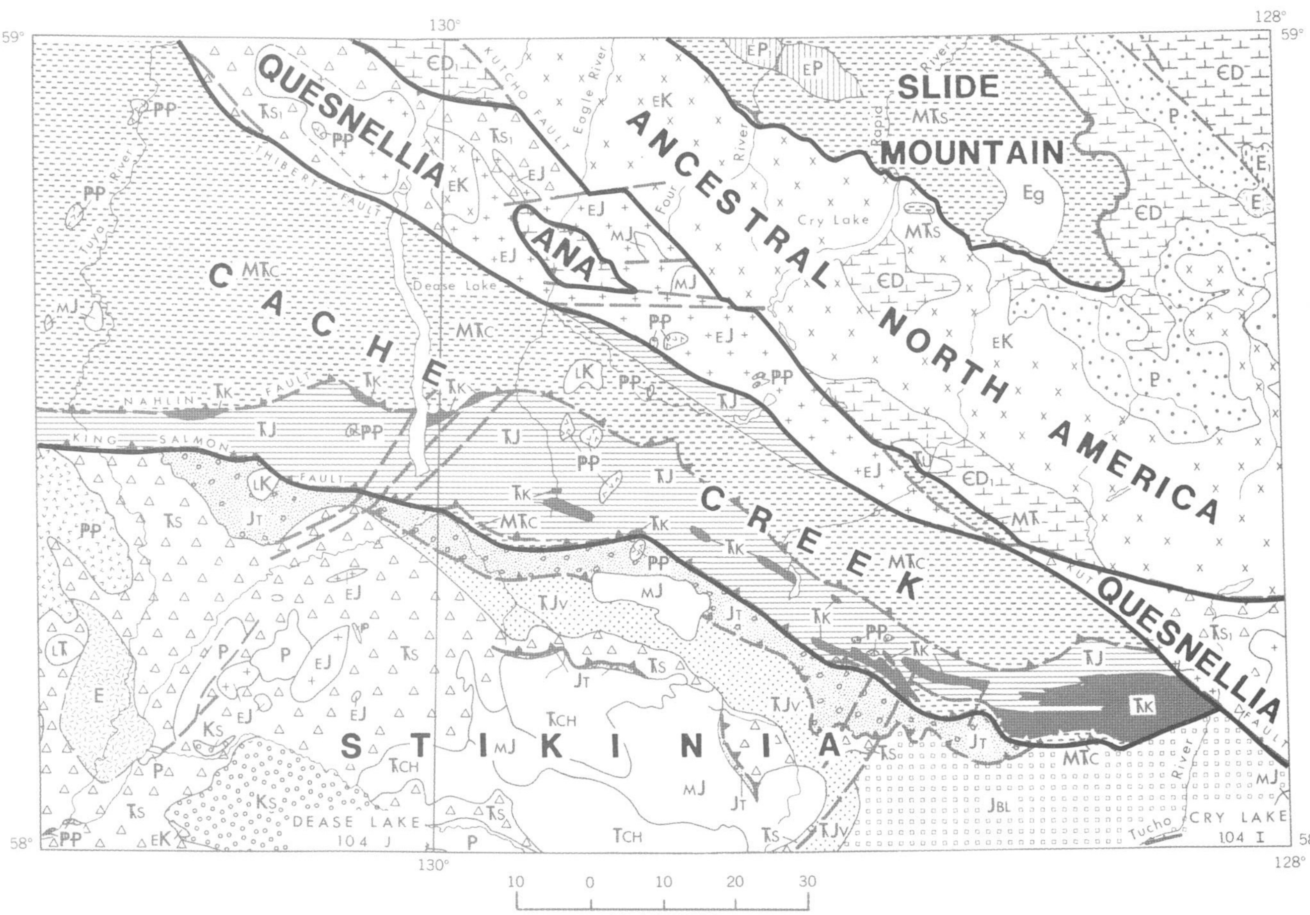

Figure 4. Terranes in Cry Lake and part of Dease Lake map areas. Geological base map from Figure 3. Abbreviation ANA = ancestral North America.

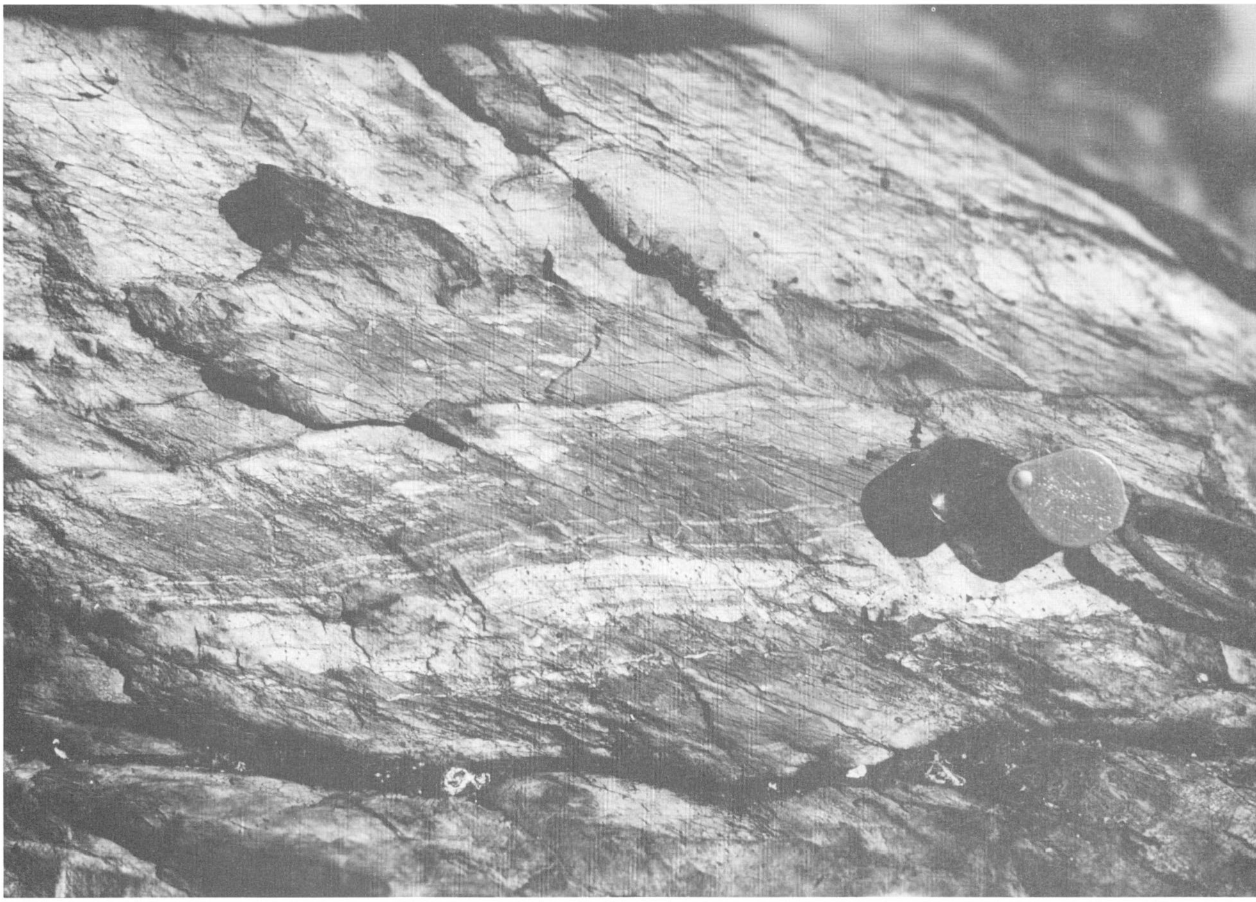

Figure 5A. Interbedded intensely cleaved greywacke and argillite of the Inklin Formation.

Creek Group, a Mississippian(?) to Triassic(?) oceanic assemblage, is generally in fault contact with other rock units although stratigraphic continuity with the King Salmon Assemblage seems probable in a few localities.

Mesozoic rocks are dominant southwest of the Nahlin Fault, occurring within and south of the west-northwest trending King Salmon Allochthon. The King Salmon Assemblage between the Nahlin and King Salmon faults includes, in ascending order, the Kutcho, Sinwa and Inklin formations (Monger and Thorstad, 1978).

The Upper Triassic Kutcho Formation is an island arc volcaniclastic sequence which may be up to 1000 m thick. Basaltic to dacitic tuff and breccia are lowermost, overlain by dacitic to rhyolitic tuff and breccia. Tuffaceous argillite, argillite and conglomerate cap the sequence.

Norian Sinwa Formation is a grey to white, well foliated marble and local micrite up to 250 m thick. Commonly it is fetid and pyritic. Layering is poorly defined and is probably transposed along the well developed foliation. Rare index fauna include the bivalves *Lima* sp.(?) and a probable *Palaeocardita*, (*Minetrigonia*, sp.) and one scleractinian coral tentatively identified by E. T. Tozer (personal communication, 1977).

Figure 5B. Strongly cleaved flat-lying siltstone and argillite of the Inklin Formation.

The Lower Jurassic Inklin Formation (Monger and Thorstad, 1978) comprises intercalated calcareous greywacke, dark grey to black shale and siltstone and black phyllite 1000-1500 m thick (Figs. 5A,B). Conglomerate is generally

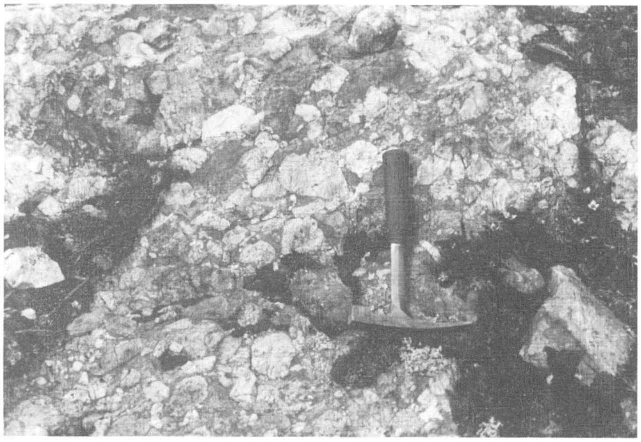

Figure 6. Conglomerate of basal Inklin (or upper Kutcho Formation?) along the Nahlin Fault 10 km east of Dease Lake. Most clasts are quartz-eye porphyry.

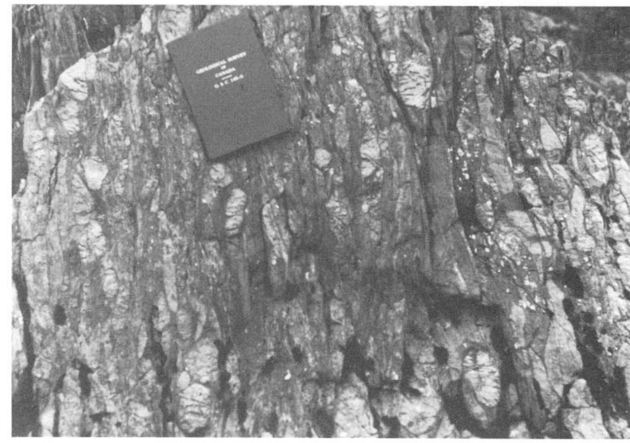

Figure 7. Strongly flattened and stretched clasts of quartz-eye porphyry and limestone along King Salmon Fault 30 km southeast of south end of Dease Lake. Compare degree of deformation with Figure 6.

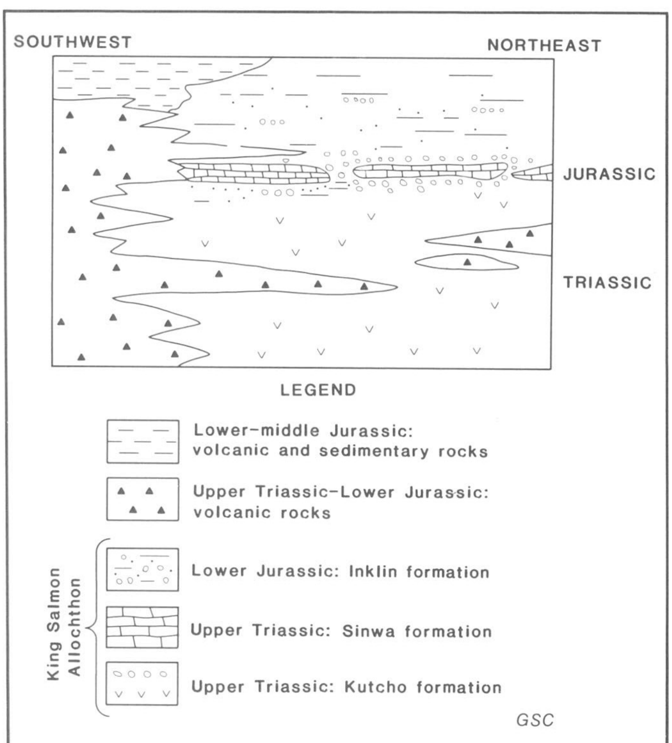

Figure 8. Stratigraphic relations among Mesozoic rocks in the Cry Lake map area, British Columbia.

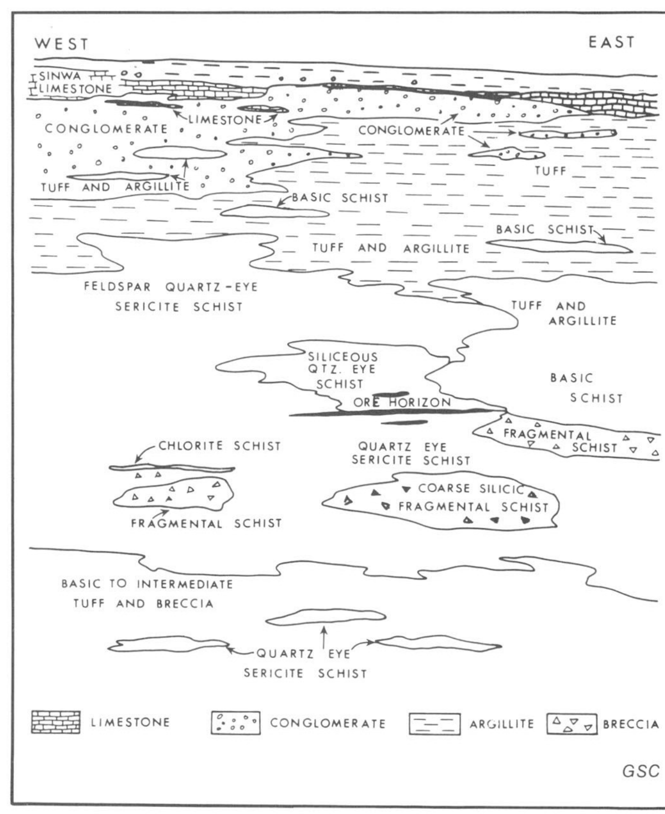

Figure 9. Interpretive facies relationships between rocks of the Kutcho Formation (true thicknesses not shown; contacts are gradational and units are commonly lenticular).

present at its base and common as layers and lenses throughout. Limestone and quartz-feldspar porphyry clasts up to 30 cm long predominate (Fig. 6). Shale rip-ups are abundant in some conglomerate units and ubiquitous in greywacke. Near the King Salmon Fault, limestone clasts are strongly flattened and stretched to form plates parallel with foliation (Fig. 7). Layering seen locally in greywacke-shale and phyllite sequences is commonly transposed in a well developed penetrative foliation. Disseminated pyrite cubes, in amounts up to 5 per cent, are widespread.

The Sinwa and Inklin formations are structurally conformable with conglomerate of the upper Kutcho Formation. Scattered limestone lenses in the upper Kutcho conglomerate increase in abundance and grade into massive Sinwa Formation limestone. In places where the Sinwa limestone is absent the lenses are the only indication of limestone deposition and it is difficult to define stratigraphic boundaries because the upper Kutcho conglomerate appears to grade into the basal conglomerate of the Inklin Formation. Nevertheless, local and possibly regional uplift and erosion of the Sinwa and Kutcho formations provided abundant Sinwa limestone and quartz porphyry clasts during deposition of the Inklin Formation conglomerate. Facies relationships (Fig. 8) between the various lithologies of the Kutcho, Sinwa and Inklin rocks are complex. A possibility exists that much of the conglomerate referred to herein as "Kutcho" may indeed be basal Inklin. This necessitates that some large exposures of Sinwa limestone are olistoliths. Another possibility is that two conglomerates are present, one of Late Triassic (Kutcho) and one of Early Jurassic (Inklin) age.

Porphyry dykes crosscut the Kutcho Formation and postdate its deformation in the southeastern part of the King Salmon Allochthon. The hornblende-feldspar porphyries are generally fresh, non-foliated and may contain grey to mauve, amethystine quartz. Rare porphyries are weakly foliated. A K-Ar isotopic age of 55.4 ± 3 Ma was defined for hornblende from one of the dykes (Stevens et al., 1982).

South of the King Salmon Allochthon the youngest plutons of the Hotailuh Batholith, a Mesozoic composite batholith and satellitic intrusions (Anderson, 1978, 1979, 1980), intrudes Mesozoic rocks comprising arc-type volcanics of Late Triassic and Jurassic age and sediments of mainly Early Jurassic age (Gabrielse et al., 1979; Tipper, 1978).

STRATIGRAPHY AND PETROGRAPHY OF THE KUTCHO FORMATION

Formal definition

The Kutcho Formation is composed predominantly of volcaniclastic rocks with intercalated sediments and subordinate volcanic flows (Fig. 9). The base of the section is not exposed.

Excellent exposures of the Kutcho Formation in the type area in the eastern part of the King Salmon Allochthon (58°12′N, 128°24′W) represent the thickest and best studied sequences (Fig. 10). Members of the Kutcho Formation are lenticular and deformed and no single locality embraces all the variations in lithology. The described sequence combines the generalized stratigraphy developed by Pearson and Panteleyev (1975) and D. Bridge (personal communication, 1977, 1979) with work by the authors. The lowest unit exposed to the east is basaltic to dacitic tuff and breccia, which is overlain by quartz-eye and quartz feldspar sericite schist interpreted to be dacitic to rhyolitic tuff and breccia. Carbonate and calcareous quartz sericite schist (originally crystal and lapilli tuffs and minor breccias) with minor basalt lenses and intercalated, lensoid massive sulphide unit overlie the quartz-eye schist. Basic schist, a basic volcaniclastic or flow overlies and in part truncates the massive sulphide in the area of the deposit (D. Bridge, personal communication, 1977). Interlayered intermediate to acidic tuff and argillite rest on and have gradational contacts with underlying acidic fragmental rocks and basic schist and with overlying conglomerate. Conglomerate, thickest in the western part of the type area, is also a facies equivalent of the tuff and argillite which dominate in the east.

The conglomerate and argillite cap the sequence and apparently grade into overlying Upper Triassic Sinwa Formation, or, where Sinwa Formation is absent, rocks of the Lower Jurassic Inklin Formation. However, an unconformity probably separates Sinwa and Inklin strata based on the conglomerate sedimentology described previously. If further work demonstrates that Sinwa limestone in the type Kutcho area occurs only as olistoliths the conglomerate should be excluded from the Kutcho Formation and included in the Inklin Formation.

Basaltic to dacitic tuff and breccia

The Kutcho Formation's basal unit accounts for up to 215 m of section and includes massive tuff, feldspar ± augite ± hornblende crystal tuff and medium to coarse chaotic breccias (fragments 1-35 cm long). Rocks are generally well foliated, form massive, resistant, dark grey to green outcrops, and show little evidence of bedding (Fig. 11). Rare lenses of acidic tuff are found throughout the sequence. Epidote is ubiquitous and replaces fragments in some layers or forms small and large (1-20 cm diameter) subspherical clots of radiating crystals. These epidote clots may be altered fragments or epidotized cores of pillows within flows.

In thin section, tuff phenocrysts and matrix are altered. Plagioclase is extensively altered to epidote, carbonate and lesser sericite and chlorite. Mafic minerals are pseudomorphed by chlorite and/or biotite and the fine matrix is replaced by chlorite, epidote, carbonate and minor sericite.

Feldspar quartz-eye sericite schist

Feldspar quartz-eye sericite schist, quartz-eye sericite schist and sericite schist are considered to be metamorphosed dacite to rhyolite tuffs and breccia. The schists enclose a massive sulphide horizon. In the hanging wall they are up to 245 m

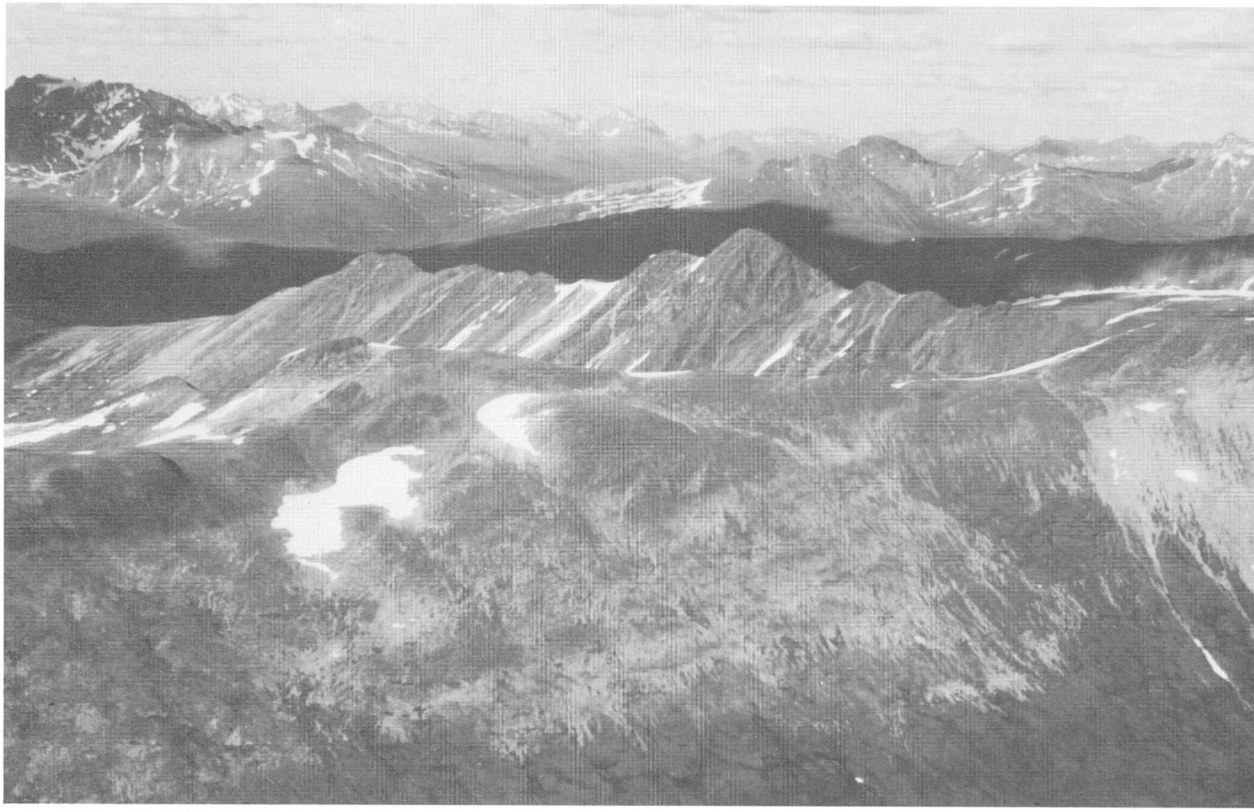

Figure 10. View east-northeast to type section of Kutcho Formation. Resistant units are basic volcanic rocks whereas slightly recessive units are acid-volcanic rocks.

Figure 11. Epidotized basic volcanic rocks of the Kutcho Formation.

thick; in the footwall they are approximately 320 m thick. A distinct north-south facies change is recognized in the footwall of the deposit by the gradation of lapilli crystal tuff into quartz feldspar crystal tuff (D. Bridge, personal communication, 1977)

Lithologies are invariably tuff, volcanic conglomerate or breccia. Although layering is typically poorly developed, there may be as many as seven fining upward cycles in the silicic footwall schist. Breccias are generally monolithologic. Fragments range from 2 to 20 cm and are highly flattened but less foliated than their matrix (Fig. 12). Some mauve quartz feldspar fragments, partially replaced by hematite were observed in some breccias. Tuff contains variable amounts (5-40%) and sizes (1-20 mm long) of quartz and feldspar crystals. Quartz and feldspar are generally subhedral and white to pale blue-green. Variable blue to green feldspar colour may be the result of sericitization. Dolomite lenses, 10 to 20 cm long, are evident throughout the section and have been flattened in the plane of the foliation. Secondary rhombic dolomite porphyroblasts are characteristic of the matrices of the rocks. Disseminated pyrite and limonitic boxwork after pyrite are ubiquitous and rocks may contain abundant secondary hematite.

In thin section quartz, feldspar and sericite dominate. The matrix is dominantly fine sericite, quartz and feldspar with lesser chlorite.

Chlorite schist

Chlorite schist occurs as thin layers and lenses throughout basaltic to dacitic tuff and breccia of the lower unit. In the type area a lens of chlorite schist (1-61 m thick) is also found in the acidic schists of the footwall. Underlying the chlorite schist is a thin (about 2.7 m thick) mineralized rhyolite breccia with disseminated sulphides (D. Bridge, personal communication, 1978).

In thin section, chlorite schist comprises chlorite, epidote clots and fine feldspar with minor amounts of sericite and tremolite-actinolite. Dolomitic rhombs deflect the well developed foliation.

Breccia

In the type area a lens of breccia within quartz-eye feldspar schist outcrops on a ridge just north of the Kutcho Creek deposit. The breccia is monolithologic with fragments of quartzeye feldspar sericite schist in a matrix of similar composition (Fig. 13). This unit is unique in that fragments are apparently more competent than those in other fragmental units. Fragments range from 2 to 30 cm in size and constitute 20 to 70 per cent of the rock. Both fragments and matrix are petrographically similar to feldspar quartz-eye sericite schists.

Basic schist

Well-foliated basic tuff, similar in lithology to basic rocks of the lowest stratigraphic unit, occurs as schist lenses within sharp or gradational contacts with enclosing tuff and argillite which are confined to the type area. They are 1 to 3 m thick (exceptionally much thicker) with variable lengths. The thickest lens is concordant with and caps the sulphide member, but they locally occur at the same stratigraphic horizon (D. Bridge, personal communication, 1978). Lithologies include feldspar chlorite schist, feldspar augite chlorite schist and augite chlorite schist.

Weathered surfaces are dark green and apparently texturally homogeneous but fresh surfaces exposed in core samples are heterogeneous. Pyrite and pyrrhotite are disseminated throughout the unit. Sulphides are flattened and restricted to foliation planes. Internal layering is defined by variation in crystal size, shape and abundance. Feldspar abundance varies from fine- to coarse-grained schist. Some fragmental textures are observed (fragments 1-10 mm long), suggesting that the rocks are both flows and tuffs.

In thin section plagioclase is the dominant phenocryst and is extensively altered to sericite, epidote, carbonate and chlorite. Original mafic grains and the fine matrix are replaced by biotite, epidote, chlorite, tremolite-actinolite and carbonate. Fine grained potassium feldspar occurs throughout the matrix.

The origin of the basic lenses is controversial. Pearson and Panteleyev (1975) considered the lenses to be intrusive because of crosscutting relationships. However, textural inhomogeneity, local fragmental nature, internal layering and gradational contacts with adjacent rocks suggest that these rocks are pyroclastic flows.

Tuff and argillite

Distribution of the tuff and argillite (Fig. 14) and intertonguing relationships with the capping conglomerate suggest the two units are a facies equivalent. Tuff and argillite thicken markedly in the eastern part of the type area where they largely replace conglomerate. In the west, conglomerate dominates and tuff and argillite are subordinate. The unit is 1-400 m thick.

The tuff and argillite unit is heterogeneous and includes: very fine grained quartz feldspar sericite schist, fine grained chlorite feldspar schist, black to green shale and siltstone with calcareous lenses, and grey to green sericite schist and greywacke. Disseminated pyrite and pyrrhotite and limonitic boxwork after pyrite are common.

Conglomerate

The conglomerate, 10 to 100 m thick, caps the Kutcho Formation and contains limestone lenses throughout. Clasts are 0.5 to 12 cm long, predominantly volcanic (white to green quartz-eye sericite schist, sericite schist, quartz-eye feldspar sericite schist and lesser chlorite schist, carbonate and quartzite), and locally derived. Matrix composition is a siliceous crystal tuff, comprising quartz, feldspar, sericite and chlorite. Crude layering is evident in the conglomerate as fine grained sandy lenses, but is commonly transposed in the well developed foliation which wraps around flattened clasts.

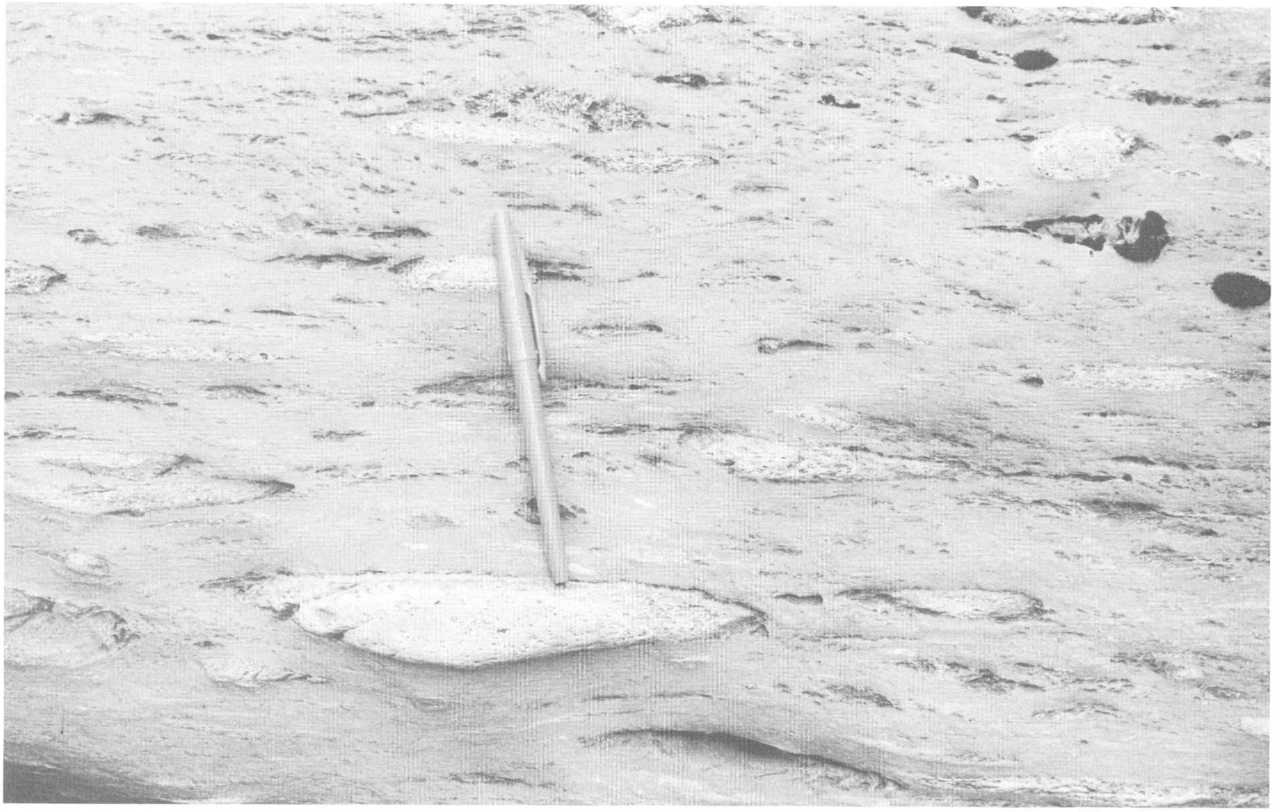

Figure 12. Fragmental acid volcanic clast in quartz-eye sericite schist.

Figure 13. Large breccia fragment in quartz-eye sericite schist.

Figure 14. Foliated tuff and argillite of Kutcho Formation.

Correlation

Except for a few small, scattered occurrences west of the type locality in Cry Lake and Dease Lake map areas volcanic rocks of similar age and lithology to the Kutcho Formation are unknown in northern British Columbia. In central British Columbia, east of the Takla Fault, possible correlative rocks are included in the Sitlika Assemblage (Monger et al., 1978). The Sitlika Assemblage has much in common with the King Salmon Assemblage in Cry Lake map area and it has been suggested that they have been separated along a system of dextral transcurrent faults (Monger et al., 1978; Gabrielse, 1985).

METAMORPHISM

The Kutcho Formation has been regionally metamorphosed in the greenschist facies. Metamorphic mineral assemblages noted within metavolcanic rocks and metasedimentary rocks of the formation, including those in the Sinwa Formation, are indicative of lowgrade metamorphism which accompanied the deformation of the King Salmon Assemblage (Fig. 15).

Metamorphic mineral assemblages and conditions

Primary mineralogies of rock units within the Kutcho Formation have been pervasively altered by the metamorphism and local metasomatism synchronous with emplacement of the King Salmon Allochthon. Metamorphic assemblages are specific to different compositions of the metavolcanic and metasedimentary rocks. Locally and, in particular, close to the Kutcho massive sulphide deposit, rock units have been subjected to hydrothermal metasomatism and metamorphism was not isochemical.

Basalt to basaltic andesite rocks are characterized by complete replacement of original iron-magnesium minerals to tremolite-actinolite, carbonate, chlorite and epidote and calcic plagioclase to epidote, white mica, carbonate and albite. Commonly very fine grained quartz is found in the groundmass. Potassium feldspar, where present, is weakly sericitized. Hornblende, in basaltic andesites, is replaced by tremolite-actinolite, chlorite, biotite, calcite and opaques.

In the basic schist unit, primary plagioclase is altered to albite and epidote and pyroxene to hornblende and chlorite.

In addition to abundant groundmass potassium feldspar, the common dolomite rhombs attest to metasomatism accompanying ore-forming processes.

In general silica-rich volcanic and volcaniclastic rocks of the Kutcho Formation are less altered than silica-poor varieties. Dacitic and rhyolitic rocks are characteristically altered to muscovite, sericite, carbonate and minor chlorite. Plagioclase alteration resembles that in basaltic rocks with the development of muscovite, sericite carbonate and lesser amounts of epidote. Quartz, plagioclase and less altered potassium feldspar are partially replaced by muscovite, sericite and carbonate along fractures and grain boundaries.

Argillic rocks are composed mainly of a fine grained quartz, white mica and chlorite. An argillaceous layer within the basic schist unit contains the mineral assemblage quartz, chlorite, biotite and stilpnomelane.

Limestone lenses in upper Kutcho rocks and the overlying Sinwa Formation are composed of recrystallized calcite, minor quartz, thin partings of fetid, carbonaceous material and locally dolomite.

Key mineral assemblages in metavolcanic and argillic rocks of the Kutcho Formation are given in Figure 15. Greenschist metamorphism of basic rocks leads to the assemblage epidote/clinozoisite, chlorite, calcite, biotite (or stilpnomelane), albite, white mica and minor quartz. Acidic metavolcanic rocks or quartz-eye schist, are metamorphosed to the assemblage white mica, potassium feldspar, quartz, chlorite, plagioclase and calcite. Argillic rocks within the basic schist unit contain the diagnostic assemblage chlorite, biotite and stilpnomelane.

These mineral assemblages indicate that the Kutcho Formation has been metamorphosed within the quartz-albite-epidote-biotite subfacies of the greenschist facies over a poorly constrained pressure interval (1 to 7 kb ($1kb = 1 \times 10^5 kPa$) from stilpnomelane stability (Winkler, 1974)) within the temperature range 300° to 450°C.

Dolomite and quartz in siliceous dolomitic lenses remained stable during metamorphism as no evidence for the formation of either talc or tremolite within the limestones was found.

The reaction:

dolomite + quartz + H_2O = talc + calcite + CO_2 is buffered to increasing temperatures (in the range 350-450°C at 1 kb) by increasing CO_2 activity and so define a maximum temperature range of metamorphism at 1 kb.

Metamorphic reactions involving one or more volatile components, such as the one above, tend to be relatively pressure insensitive. Although no pressure sensitive mineral assemblages occur in the King Salmon Assemblage, physical characteristics and deformational history of the rocks indicate that they have been subjected to considerable strain, probably under moderate pressure.

Timing of metamorphism

Textural evidence suggests that metamorphic recrystallization took place throughout the deformational event which affected the King Salmon Assemblage. Prekinematic textures include bent plagioclase grains with deformation twins, bent platy grains and flattened and deformed carbonate grains. Synkinematic textures include the alignment of porphyroblasts parallel with and slightly deflecting the foliation. Postkinematic textures include polygonal arcs of micaceous minerals and feldspar overprinting of the micaceous foliation.

CHEMISTRY

Volcanic activity in different geological environments has been shown to produce magma types whose chemistry reflects their particular tectonic setting. Lavas of an oceanic environment, including mid-ocean ridges and intraplate oceanic islands, the island-arc environment at converging plate margins, and the environment of rifting within continents, all tend to have distinct chemical characteristics. The voluminous basalts erupted at mid-ocean ridges and which comprise most of the oceanic crust, are tholeiitic. These differ compositionally from basalts of intraplate oceanic islands which may be derived from a deeper source within the undepleted mantle. Volcanism at modern day island arcs and continental margins is associated with a seismic Benioff zone along which magmas are generated under differing physical conditions. These differing physical conditions may be reflected in the bimodal nature of the magma series observed in these environments. Lavas erupted from different depths across an arc range in composition from tholeiites to calc-alkaline andesites. Chemical changes, such as potash content of calc-alkaline rocks, may reflect variations in source depth. Alkaline lavas in back arc basins are commonly found in association with calc-alkaline arcs. Similar alkaline lavas are the main products of post orogenic continental volcanism. Lavas associated with continental rift environments are peralkaline and display characteristics of extreme alkali enrichment.

This concept of different magma type reflecting different tectonic environment may be applied to ancient volcanic terranes in an attempt to define ancient environments of volcanic activity in the light of modern plate-tectonic theory.

Several classification schemes exist for defining rock names, chemical affinities and tectonic environments of volcanic rocks based on their chemical composition. These are based on comparative plots of various parameters including major and trace element concentrations, colour indices and normative minerals (Irvine and Baragar, 1971; Middlemost, 1973; Winchester and Floyd, 1976, 1977; Floyd and Winchester, 1978; Baragar and Goodwin, 1969).

The Irvine and Baragar (1971) classification is based on plots of normative colour index versus normative plagioclase

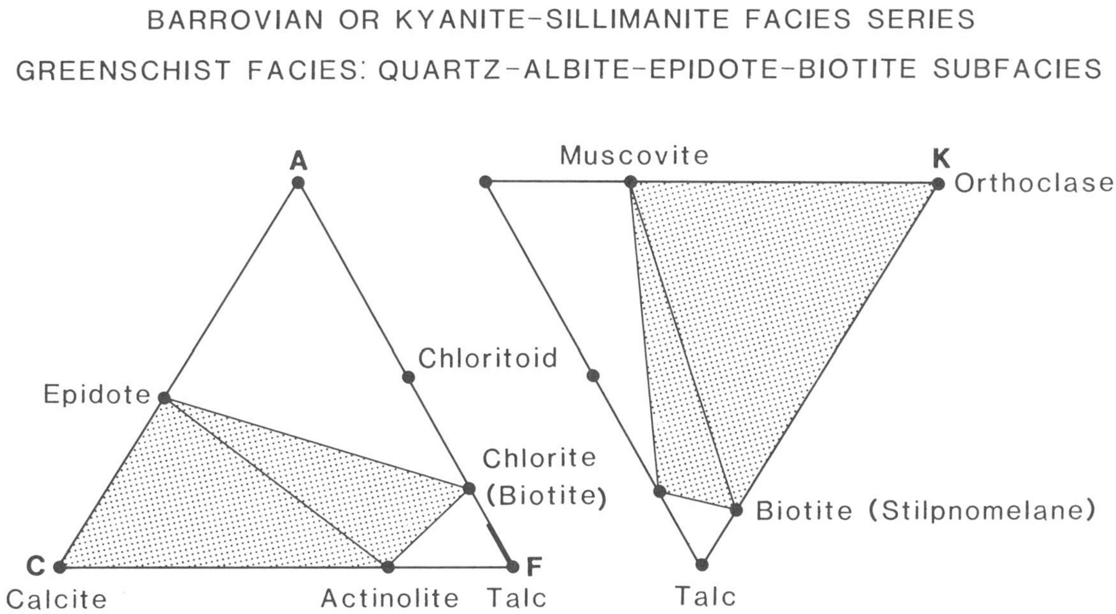

Figure 15. Metamorphic mineral assemblages of the Kutcho Formation; shown on ACF, AKF and AFM diagrams for the quartz-albite-epidote-biotite subfacies of the green-schist facies (indicated by stippled areas). ACF diagram after Miyashiro (1973); AKF and AFM diagrams after Greenwood (personal communication, 1976).

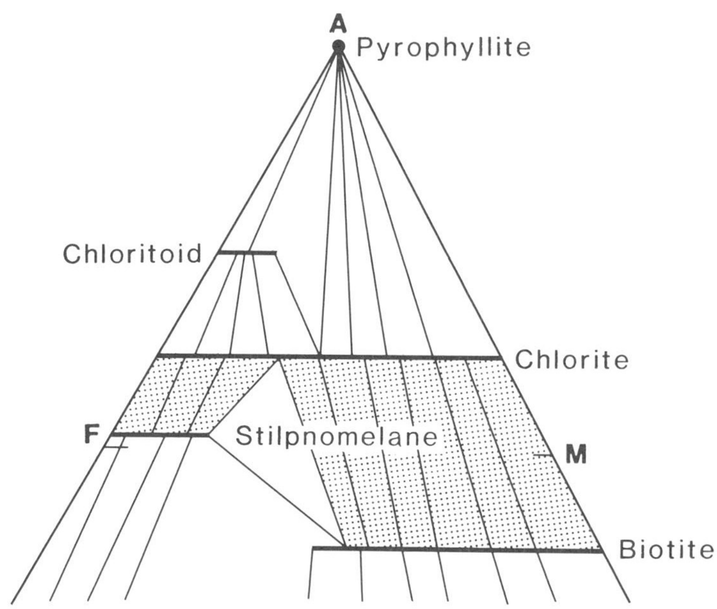

GSC

and modified as K-rich and K-poor as defined by a triangular plot of normative albite, orthoclase and anorthite. Although this classification was derived from Cenozoic to Recent volcanic rocks, many authors have used modern island arc nomenclature for older rocks (e.g. Goodwin, 1977). Irvine and Baragar (1971) have also applied the diagrams to older rock suites from the Yellowknife Greenstone Belt, Northwest Territories and Noranda, Quebec.

Various plots of chemical data have been utilized to describe volcanic rocks. Due to the high mobility of components such as K_2O, Na_2O, CaO, Rb, Sr and to a lesser extent SiO_2 and Fe_2O_3 during secondary processes such as weathering and metamorphism (Davies et al., 1979) the validity of information derived from plots involving these elements may be questionable. Many authors, (Hart et al., 1970; Gelinas et al., 1977; Strong, 1977) have argued, however, that despite the high mobility of these elements there is little change in overall bulk composition and that useful generalizations may therefore be derived from them. Other less mobile components, including TiO_2, Al_2O_3, P_2O_5, Zr, Cr and Co (Davies et al., 1979; Floyd and Winchester, 1978) may provide more definitive information.

Condie (1976) suggested that little or no change in concentration occurs for Ti, Y, Zr, Zn, Cr, V, Sr, Co and Ni during metamorphism and Davies et al. (1979) concurred that Y, Zr, Cr, Co, Ni and Ti are relatively immobile during secondary processes; Sr, however, is very mobile. It is reasonable to assume, then, that most of the above trace element concentrations of the Kutcho suite are little affected by metamorphism and weathering and may cautiously be compared to data from modern orogenic zones.

Immobile trace elements such as Cr, Ti, Zr, Y and more mobile Sr have been used by Floyd and Winchester (1975, 1976) and Pearce (1975) to classify and define tectonic environments of emplacement for volcanic rocks. Winchester and Floyd (1976) stated that the "utilization of immobile elements enables a more meaningful interpretation to be placed on ancient volcanic suites in terms of magma type and degree of differentiation". Advantages to the use of such immobile elements include their large variation in concentration between magma types and their insensitivity to secondary processes (Pearce, 1975). Drawbacks in their application is a limitation to basaltic compositions and the fact that elements commonly occur in concentrations below detectable limits for conventional analytical methods.

Rocks of the Kutcho Formation are metasomatized, the most obvious result of which is abnormally high amounts of calcite (up to 24% CaO) in the volcanic rocks. Enrichment and depletion of CaO, Na_2O and K_2O in rocks near massive sulphide mineralization may also have significantly altered original bulk compositions. The chemical analyses given in Appendix 1 were re-calculated by deleting the CO_2 and H_2O content with the object of minimizing alteration effects. The re-calculated values were used for the various plots shown in this section. CIPW normative minerals, presented in Appendix 1, are not discussed in detail due to metasomatic changes.

Despite the high mobility of alkalis during weathering and metamorphism (Davies et al., 1979) this plot is used extensively for the classification of altered volcanic suites and appears reasonably effective according to Irvine and Baragar (1971). This is because of the ease with which the major element concentrations can be measured and because of the abundance of existing data plotted on AFM diagrams that are available for comparative purposes.

MgO, FeO, Fe_2O_3 and Al_2O_3, only slightly mobile during metamorphism and weathering (Pearce, 1975), are reasonable parameters to use in defining tectonic environments. Samples with low silica (51 to 56% SiO_2) appear to be sensitive tectonic indicators (Pearce et al., 1976). The MgO-FeO(total)-Al_2O_3 diagram of Figure 16 has been subdivided using Cenozoic rocks, but also has been applied to Archean rocks with some success (Pearce et al., 1976).

Chemical composition

This section deals with the chemical characteristics of Upper Triassic and Cache Creek Group volcanic rocks within the study area and applies a consistent nomenclature to them. Analyses of Kutcho Formation samples (Appendix 1) cover a wide range of compositions within the subalkaline series as defined by Irvine and Baragar (1971). Compositionally, the rocks range from tholeiitic, calc-alkaline and high alumina basalt to calcalkaline rhyolite.

Rocks have been named using both a descriptive field term and the Irvine and Baragar classification (Appendix 2). The basis for the Irvine and Baragar nomenclature has been discussed in introductory comments, but further comment on the reliability of the classification system is in order. The classification scheme is based on Na_2O, CaO and K_2O compositions which are susceptible to change during metamorphism (Pearce, 1975). For example, a chlorite, sericite schist (48.3% SiO_2) classified as a calcalkaline dacite and a coarse-bladed feldspar and chlorite schist (53.5% SiO_2) classified as a calc-alkaline rhyolite have anomalous K_2O and CaO concentrations. Nonetheless the Irvine-Baragar classification is generally useful. Accordingly, rocks of the Kutcho suite are predominantly calc-alkaline basalt to rhyolite, rocks of the Stuhini Formation are tholeiitic and calcalkaline basalt and andesite, and those of the Cache Creek Group are predominantly tholeiitic basalts.

Chemical Affinities

Diagrams involving different elemental parameters have been employed to determine the character of the Kutcho suite. These include the total alkalies-silica diagram and the AFM diagram (Irvine and Baragar, 1971). The total alkalis-silica diagram discriminates between alkaline and subalkaline rocks and the AFM ternary diagram differentiates tholeiitic and calc-alkaline rock series.

The alkaline-subalkaline fields on the total alkalis-silica diagram (Fig. 17) discriminates the alkaline basic schist from

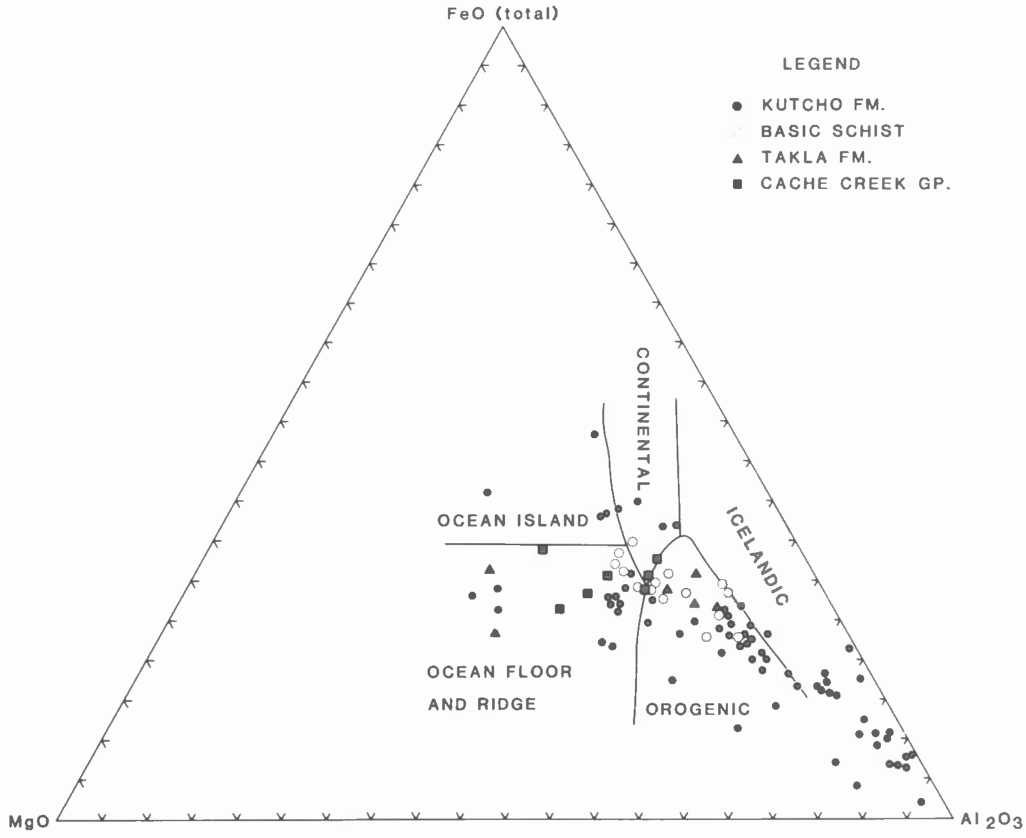

Figure 16. MgO-FeO (total)-Al_2O_3 diagram for rocks of the Cry Lake map area. Solid lines divide tectonic environments (after Pearce et al., 1977).

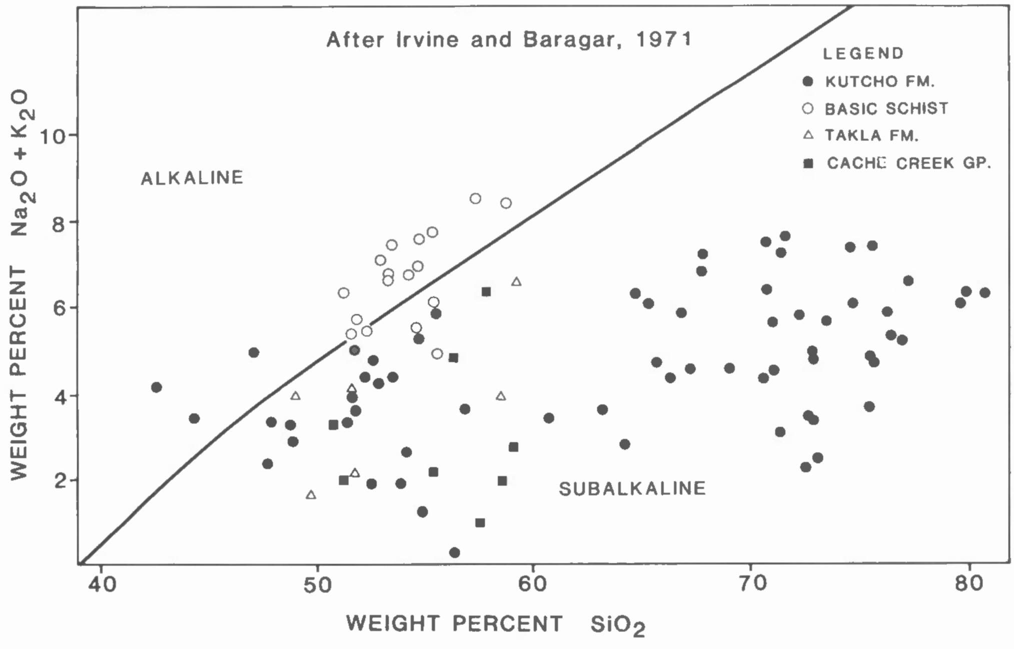

Figure 17. Total alkalis-silica diagram for volcanic rocks of the Cache Creek Terrane of the Cry Lake map area

calc-alkaline rocks in most of the Kutcho suite. Rocks of the Stuhini Formation in the study area are subalkaline. Rocks of the Takla Group (Monger, 1977b) and Nicola Group (Preto, 1977) have been shown to be dominantly alkaline in their type areas. Rocks of the Cache Creek Group are subalkaline.

According to fields on an AFM diagram (Fig. 18), Kutcho Formation rocks are predominantly calc-alkaline but some samples are tholeiitic. The Kutcho data strongly resemble modern, orogenic, calc-alkaline suites (McBirney, 1969a,b; Irvine and Barager, 1971; Pichler and Zeil, 1969). Tholeiitic basic rocks are common in modern arc environments, particularly in initial stages of development (Miyashiro, 1974, 1975).

Both Cache Creek Group and Takla Group rocks plot in tholeiitic to calc-alkaline fields. The Cache Creek is dominantly tholeiitic and the Takla is dominantly calc-alkaline.

Several other plots of volcanic rock chemistry are routinely used in the literature to help define magma series and tectonic environments of volcanic terranes. The tectonic environment of volcanic suites can be ascertained using diagrams such as the MgO-FeO(total)-Al_2O_3 (Pearce et al., 1976); TiO_2-K_2O-P_2O_5 (Pearce et al., 1975; Yellur, 1977); Ti-Zr (Pearce, 1975; Pearce and Cann, 1973); Ti-Cr (Pearce, 1975); Zr-Cr (Bloxam and Lewis, 1972); Zr-TiO_2 (Bloxam and Lewis, 1972); and TiO_2-Zr-Cr (Bloxam and Lewis, 1972). The most applicable plot in this study was the MgO-FeOtotal-Al_2O_3 diagram (Fig. 16).

Low silica samples from the Kutcho suite plot mainly in the orogenic field of Pearce et al., (1976) and only a few data have ocean floor and ridge or "continental" affinities. The diagram is not intended for silica-rich samples. Rocks of the Takla Group plot both in the ocean floor and calc-alkaline basalt fields; those of the Cache Creek Group plot in the ocean floor and ridge field.

The bimodal composition of the Kutcho Formation volcanic rocks is further emphasized by a frequency (N) versus silica (SiO_2) plot of analyzed samples (Fig. 19). There is a distinct paucity of intermediate (55 to 62%) silica values corresponding to the average silica content of andesites (Manson, 1967). The suite is different from recent mature island arcs where a large percentage of rocks is andesitic (Miyashiro, 1974; McBirney, 1969b; Dickinson, 1968).

Conclusions

Major and minor element geochemistry of rocks of the Kutcho volcanic suite is similar to that of modern orogenic volcanic series as defined by Ewart (1976), Carmichael et al. (1974), Taylor (1969) and McBirney (1969a). A unique characteristic that distinguishes the Kutcho volcanic suite from "average" modern orogenic suites is the apparent lack of andesites which characterize most volcanic island arcs (Dickinson and Hatherton, 1967; Dickinson, 1970; Taylor, 1969; and McBirney, 1969b). Rather, the Kutcho rocks tend to be bimodal with basalt or basaltic andesite and rhyodacite or rhyolite being the major volcanic rock types. The suite is characteristically calc-alkaline and compositionally akin to volcanics in an island arc setting. A notable exception is the basic schist unit which may be transitionally alkaline and similar to rocks of the Takla Formation (Monger, 1977a). However, this may also be the result of metasomatism adjacent to massive sulphide deposits.

A wide range of CaO, Na_2O and K_2O concentrations for a given SiO_2 concentration, coupled with the documented mobility of these elements during secondary processes (Pearce, 1975) and high CO_2 and H_2O concentrations reflect alteration in rocks of the Kutcho volcanic suite.

Rocks of the Kutcho Formation are contemporaneous with other Upper Triassic island arc assemblages such as the Takla Group (Monger, 1977b). The Kutcho Formation and other Upper Triassic volcanic rocks in the Cry Lake area have similar calc-alkaline characteristics. The peculiar alkaline nature of the Takla volcanic rocks has been attributed to oblique subduction (Monger, 1977b; Paterson, 1973; 1977) because the chemistry of some of the rocks is similar to that of Pliocene-Pleistocene volcanics above "bleeding" transform faults in the Aleutian arc (Scholl et al., 1973). Rocks of the Cry Lake area also have similar chemical characteristics to Stuhini volcanic rocks in the Stikine area, which have been included as part of the terrane known as Stikinia (Coney et al., 1980; Monger and Berg, 1984). The complex nature of late Triassic island arc volcanism in British Columbia, in which apparently equal amounts of alkaline and subalkaline rocks were erupted, has also been attributed to rapid subduction accompanied by rifting along plate margins (Souther, 1977).

Major and trace element distribution for rocks of the Cache Creek Group differ from those of the Kutcho volcanic suite, in that the Cache Creek Group rocks are dominantly tholeiitic and have ocean floor basalt affinities.

AGE OF KUTCHO FORMATION

On the basis of its minerology the Kutcho Formation was originally correlated with acidic volcanic rocks of the Permian Asitka Group (Monger, 1977c). Stratigraphic evidence although equivocal (see sections on regional geology and stratigraphy) and a Rb-Sr isochron age of 210 ± 10 Ma, however, suggest a Late Triassic age for the rocks. Rocks of the Kutcho Formation are probably contemporaneous with the Upper Triassic Takla Group (Monger, 1977b).

Paleontological evidence

The Kutcho Formation is apparently devoid of fossils due to the degree of deformation or to their absence originally. Fossils collected from limestone of the Upper Triassic Sinwa Formation near the Kutcho Creek sulphide deposit indicate a Late Triassic age (see section on King Salmon Assemblage). The age of the limestone is important because, if in place, it apparently overlies conglomerate of the Kutcho Formation.

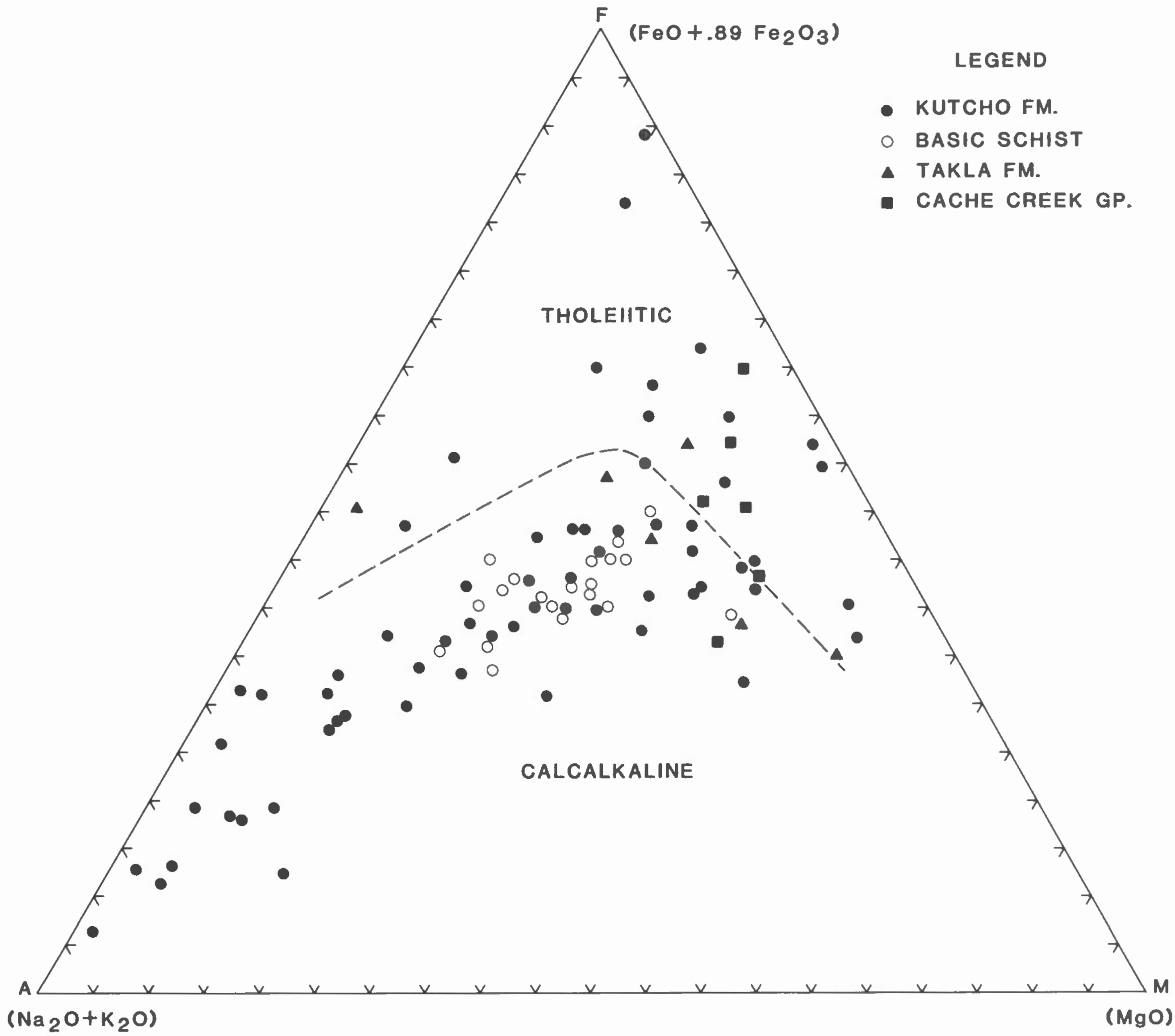

Figure 18. AFM composition for volcanic rocks of the Cache Creek Terrane of the Cry Lake map area.

Rb-Sr isotopic age

Silicic acidic and basic samples analyzed were chosen for little alteration and to provide a range of Rb/Sr ratios.

A Rb-Sr isochron calculated for rocks of the Kutcho Formation gives an age of 210 ± 10 Ma (Fig. 20A). Sample data are in Tables 1 and 2. The isochron date is similar to a 223 ± 28 Ma isochron generated for Takla Group samples collected by Monger and run by R.L. Armstrong (Fig. 20B). An age of 215 ± 14 Ma is generated by combining Rb-Sr data for the Takla Group and Kutcho Formation (Fig. 20C).

A previously reported age of 275 ± 30 Ma for the Kutcho Formation (Panteleyev and Pearson, 1977) was based on limited data (R.L. Armstrong, personal communication, 1978) and is no longer considered valid.

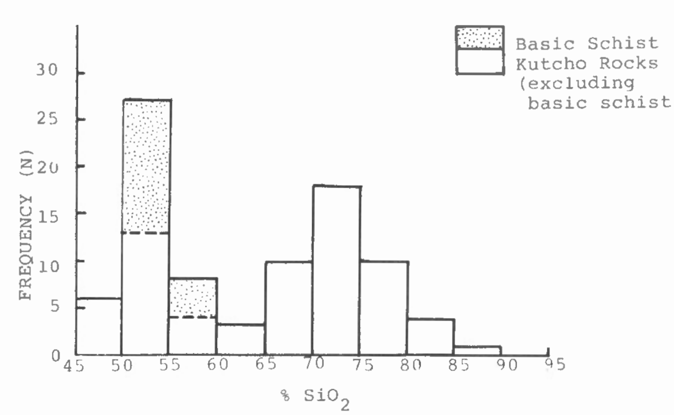

Figure 19. Silica histogram for rocks of the Kutcho Formation.

Table 1. . Rb-Sr data for rocks of the Kutcho Formation, Cry Lake map area, British Columbia.

Sample Number	Description	Location	Latitude	Longitude	%	Sr (ppm)	Rb (ppm)	Rb/Sr	$^{87}Rb/^{86}Sr$	$^{87}Sr/^{86}Sr$
A.12	Quartz-eye feldspar-sericite schist	Cry Lake Map Area	58°11′	128°20′	69.0	197	18.3	0.093	0.268	.7048
A.13	Quartz-eye sericite schist	Cry Lake Map Area	58°12′	128°24′	68.4	29.1	14.7	0.504	1.46	.7086
A.28	Feldspar-quartz-eye sericite schist	Cry Lake Map Area	58°10′	128°15′	61.1	57.6	8.6	0.149	0.432	.7054
A.32	Feldspar-quartz-eye sericite schist	Cry Lake Map Area	58°13′	128°24′	68.5	69.1	3.7	0.053	0.153	.7049
A.47[1]	Quartz-feldspar-chlorite sericite schist	Cry Lake Map Area	58°10′	128°20′	73.64	46.3	1.4	0.030	0.087	.7044
A.481	Chlorite schist	Cry Lake Map Area	58°11′	128°20′	50.87	147.0	1.0	0.007	0.020	.7042
A.53	Quartz-feldspar-sericite schist	Cry Lake Map Area	58°13′	128°23′	7.570	136.4	8.7	0.063	0.182	.7047
AP.63[1]	Quartz-feldspar sericite schist	Cry Lake Map Area	58°10′	128°20′	—	51.1	2.3	0.046	0.133	.7047

[1] (Analyses performed by R.L. Armstrong, University of British Columbia on samples provided by A. Panteleyev). Other analyses by L.E. Thorstad at the University of British Columbia.

Table 2. Rb-Sr data for rocks of the Takla Group, McConnell Creek map area, British Columbia.

Sample Number	Description	Location	Latitude	Longitude	%	Sr (ppm)	Rb (ppm)	Rb/Sr	$^{87}Rb/^{86}Sr$	$^{87}Sr/^{86}Sr$
MV-75-14a	Savage Mountain Formation	McConnell Creek Map Area	56°35′30″	126°25′	48.4	259	27.8	0.107	0.310	.7044
MV-75-82	Savage Mountain Formation	McConnell Creek Map Area	56°33′30″	126°33′	49.1	470	36.0	0.077	0.222	.7050
MV-75-141C	Savage Mountain Formation	McConnell Creek Map Area	58°32′	126°29′	49.3	382	28.8	0.075	0.217	.7049
10B-RML-75	Savage Mountain Formation	McConnell Creek Map Area	56°36′	126°32′	47.3	291	16.7	0.057	0.165	.7048
11B-RML-75	Savage Mountain Formation	McConnell Creek Map Area	56°35′	126°32′	49.2	417	17.9	0.043	0.124	.7046
MV-75-209C	Moosevale Formation	McConnell Creek Map Area	56°41′	126°54′	57.3	312	42.9	0.138	0.399	.7050
MV-75-22a	Moosevale Formation	McConnell Creek Map Area	56°40′	126°52′	41.2	202	14.4	0.071	0.205	.7043
MV-322-66		Jennings River Map Area	58°56′	130°30′	—	130	49.3	0.379	1.097	.7076
99A1075-RWD		E. of Pinchi Fault McConnell River	56°44′33″	126°33′	—	217	25.5	0.118	0.341	.7049
129A-75-RWD		E. of Pinchi Fault McConnell River	56°25′	126°11′	49.8	240	3.9	0.016	0.046	.7040

[2] (Analyses by R.L. Armstrong, University of British Columbia on samples provided by J.W.H. Monger).

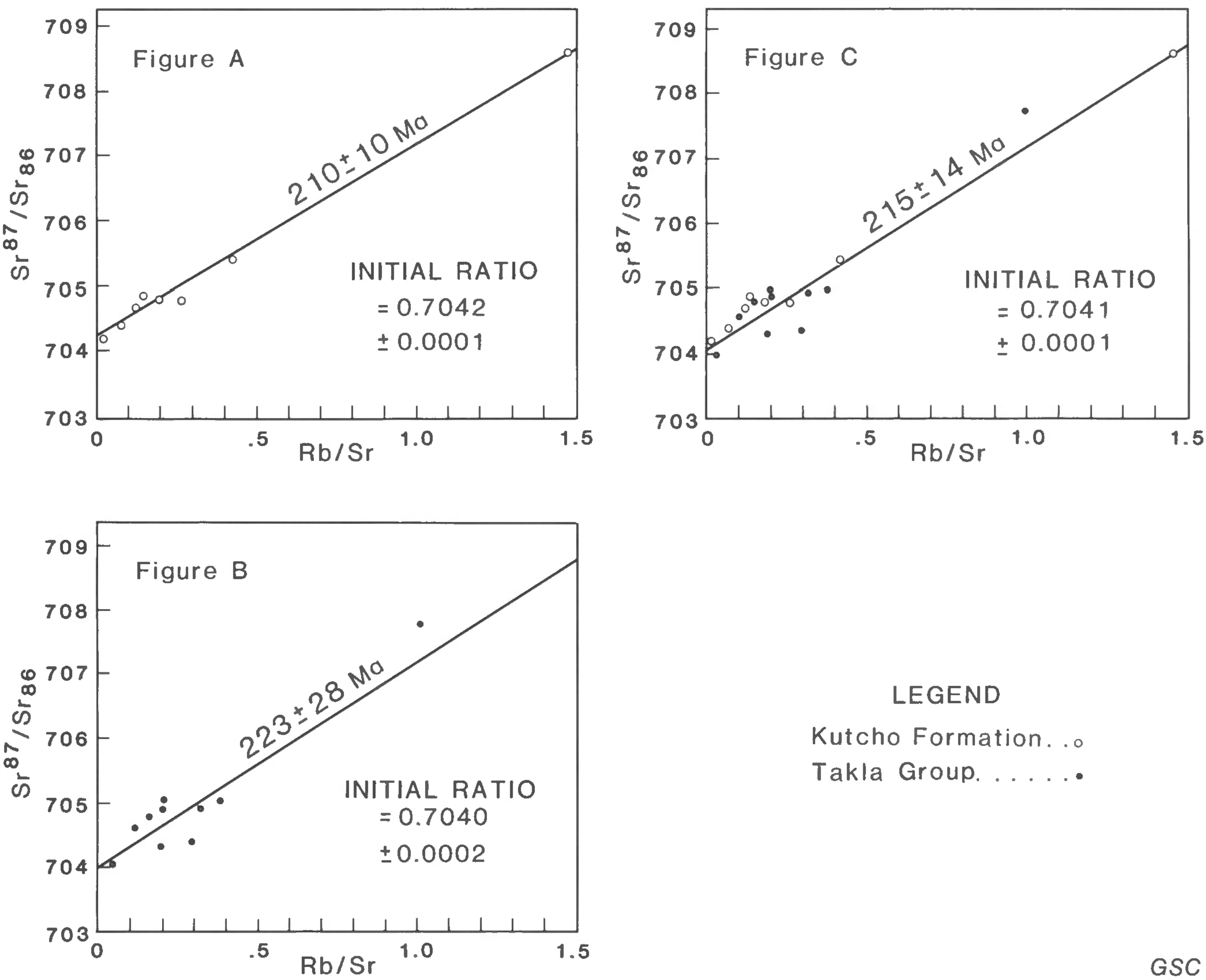

Figure 20

A Rb-Sr isochron diagram for rocks of the Kutcho Formation. Rb and Sr concentrations were determined by replicate analysis of pressed powder pellets using X-ray fluorescence. United States Geological Survey rock standards were used for calibration; mass absorption coefficients were obtained from Mo K Compton scattering measurements. Rb/Sr ratios have a precision of 0.2% (1 sigma) and concentrations a precision of 5% (1 sigma). Sr isotopic composition was measured on unspiked samples prepared using standard ion exchange techniques. The mass spectrometer (60° sector, 30 cm radius, solid source) is of United States National Bureau of Standards design, modified by H. Faul. Data acquisition is digitized and automated using a NOVA computer. Experimental data have been normalized to a $^{86}Sr/^{88}Sr$ ratio of 0.1194 and adjusted so that the NBS standard $SrCO_3$ (SRM987) gives a $^{87}Sr/^{86}Sr$ ratio of 0.71022 ± 2 and the Eimer and Amend Sr ratio is −.00013 at 1 sigma. Rb-Sr dates are based on a Rb decay constant of $1.42 \times 10^{-11}a^{-1}$. The regressions are calculated according to the technique of York (1967)

B Rb-Sr isochron diagram for rocks of the Takla Formation, McConnell Creek map area. Data from R.L. Armstrong (personal communication, 1979). Samples collected by J.W.H. Monger.

C Rb-Sr isochron diagram for combined data from Figures 20A and B for rocks of the Kutcho Formation and Takla Group.

STRUCTURE

Rocks of the King Salmon Assemblage, including the Kutcho Formation, are folded by upright to overturned, southwesterly vergent tight and asymmetric to near isoclinal folds during a single phase of deformation, probably related to the thrusting event that emplaced the allochthon. Later vertical and strike-slip faults dismembered the allochthon.

Poles to bedding, foliation and minor folds from five structural domains (Fig. 21) are plotted on Mellis equal area stereonet projections using a computer program (G. Woodsworth, personal communication, 1977).

The intensity diminishes and style of deformation changes to the northeast of the King Salmon Fault and to the northwest along strike (Fig. 22). In the southeast, high amplitude, overturned, isoclinal folds with well defined axial plane foliation and imbricate thrust sheets are common near the sole of the King Salmon Fault. To the northwest, open, similar-style folds with weakly developed axial foliations predominate and imbricate zones are uncommon or undefined. Inklin Formation rocks 35 km east of Dease Lake show two directions of fold axes, an early north trending, steeply plunging set and a later, predominant, more intense west-northwest trending set which obliterated the earlier set during the more intense, later deformation in the east. Strike-slip or normal faults, perpendicular to the main thrusts, occur throughout the belt.

Folds

Isoclinal folds predominate over open, upright, similar-style folds both outlined by the marker Sinwa Formation or conglomerate with Sinwa clasts (Fig. 22). Isoclinal folds are characterized by highly attenuated fold limbs and by transposed layering and suspected thrusts within hinge regions. Folds have amplitudes of 1 to 4 km and wavelengths of 0.5 to 2 km. Major fold axes plunge gently northwest and are local in extent. North trending fold axes are related to folds with amplitudes of a few tens of metres and wavelengths of a few hundred metres.

In the eastern part of the map area (Fig. 22, section C, D), where deformation is most intense, fold amplitudes increase and wavelengths decrease. A large, south vergent, west plunging anticline with smaller parasitic folds on its southern limb dominates the structure. Beds are moderate to steeply dipping in this area, but drillhole information suggests they tend to flatten at depth to 45° dips (D. Bridge, personal communication, 1978).

Transposition of layering and the massive and fragmental character of rocks within the Kutcho Formation obscures primary layering except in areas of lesser deformation. Easterly trends with a singular concentration of poles to bedding, typify the eastern part of the belt (Fig. 23A) but change to northwesterly trends in the central and western parts of the belt (Fig. 23B, C). In the central zone (Fig. 23B), even distribution of two bedding pole maxima along a great circle is an artifact of greater sampling of more open folds in the northeast parts of the zone. In the west (Fig. 23C) two maxima of poles to bedding suggest isoclinal folds. Figure 23D summarizes bedding measurements from the entire belt to yield an average plane striking 107° with a 56° northeasterly dip.

Isoclinal folds in Cache Creek Group rocks are refolded about west-northwest trending second phase fold axes substantiating the presence of multiple phases of deformation.

Minor folds

Minor folds are readily observed in weathered float but are not so evident in outcrop. Minor folds are difficult to recognize in greenschist rocks but are easily recognized in chert-argillite sequences. Orientations of minor fold axes are scattered (see Fig. 26C), but generally plunge shallowly to the west-northwest.

Foliation

Penetrative axial planar foliation is common in the King Salmon Assemblage (Fig. 24). Intensity of foliation diminishes with deformation intensity along and across strike. It typically trends west-northwesterly and dips moderately to steeply north and steepens to the northeast. The foliation fan is also evident farther northeast in the Cache Creek Group rocks where steep southwesterly dips predominate. Attitudes in the Kutcho Formation north of the main belt (Fig. 25G) are similar in northwesterly strike to the main belt, but dip steeply southwest.

The foliation is marked by the alignment of micaceous minerals, tremolite-actinolite laths and flattened grains of epidote and carbonate. Textural features noted during thin section examination indicate that constituent minerals have been subjected to extreme cataclasis, presumably during emplacement of the allochthon. Common cataclastic textures include augen-shaped quartz and feldspar grains, highly comminuted quartz and feldspar crystals, recrystallized mineral aggregates within pressure shadows and fractured twins in feldspar and calcite crystals. Large quartz and feldspar crystals are corroded, crushed and exhibit undulose extinction. Annealed crystalline mosaics of quartz are suggestive of later recrystallization.

Stereonet projections of poles to foliation show a relative homogeneity of attitudes within the belt (Fig. 25A-E). In the eastern part (Fig. 25A), east-west strikes and moderately steep northerly dips are dominant with some flattening of dips near the leading edge of the King Salmon Thrust. In central and west zones of the belt northwesterly strikes and steep northeasterly dips prevail, but steep southwesterly dips are also present (Fig. 25B,D,E). An obvious exception to the relatively homogeneous attitudes is evident in Figure 25C, in which the average plane of foliation is significantly different and is interpreted as a rotated fault block. Figure 25F, a cumulative plot of poles to foliation gives an average plane of 108° with a dip of 70° northwest.

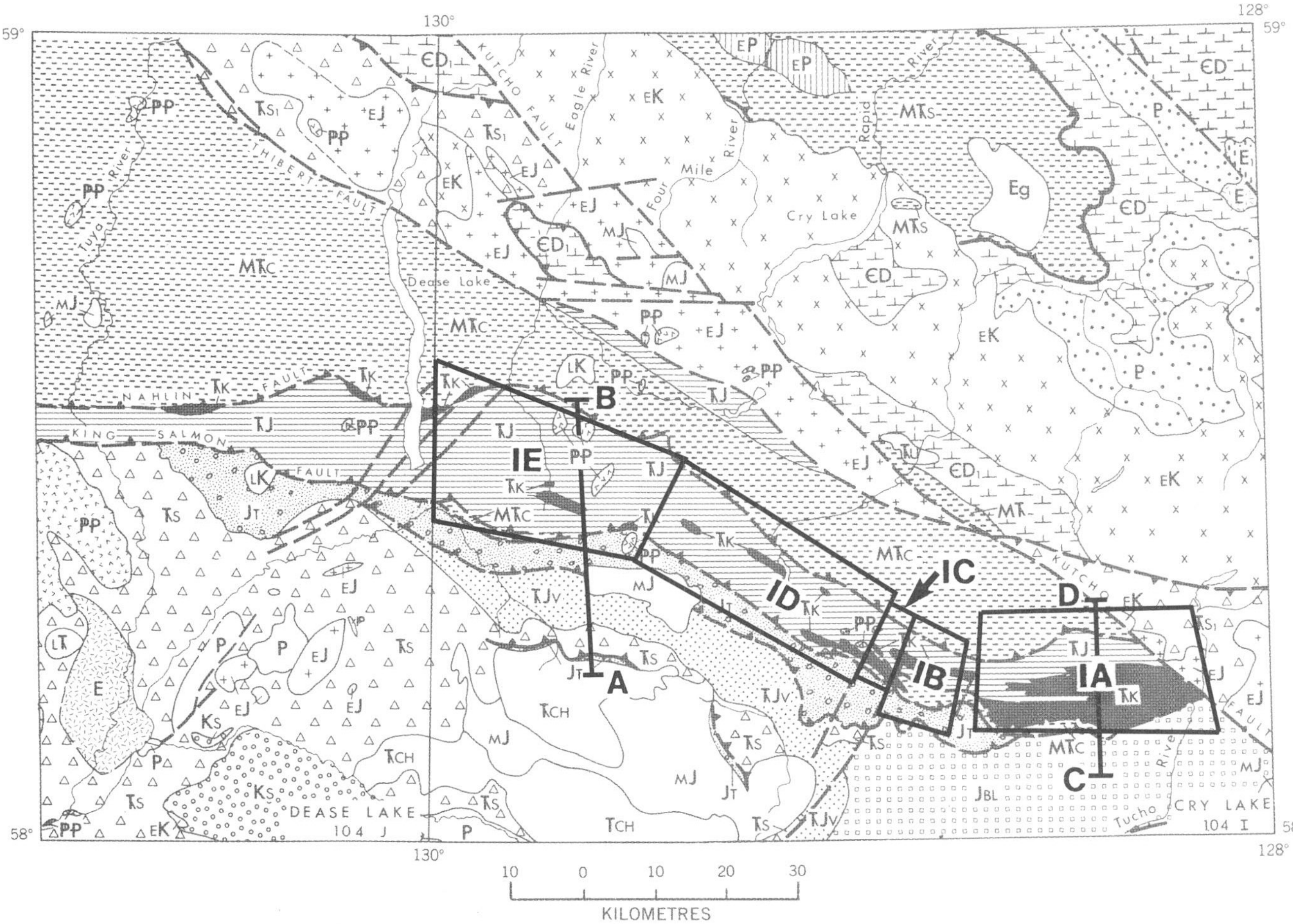

Figure 21. Structural domains and locations of structural cross-sections A-B and C-D.

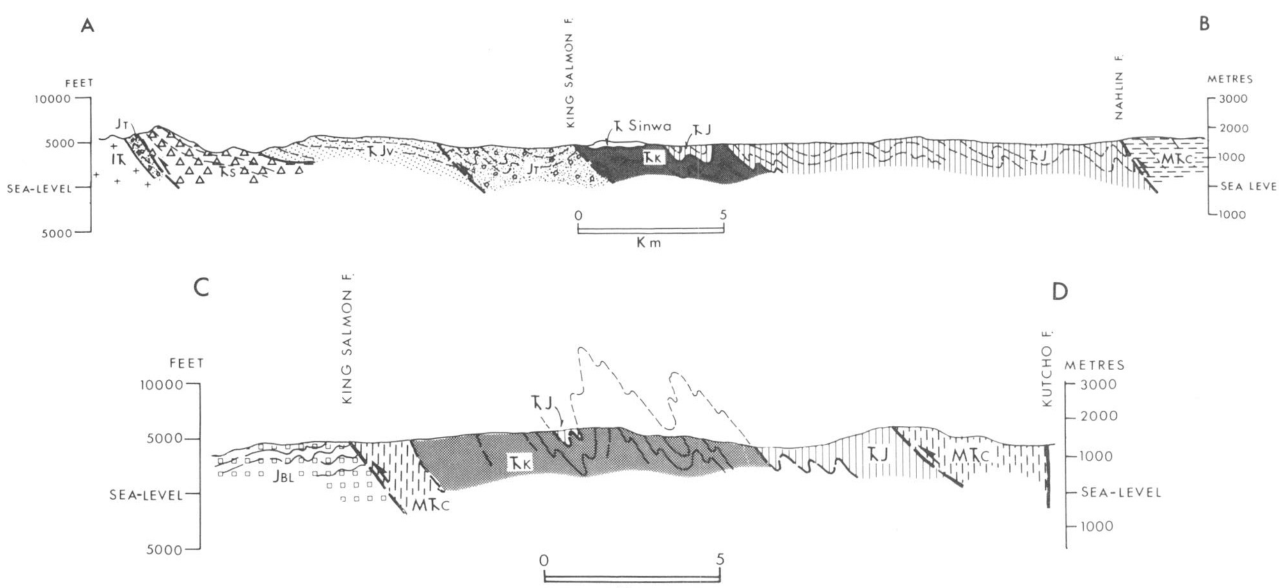

Figure 22. Diagrammatic structural cross-sections A-B and C-D. See Figure 21 for locations.

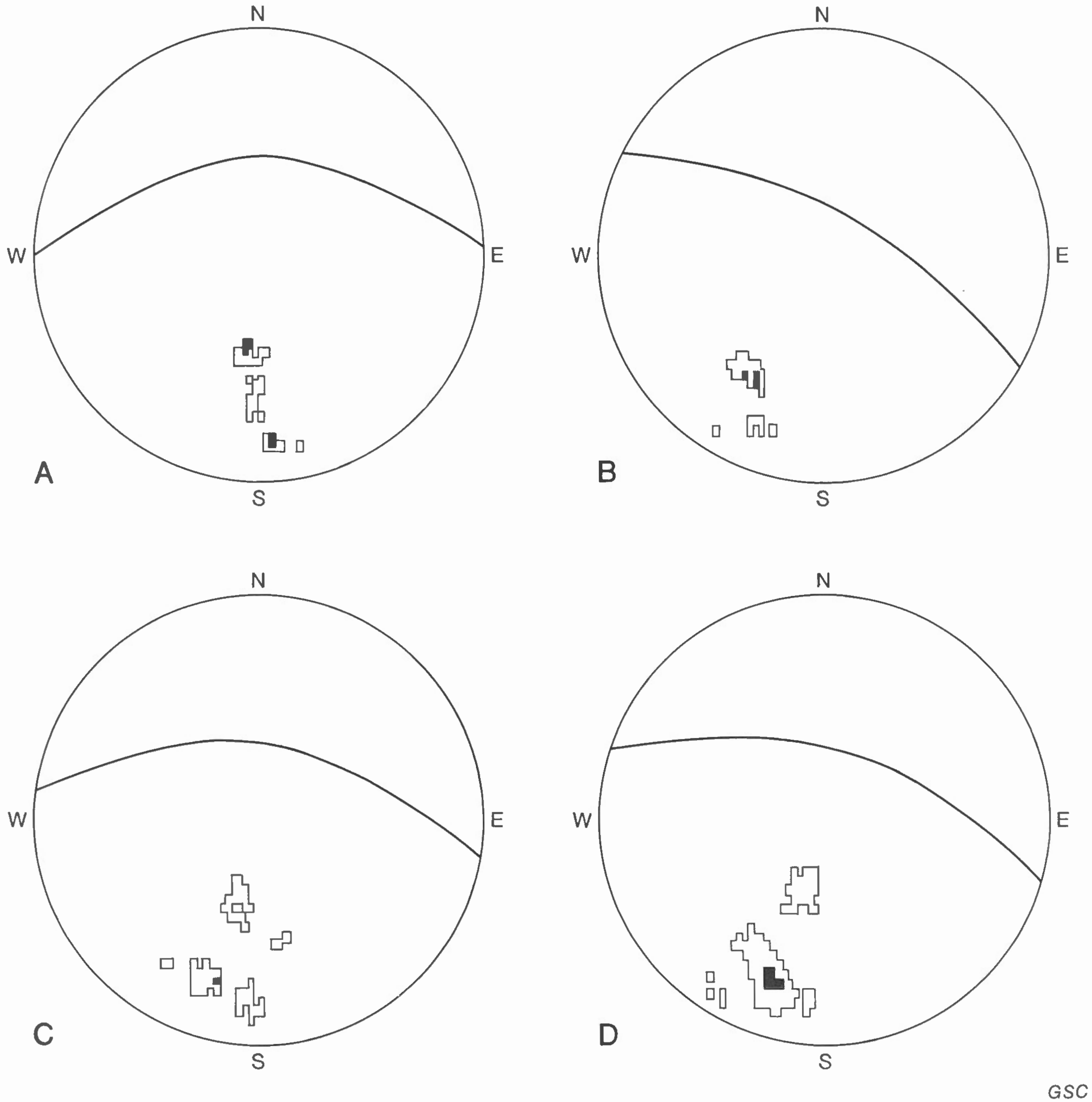

A Domain 1A; Average of 35 beds 088°/46° NW

B Domain 1D; Average of 50 beds 116°/64° NE

C Domain 1E; Average of 53 beds 099°/51° NE

D Domains 1B,1D,1E; Average of 104 beds 107°/56 NE

Figure 23. Contoured Mellis stereonets of poles to bedding planes for rocks of the King Salmon Allochthon.

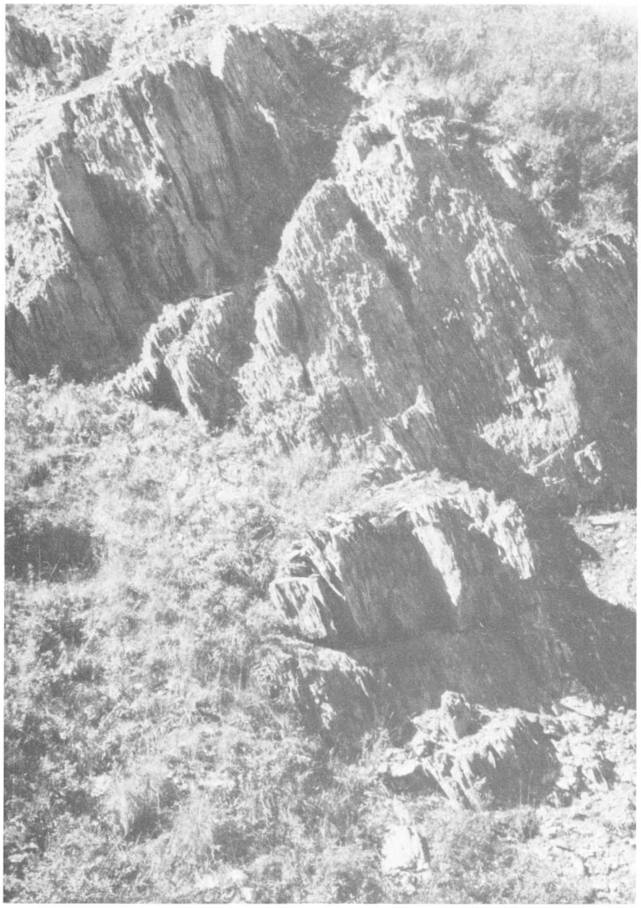

Figure 24. Penetrative foliation in conglomerate of the Inklin Formation; exposure about 5 m high.

In summary, northwesterly trends with steep northeasterly dips fanning to steep southwesterly dips characterize the foliation. Foliation parallels the leading edge of the King Salmon Thrust. Foliation and the leading edge of the thrust parallel the regional structural grain in the Cry Lake map area.

Faults

The King Salmon Assemblage is crosscut by low-angle thrust faults and high-angle, strike-slip and normal faults (Fig. 3). The King Salmon Thrust Fault floors the King Salmon Assemblage and the Nahlin Fault bounds it to the north. The Nahlin Fault varies in character along its strike length (Gabrielse, 1978, 1985) from a thrust fault along its westerly trend to a possible dextral strike-slip fault along its northwestern trend. Imbricate thrusts at the leading edge of the King Salmon Fault are the large-scale manifestation of common thrusts in highly attenuated fold hinges within the assemblage.

Remarkable examples of flattened and stretched cobbles occur in basal conglomerate of the Inklin Formation in the hanging wall of the King Salmon Fault between 16 and 30 km east-southeast of the south end of Dease Lake (Fig. 7). The sequence, more than 100 m thick, comprises phyllitic slate, minor quartz-feldspar-volcanic greywacke and conglomerate which increases in shale matrix in the upper part. Blue-grey weathering limestone and green to buff weathering quartz-eye feldspar porphyry predominate in the pebbles and cobbles. Triaxial ellipsoid shape of the porphyry clasts has the long axis oriented down the foliation dip, intermediate axis parallel with the strike of foliation and minor axis perpendicular to the foliation. Maximum aspect ratios are 3. Limestone clasts are plate-like in sections perpendicular to the strike and have aspect ratios up to 35 (Godwin, 1962). Well developed, conjugate fracture sets in the porphyry are filled with calcite and commonly subtend obtuse angles to the minor axes. Some porphyry cobbles are cut by similarly oriented small scale surfaces which are slickensided and offset the cobbles more than 2 cm. In many places limestone has flowed along the contacts of the relatively more competent porphyry clasts.

The degree of deformation in the cobbles is clearly related to proximity to the sole of the King Salmon Fault. Although penetrative foliation is characteristic of the Inklin rocks clasts in conglomerates well removed from the fault are much less strained.

Structural comparison between the King Salmon Assemblage and Cache Creek Group

Similar in certain respects, the structural styles of the King Salmon Assemblage and Cache Creek Group rocks are nonetheless distinct. Both were deformed in the last major deformational event but Cache Creek Group rocks (Fig. 26) suffered two phases of deformation, including the event affecting the King Salmon Assemblage rocks.

The most important structural contrast is in foliation style. The King Salmon Assemblage is characterized by one penetrative cleavage giving rise to distinctive, platy talus in which cleavage-bedding relationships are commonly well displayed. Two or more cleavage directions in the Cache Creek Group, one that is well defined and parallels that in the King Salmon Assemblage and one that is fainter and easterly trending (Fig. 26A) give rise to a blocky talus. The contrast in cleavage styles expressed in talus shape was used to differentiate nondescript greenstones during field mapping.

Structural similarities exist between Cache Creek Group and King Salmon Assemblage rocks in the structural elements produced in the last deformational event.

Timing of deformation and metamorphism

Stratigraphic, structural and isotopic age evidence bear on the timing of deformation and metamorphism of the King Salmon Assemblage. Sinwa limestone clasts in Lower Jurassic conglomerate (pre-thrusting) are fine grained and massive whereas in Middle Bajocian (Middle Jurassic) conglomerate (post-thrusting) they are coarsely crystalline, veined and sheared (Tipper, 1978). The King Salmon Thrust

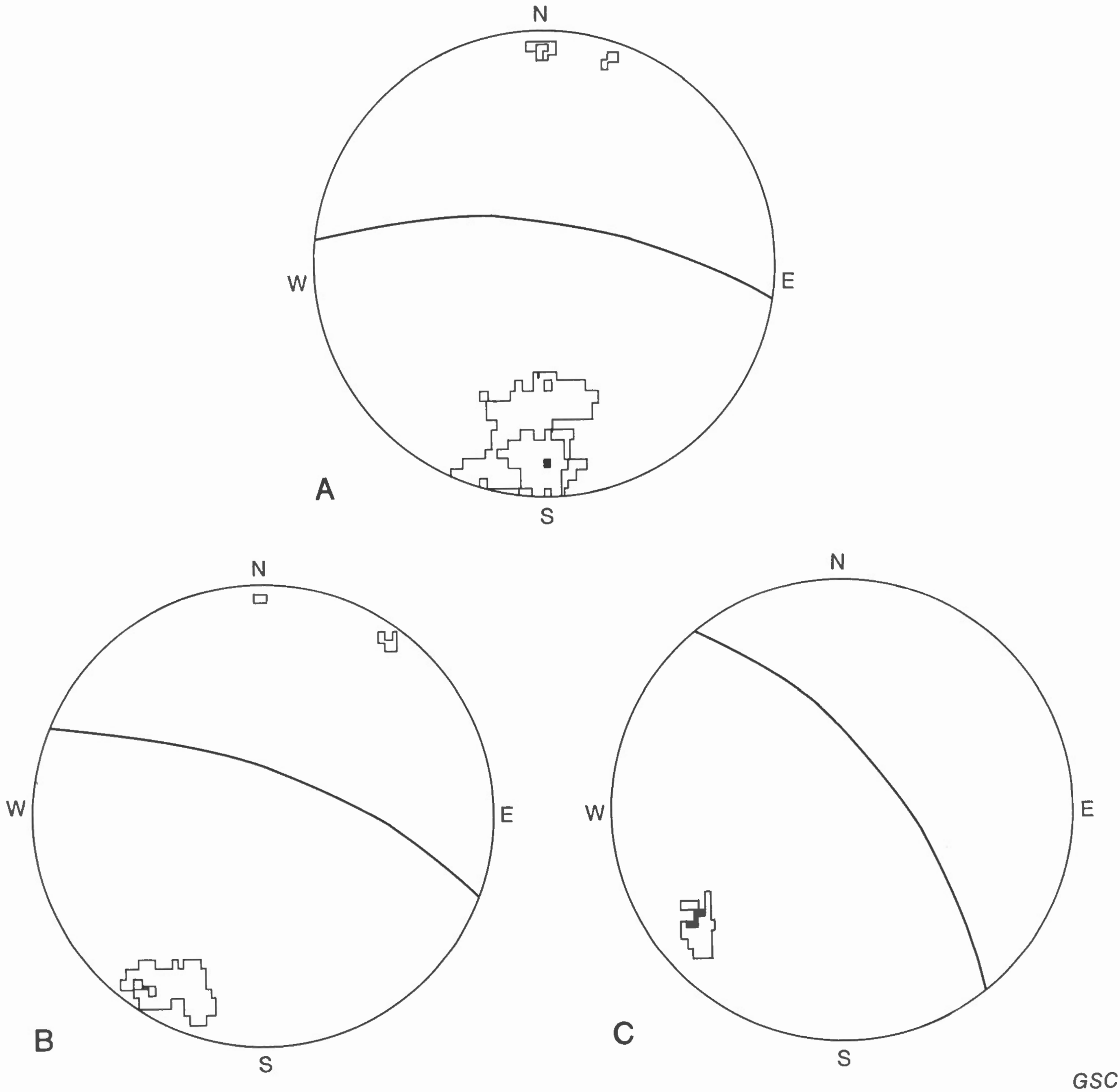

A Domain 1A; Average of 103 planes 093°/71° NE

B Domain 1B; Average of 73 planes 112°/74° NE

C Domain 1C; Average of 34 planes 140°/67° NE

D Domain 1D; Average of 37 planes 109°/75° NE

E Domain 1E; Average of 45 planes 107°/69° NE

F Domains 1A,1B,1C,1D,1E; Average plane 108°/70° NE

G Upper Paleozoic(?) and Lower Mesozoic(?) rocks northeast of the Kutcho Fault; Average of 32 planes 130°/80° SW

Figure 25. Contoured Mellis stereonets of poles to foliation for rocks of the King Salmon Allochthon.

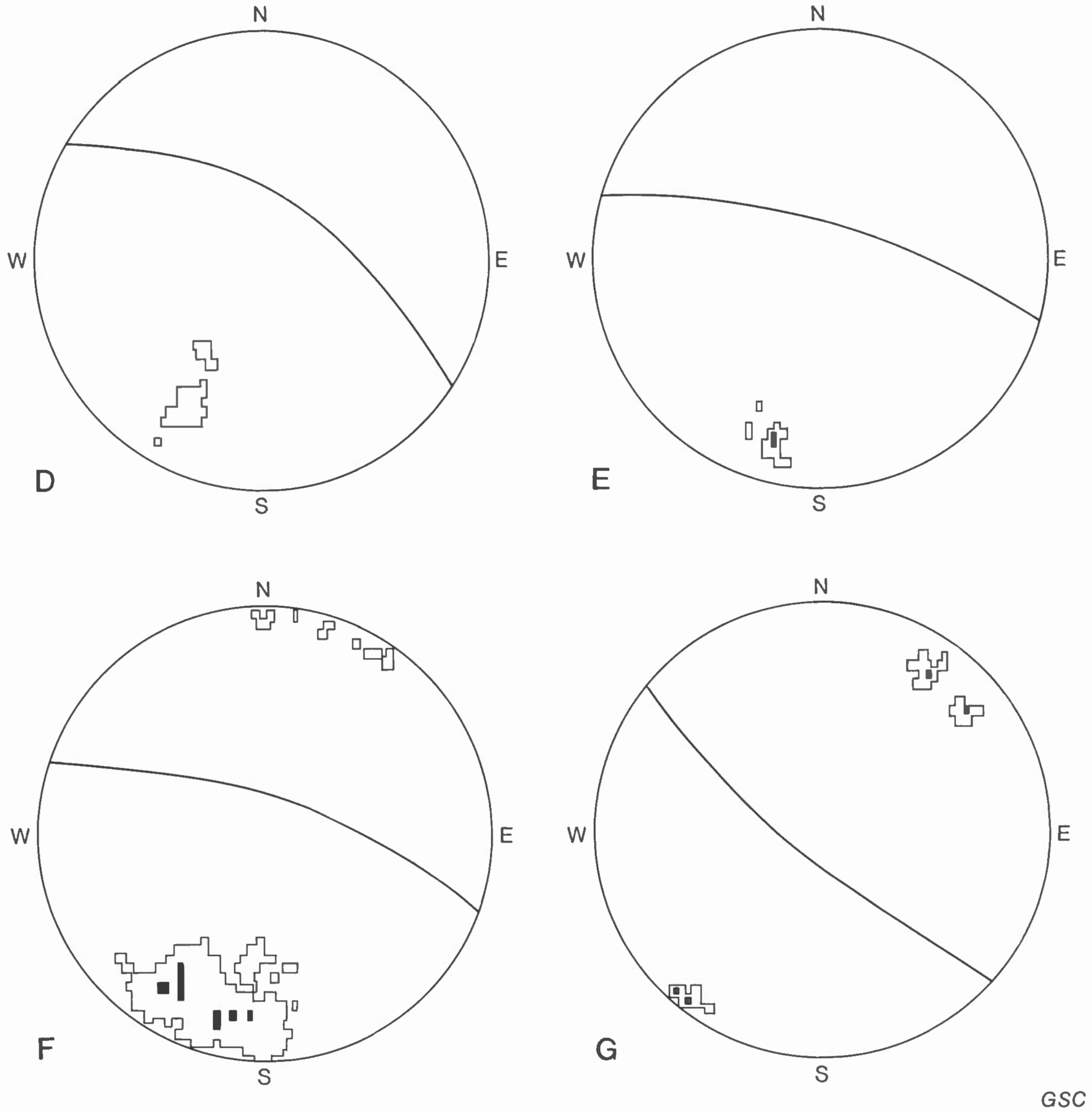

Figure 25 (cont.)

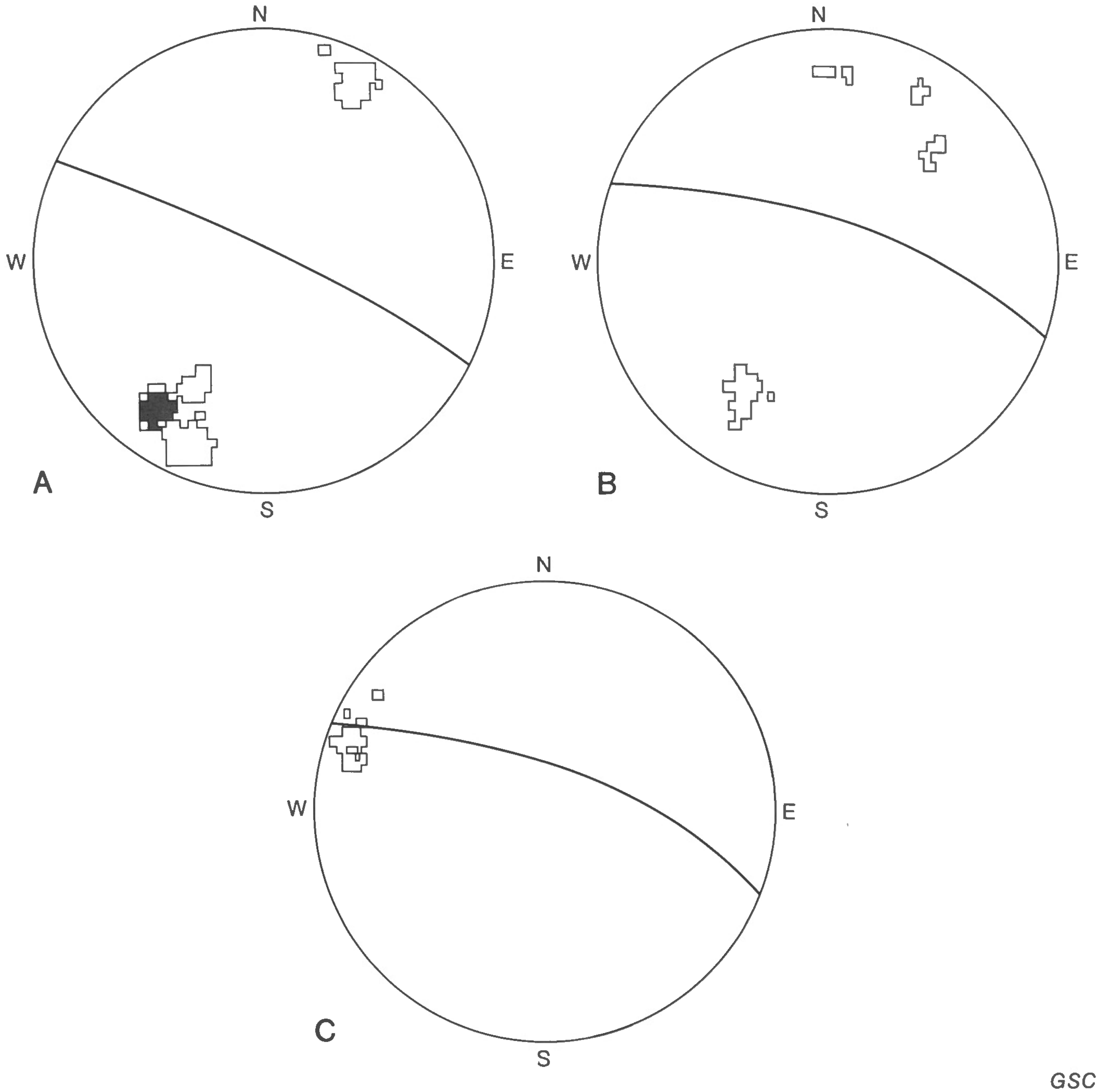

A Poles to 159 foliation planes; Average plane 117°/84° NE

B Poles to 47 bedding planes; Average plane 107°/67° NE

C Minor folds, 30 axes; Average axis is 292°/28° NW

Figure 26. Contoured stereonets of poles to foliation and bedding and axes of minor folds for Cache Creek Group rocks.

Fault places Pliensbachian (Lower Jurassic) and older rocks on Upper Triassic to Bajocian (?) volcanic and sedimentary rocks to the south. Footwall Lower Jurassic rocks are involved in complex imbricate thrust sheets and Middle Bajocian sediments and volcanics are locally deformed adjacent to the fault.

About 35 km southeast of the south end of Dease Lake a biotite-hornblende-quartz granodiorite crosscuts footwall structures related to the King Salmon Fault. Two of three K-Ar isotopic ages (147 ± 5 Ma, 158 ± 2 Ma and 161 ± 2 Ma) are essentially concordant (Stevens et al., 1982; J.C. Roddick, personal communication, 1984), suggesting that much of the deformation predated the early Late Jurassic.

Folding, development of penetrative cleavage, and metamorphism are considered to be contemporaneous with thrusting. Vergence of overturned isoclinal folds are perpendicular to and foliation and fold axis trends are parallel with the strike of the King Salmon Thrust. The fabric of most metamorphic minerals in the Kutcho Formation suggests that metamorphism was synkinematic with folding and thrusting. Stratigraphic and structural studies (Tipper, 1978) have shown that rocks of the King Salmon Allochthon have been thrust over Lower to Middle Jurassic volcano-sedimentary rocks. Lower Jurassic rocks are found in imbricate thrust sheets near the sole of the King Salmon Thrust. Rocks of middle Bajocian (Middle Jurassic) age, however, are little involved in thrusting. Thrusting, folding and metamorphism therefore probably occurred between Toarcian and pre-Middle Bajocian time. Sericite from quartz sericite schist about 2 km west of the Kutcho Creek sulphide deposit gave a K-Ar age of 189 ± 3 Ma and may indicate the time of metamorphic crystallization. (A. Panteleyev, personal communication, 1981). The main period of deformation and metamorphism is probably related to a Toarcian to pre-Middle Bajocian deformational event.

Available evidence suggests that rocks of the King Salmon Allochthon were folded and thrust into their present location in early Toarcian to Middle Bajocian time. Some movement may have continued into the Late Jurassic.

Summary

Early Toarcian to Middle Bajocian deformation and metamorphism of the King Salmon Assemblage produced mainly isoclinal folds, a single, synkinematic metamorphic penetrative foliation and the King Salmon Allochthon floored by the King Salmon Thrust Fault. Macro and microscopic tectonic fabrics are parallel with the regional grain in the Cry Lake map area. Second phase, congruent structures in Cache Creek Group rocks suggest that they and the King Salmon Assemblage rocks were deformed together.

ALTERATION AND MASSIVE SULPHIDE MINERALIZATION

Kutcho Creek deposit

The Kutcho Creek is a volcanogenic, exhalative, stratabound massive sulphide (Cu-Zn-Ag) deposit, hosted by volcanic rocks of the Kutcho Formation in the southeastern part of the Cry Lake map area (Fig. 4). The deposit was discovered by a regional geochemical program in the early 1970s and has been further explored and assessed with geological mapping, diamond drilling, electromagnetics, gravity, induced polarization and charged potential methods. Sulphide minerals include pyrite, sphalerite, chalcopyrite, chalcocite, bornite and minor galena, digenite, tetrahedrite-tennantite, covellite and pyrrhotite. The deposit has many affinities with Kuroko deposits hosted in Cenozoic rocks of Japan (Tatsumi, 1970; Ishihara, 1974).

General setting and morphology of the deposit

The massive sulphide unit lies within a felsic sequence of volcaniclastic rocks (Fig. 9). Three distinct, ellipsoidal sulphide bodies, 30 m thick and separated up to 200 m along a strike length of 3.5 km are divided into four main lenses (Bridge and Maar, in press): the ore-grade "Kutcho" lens, a fine grained, pyritic "Sumac West" lens and two ore-grade "Esso West" lenses texturally similar to the Kutcho lens. These are interpreted to occur on the flank of a pyroclastic rhyolite dome (Bridge et al., 1977). Thin lenses of massive sulphide and disseminated pyrite are common in both footwall and hanging wall of the main deposit.

Massive sulphide mineralization

Mineralization

The main mineralized lens (80-85% sulphides) is composed predominantly of pyrite, chalcopyrite, sphalerite, lesser bornite and chalcocite, and trace tetrahedrite-tennantite, digenite and galena. Pyrrhotite was reported by D. Bridge (personal communication, 1978) and by Weber (1977); no pyrrhotite, however, was observed in polished sections examined by the writers.

Silver values appear to be associated with copper sulphides (D. Bridge, personal communication, 1978); polished section work by the writers supports this.

The largest sulphide body, the Kutcho lens, is estimated to contain 17 million tonnes of reserves amenable to open pit mining with an average grade of 1.62% Cu, 2.32% Zn, 29.2 g/t Ag and 0.3 g/t Au (Bridge and Maar, in press). The Sumac West deposit has not been completely delineated by drilling but has geological reserves estimated at 10 million tonnes grading 1.0% Cu and 1.2% Zn (Bridge and Maar, in press). Gold and silver contents are not available. The Esso West, most westerly of the massive sulphide lenses, is estimated to contain 1 to 1.5 million tonnes of massive sulphides with an average grade that is approximately twice that of the Kutcho Zone (Bridge and Maar, in press).

Gangue

Gangue is predominantly carbonate, sericite and quartz. Banded dolomite lenses occur in the massive ore.

Thin carbonate laminae gangue in ore zones is predominantly ferroan dolomite (from X-ray diffraction and Alizarin Red stain results). Dolomite and ferroan dolomite ($Ca(Mg_{.67}Fe_{.33})(CO_3)_2$) occur throughout the ore horizon as massive lenses or matrix or both. Dolomite and ferroan dolomite also form thin layers in the sericite schist generally parallel with the foliation and as veinlets filling fractures. Dolomite rhomb porphyroblasts, common in the hanging wall, are believed to be related to original mineralizing fluids, but have been derived from partially remobilized carbonate during metamorphism. Carbonate is believed to be an exhalative product related to volcanism contemporaneous with sulphide deposition.

Milky white to clear quartz constitutes a major part of the gangue especially as fragments in breccias, as granular aggregates and quartz-eyes in sericite schist but also occurs alone or with carbonate in pre- and post-tectonic veins. Pretectonic veins commonly contain bornite and chalcopyrite. Post-tectonic or syntectonic quartz veins are generally barren, but commonly associated with a gossan halo.

Hanging wall and footwall sulphides

Several lenses of massive sulphide, conformable with host rock schist and carbonate, occur in the hanging wall of the deposit. Three lenses are recognized in successive stratigraphic horizons and may represent three mineralizing events (C. Scott, personal communication, 1977).

Footwall sulphides, comprising disseminated pyrite or very small massive sulphide lenses, are found in quartz, sericite and carbonate gangue up to 39 m below the main zone of mineralization.

Mineral zonation

Vertical mineral zonation is not defined within the massive sulphides, but a lateral outward enrichment in zinc relative to copper occurs within the plane of the sulphide bodies (Bridge and Maar, in press). Disseminated sulphide feeder zones are barren of copper and zinc.

Ore textures

The ore ranges from massive to well-layered. Massive ore is generally a very dense, compact granular aggregate that grades into disseminated anhedral to euhedral grains (predominantly pyrite). Poorly to well developed layering is defined by layered laminations 1-20 m thick.

The penetrative foliation has obscured most but not all of the primary minerals and structures. For example, convoluted sulphide laminations enveloped by planar sulphide laminae may reflect syndepositional slumps. Breccia textures are rare but appear to be of primary origin because the gangue and sulphide matrix is undeformed. Microfaulting is evident with offsets on quartz veinlets and sulphide blebs from 2-10 mm.

Alteration associated with massive sulphide mineralization

An alteration envelope related to sulphide mineralization can be recognized despite a regional metamorphic overprint which produced extensive sericitization. It consists of sericite, dolomite and very minor silica (Bridge and Maar, in press). A mantle with Na_2O-depletion and K_2O-enrichment has been defined laterally for at least 500 m from the sulphide horizon and vertically at least 290 m beneath the horizon. In hanging wall rocks a Na_2O-poor and K_2O-rich mantle extends approximately 100 m laterally beyond the sulphide lenses and 180 m above them (Bridge and Maar, in press). Data from unpublished reports show a strong sevenfold enrichment of MgO and CaO, twofold K_2O enrichment and anomalously high SiO_2 content in comparison to country rocks. The lack of textural evidence for secondary introduction of SiO_2 suggests that the high silica content reflects the primary composition of an exhalative horizon (Bridge and Marr, in press). Hematite is abundant in hanging wall rocks but is absent in altered footwall rocks.

Detailed mineralogy of Kutcho Creek deposit

Copper, zinc and minor amounts of silver are the major commodities of the Kutcho Creek deposit. They are contained within the sulphide minerals pyrite, sphalerite, chalcopyrite, bornite, lesser chalcocite and trace tetrahedrite-tennantite, galena, digenite and covellite.

Pyrite

Massive pyrite, ubiquitous throughout the ore, also occurs as disseminations ranging from 10-50% in the footwall and hanging wall rocks. It occurs as dense, anhedral, granular aggregates and euhedral to subhedral grains in other sulphides. The common euhedral pyrite is interpreted to be the result of recrystallization. Fine to coarse disseminated grains are anhedral to subhedral and flattened in the foliation plane.

Brittle deformation of pyrite produces angular subgrains (pyrite grains generally deform in a brittle manner), whereas ductile deformation results in grain flattening parallel with the foliation.

Minor sphalerite, chalcopyrite, and predominantly bornite replace pyrite along fractures and grain boundaries as embayments and irregular blebs within it. In one sample, irregular pyrite fragments are sequentially rimmed by sphalerite and pyrite.

Sphalerite

Sphalerite is interstitial to pyrite and gangue, has mutual grain boundaries with bornite and chalcopyrite, and may contain tiny, subrounded chalcopyrite inclusions, the result of exsolution or metamorphism.

Chalcopyrite

Chalcopyrite is interstitial to pyrite and gangue. It occurs both as foliated blebs oriented parallel with the penetrative foliation and as massive, randomly oriented, irregular blebs. In the latter crystal habit it bounds sphalerite and bornite suggesting syndepositional relations. Chalcopyrite also occurs in bornite as thin, cubic or minor rhombic lamellae, small irregular blebs, or with it as rims and myrmekitic intergrowths. Chalcopyrite lamellae in bornite are commonly offset and truncated by fractures. Covellite occurs at grain boundaries between bornite and chalcopyrite and may replace both. Digenite also appears to replace chalcopyrite. Chalcopyrite also occurs along fractures and microveinlets perpendicular to the layering.

Bornite

Bornite, interstitial to gangue and pyrite, bounds sphalerite and chalcopyrite. Foliated, disseminated blebs of bornite are commonly truncated by massive, non-foliated blebs, commonly associated with chalcocite, produced by remobilization. Bornite also occurs along veins and fractures. Digenite in bornite occurs along fractures as thin vein-like bodies or irregular blebs.

Chalcocite

Chalcocite occurs as myrmekitic to subgraphic intergrowths and as thin lamellae in bornite.

Digenite

Digenite is present in only small amounts replacing primary minerals. It is found along fractures in bornite and is also observed cutting across chalcopyrite lamellae, supporting the idea that it postdates initial crystallization and cooling. It also occurs at grain boundaries between chalcopyrite and bornite, possibly as a reaction zone between the two minerals or as a mutual exsolution product.

Covellite

Covellite is rare, occurring as rims on and along fractures in bornite and between chalcopyrite and bornite. It is interpreted to be a secondary replacement sulphide mineral.

Tetrahedrite-Tennanite

Tetrahedrite-tennantite occurs with bornite and chalcopyrite as irregular grains. In one sample it is discontinuously rimmed by (and partly replaced by?) chalcopyrite.

Galena

Rare galena occurs as irregular grains both in and beside bornite.

Discussion

The Kutcho Creek deposit is similar to Kuroko-type deposits of Japan. This comparison is supported by its association with acidic volcanic rocks, formation near the end of the volcanic cycle, the stratiform nature of the ore body, diffuse footwall contacts, and proximity in the section of overlying tuff and argillite. The stratiform character and the presence of sedimentary features such as layering, graded layering, and possible load structures suggest a syngenetic origin. The sulphide lenses overlie feeder zones of disseminated pyrite which generally coincide with areas of intense sodium depletion and potassium enrichment. A syngenetic, volcanogenic origin is inferred for the deposit.

REFERENCES

Anderson, R.G.

1978: Preliminary report on the Hotailuh Batholith, its distribution, age and contact relationships in the Cry Lake, Spatsizi and Dease Lake map areas north-central British Columbia; *in* Current Research, Part A, Geological Survey of Canada, Paper 78-1A, p. 29-31.

1979: Distribution and emplacement history of plutons within the Hotailuh Batholith in the Cry Lake and Spatsizi map areas, north-central British Columbia; *in* Current Research, Part A, Geological Survey of Canada, Paper 79-1A, p. 393-395.

1980: Satellitic stocks, volcanic and sedimentary stratigraphy and structure around the northern margins of the Hotailuh Batholith, north-central British Columbia; *in* Current Research, Part A, Geological Survey of Canada, Paper 80-1A, p.37-40.

Baragar, W.R.A. and **Goodwin, A.M.**

1969: Andesites and Archean volcanism of the Canadian Shield; *in* Proceedings of the Andesite Conference, A.R. McBirney, ed., Oregon Department of Geology and Mineral Industry, Oregon, Bulletin 65, p. 121-141.

Bloxam, T.W. and **Lewis, A.D.**

1972: Ti, Zr and Cr in some British pillow lavas and their petrogenetic affinities; Nature Physical Science, v.237, p. 134.

Bridge, D.A.

1978: Geology of the Kutcho Creek massive sulphide deposit, northern British Columbia; (unpublished internal report for Esso Minerals Ltd.).

1979: Geology and mineralization at the Kutcho Creek Cu-Zn deposit, northern British Columbia; Abstract Geoscience Forum, Whitehorse, Yukon Territory.

Bridge, D.A. and **Maar, J.M.**
in press: Geology of the Kutcho Creek volcanogenic massive sulphide deposits, northern British Columbia; A manuscript for Mineral Deposits of the Northern Cordillera, C.J. Morin, (ed.), Canadian Intitute of Mining and Metallurgy – Geology Division.

Bridge, D.A., Maar, J.M., and **Oddy, R.D.**
1977: Geology of the Kutcho Creek massive sulphide deposit, northern British Columbia; Geological Association of Canada, Program with Abstracts v. 2, p. 9.

Carmichael, I.S.E., Turner, F.J., and **Verhoogen, J.**
1974: Igneous petrology; McGraw-Hill Book Company, 739 p.

Condie, K.C.
1976: Trace element geochemistry of Archean greenstone belts; Earth Science Review, v. 12, p. 393-417.

Coney, P., Jones, D.L., and **Monger, J.W.H.**
1980: Cordilleran suspect terranes; Nature, v. 288, p. 329-333.

Davies, J.F., Grant, R.W.E., and **Whitehead, R.E.S.**
1979: Immobile trace elements and Archean volcanic stratigraphy in the Timmins mining area, Ontario; Canadian Journal of Earth Science, v. 16, no. 2, p. 305-311.

Dickinson, W.R.
1968: Circum-Pacific andesite types; Journal of Geophysical Resources, v. 75, p. 2261-2269.
1970: Relations of andesites, granites and derivative sandstones to arc trench tectonics; Review of Geophysic and Space Physics, v. 8, p. 813-860.

Dickinson, W.R. and **Hatherton, T.**
1967: Andesite volcanism and seismicity around the Pacific; Science, v. 157, p. 801-803.

Ewart, A.
1976: Mineralogy and chemistry of modern orogenic lavas-some statistics and implications; Earth and Planetary Science Letters, v. 31, p. 417-432.

Floyd, B.A. and **Winchester, J.A.**
1975: Magma type and tectonic setting discrimination using immobile elements; Earth and Planetary Science Letters, v. 27, p. 211-218.
1976: Geochemical discrimination of different magma series and their differentiation products using immobile elements; Chemical Geology, v. 20, p. 325-343.
1978: Identification and discrimination of altered and metamorphosed volcanic rocks using immobile elements; Chemical Geology, v. 21, p. 291-306.

Gabrielse, H.
1962: Cry Lake, British Columbia; Geological Survey of Canada, Map 29-1962.
1978: Operation Dease; *in* Report of Activities, Part A, Geological Survey of Canada, Paper 78-1A, p. 1-4.
1985: Major dextral transcurrent displacements along the northern Rocky Mountain Trench and related lineaments in north-central British Columbia; Bulletin Geological Society of America, v. 96, p. 1-14.

Gabrielse, H., Anderson, R.G., Leaming, S.F., Mansy, J.L., Monger, J.W.H., Thorstad, L.E., and **Tipper, H.W.**
1979: Cry Lake, British Columbia; Geological Survey of Canada, Open File 610.

Gelinas, L., Brook, C., Perrault, G., Carrignan, J., Trudel, P., and **Grasso, F.**
1977: Chemo-Stratigraphic divisions within the Abitibi Volcanic Belt, Rouyn-Noranda District, Quebec; *in* W.R.A. Baragar, L.C. Coleman, J.M. Hall, ed., Volcanic Regimes in Canada, Geological Association of Canada, Special Paper 16, p. 276-277.

Godwin, C.I.
1962: Cobble conglomerate near Squaw Creek, British Columbia; unpublished B.A.Sc. thesis, University of British Columbia.

Goodwin, A.M.
1977: Archean volcanism in Superior Province, Canadian Shield; *in* W.R.A. Baragar, L.C. Coleman, and J.M. Hall, eds., Volcanic Regimes in Canada, Geological Association of Canada, Special Paper 16, p. 205-241.

Hart, S.R., Brooks, C., Krogh, T.E., Davis, S.L., and **Nava, D.**
1970: Ancient and modern volcanic rock: a trace element model; Earth and Planetary Science Letters, v. 10, p.17-28.

Irvine, T.N. and **Baragar, W.R.A.**
1971: A guide to chemical classification of the common volcanic rocks; Canadian Journal of Earth Sciences, v.8, p. 523-548.

Ishihara, A.
1974: Geology of Kuroko deposits; Mining Geological Special Issue Number 6, p. 1-9.

Manson, V.
1967: Geochemistry of basaltic rocks 1. Major Elements; *in* The Poldervaart Treatise on Rocks of Basaltic Composition, H.H. Hess, and A. Poldervaart, ed., Interscience New York, p. 215.

McBirney, A.R.
1969a: Compositional variations in Cenozoic calc-alkaline suites of Central America; *in* Proceedings of the Andesite Conference, Department of Mineral Research, Oregon, Bulletin 65, p. 185-189.
1969b: Andesite and rhyolitic volcanism of orogenic belts; American Geophysical Monograph 13, p. 501-507.

Middlemost, E.A.K.
1973: A simple classification of volcanic rocks; Bulletin Volcanologique, v. 36, p. 382-397.

Miyashiro, A.
1973: Metamorphism and Metamorphic Belts; George Allen and Unwin Company Limited, London, 492 p.
1974: Volcanic rock series in island arcs and continental margins; American Journal of Science, v. 274, p. 321-355.
1975: Volcanic rock series and tectonic setting; Annual Review, Earth and Planetary Science Letters, v. 3, p. 251-269.

Monger, J.W.H.
1974: Upper Paleozoic rocks of the Atlin Terrane, northwestern British Columbia and south-central Yukon; Geological Survey of Canada, Paper 74-47, 63 p.

1977a: Upper Paleozoic rocks of the western Cordillera and their bearing on Cordillera evolution; Canadian Journal of Earth Sciences, v. 14, p. 1832-1859.
1977b: The Triassic Takla Group in McConnell Creek map area, north-central British Columbia; Geological Survey of Canada, Paper 76-29, 45 p.
1977c: Upper Paleozoic rocks of northwestern British Columbia; *in* Report of Activities, Part A, Geological Survey of Canada, Paper 77-1A, p. 255-262.

Monger, J.W.H. and **Berg, A.C.**
1984: Lithotectonic terrane map of western Canada and southeastern Alaska; United States Geological Survey, Open File 84-523, Part B.

Monger, J.W.H. and **Thorstad, L.**
1978: Lower Mesozoic stratigraphy, Cry Lake (104I) and Spatsizi (104H) map areas, British Columbia; *in* Current Research, Part A, Geological Survey of Canada, Paper 78-1A, p. 21-24.

Monger, J.W.H., Richards, T.A., and **Paterson, I.A.**
1978: The Hinterland Belt of the Canadian Cordillera: new data from northern and central British Columbia; Canadian Journal of Earth Sciences, v. 15, no. 5, p.823-830.

Monger, J.W.H., Souther, J.G., and **Gabrielse, H.**
1972: Evolution of the Canadian Cordillera: a plate tectonic model; American Journal of Science, v. 272, p. 577-602.

Panteleyev, A.
1974: Kutcho Creek massive sulphide deposit; Geology, exploration and mining in British Columbia Ministry of Mines and Petroleum Resources, p. 343-347.

Panteleyev, A. and **Pearson, D.E.**
1977: Kutcho Creek map area (104I/1W); Geological Field Work, British Columbia Ministry of Mines and Petroleum Resources, p. 74-76.

Paterson, I.A.
1973: The geology of the Pinchi Lake area, central British Columbia; unpublished Ph.D. thesis, University of British Columbia.
1977: The geology and evolution of the Pinchi fault zone at Pinchi Lake, central British Columbia; Canadian Journal of Earth Sciences, v. 14, p. 1324-1342.

Pearce, J.A.
1975: Basalt geochemistry used to investigate past tectonic environments on Cypress; Tectonophysics, v. 25, p. 41-67.

Pearce, J.A. and **Cann, J.R.**
1973: Tectonic setting of basic volcanic rocks determined using trace elements analysis; Earth and Planetary Science Letters, v. 19, p. 290.

Pearce, T.H., Gorman, B.E., and **Birkett, T.C.**
1975: The Ti02-K20-P205 diagram: A method of discriminating between oceanic and nonoceanic basalts; Earth and Planetary Science Letters, v. 24, p. 419-426.
1976: Tectonic setting inferred from chemistry of Cenozoic and Archean volcanics; EOS Transactions of the American Geophysical Union, v. 57, p. 343-344.
1977: The relationship between major element chemistry and tectonic environment of basic and intermediate volcanic rocks; Earth Planetary and Science Letters, v. 36, p. 121-132.

Pearson, D.E. and **Panteleyev, A.**
1975: Cupiferous iron sulfide deposits, Kutcho Creek map area (104I/1W); Geological Field Work, British Columbia Ministry of Mines and Petroleum Resources, Geology, Exploration and Mining Report, p. 86-93.

Pichler, H. and **Zeil, W.**
1969: Andesites of the Chilean Andes; *in* A.R. McBirney, ed., Proceedings of the Andesite Conference, Department of Mineral Research, Oregon, Bulletin 65, p. 165.

Preto, V.A.
1977: The Nicola Group: Mesozoic volcanism related to rifting in southern British Columbia; *in* W.R.A. Baragar, L.C. Coleman, and J.M. Hall, ed., Volcanic Regimes in Canada; Geological Association of Canada, Special Paper 16, p. 39-60.

Scholl, D.W., Marlow, M.S., and **Buffington, E.C.**
1973: Pliocene and Pleistocene eruptive rocks of the Western Aleutian Ridge - a bleeding strike slip boundary? (abstract); Geological Society of America, Abstracts with Programs, v. 5, no. 1, p. 101.

Souther, J.G.
1977: Volcanism and tectonic environments in the Canadian Cordillera - A second look; *in* W.R.A. Baragar, L.C. Coleman, and J.M. Hall, ed., Volcanic Regimes in Canada, Geological Association of Canada, Special Paper 16, p. 3-24.

Stevens, R.D., Delabio, R.N., and **Lachance, G.R.**
1982: Age determinations and geological studies, K-Ar isotopic ages, Report 15; Geological Survey of Canada, Paper 81-2, p. 4.

Strong, D.F.
1977: Volcanic regimes of the Newfoundland Appalachians; *in* W.R.A. Baragar, L.C. Coleman, and J.M. Hill, ed., Volcanic Regimes in Canada; Geological Association of Canada, Special Paper 16, p. 61-90.

Sutherland Brown, A., Cathro, R.J., Panteleyev, R.J., and **Ney, C.S.**
1971: Metallogeny of the Canadian Cordillera; Canadian Institute of Mining Metallurgy Transactions, v. 74, p.121-145.

Tatsumi, T. (editor)
1970: Volcanism and ore genesis; University of Tokyo Press, Tokyo, p. 153-180 and p. 197-206.

Taylor, S.R.
1969: Trace element chemistry of andesites and associated calc-alkaline rocks; *in* A.R. McBirney, Proceedings of the Andesite Conference, Department of Geology and Mineral Research, Oregon, Bulletin 65, p. 43-64.

Thorstad, L.
1979: The lower Mesozoic King Salmon Assemblage-Cry Lake map area, British Columbia; *in* Current Research, Part A, Geological Survey of Canada, Paper 79-1A, p. 21-24.

Tipper, H.W.
1978: Jurassic biostratigraphy, Cry Lake map area, British Columbia; *in* Report of Activities, Part A, Geological Survey of Canada, Paper 78-1A, p. 25-27.

Weber, M.
1977: The geology and mineralogy of the Cu-Zn-Fe massive sulfide deposit at Kutcho Creek, British Columbia; unpublished B.Sc. thesis, University of British Columbia, 61 p.

Wheeler, J.O. and **Gabrielse, H.**
1972: The Cordilleran Structure Province; *in* R.A. Price, and J.W. Douglas, ed., Variations in Tectonic Styles in Canada; Geological Association of Canada, Special Paper 11, p. 1-81.

Winchester, J.A. and **Floyd, P.A.**
1976: Geochemical magma type discrimination - application to altered and metamorphosed basic igneous rocks; Earth and Planetary Science Letters, v. 28, p. 459-469.
1977: Geochemical discrimination of different magma series and their differentation products using immobile elements; Chemical Geology, v. 20, p. 325-343.

Winkler, H.G.F.
1974: Petrogenesis of metamorphic rocks. Third edition; SpringerVerlag, 334 p.

Yellur, D.D.
1977: Geochemical clues in the investigation of the tectonic environment of the Dalma Greenstones, Bihar India, Chemical Geology, v. 20, p. 345-363.

York, D.
1967: The best isochron; Earth and Planetary Science Letters, v. 2, p. 479-482.

APPENDIX 1

Chemical analyses and normative minerals for rocks from north-central British Columbia

Sampling, analytical procedures, and error

Ninety-two analyses of volcaniclastic rocks from the King Salmon Assemblage were generated and reviewed. For comparative purposes, six analyses from the Takla Formation and eight analyses from the Cache Creek Group were also reviewed. Sample names and locations are given in Appendix 2.

Chemical composition

The chemical analyses in Appendix 1 were done by the Analytical Chemistry Section of the Geological Survey of Canada, Ottawa. To minimize the effects of alteration all analyses have been normalized by recalculation eliminating CO_2 and H_2O. The normalized values are used to calculate the normative percentages. Variation diagrams for chemical data also are based on normalized values.

XRF was used for MnO, Na_2O, CaO, K_2O, P_2O_5, TiO_2 and S. FeO, Co_2 and H_2O were determined by chemical methods; F and C1 were analyzed using the specific ion electrode method. Trace elements were analyzed by emission spectroscopy.

Estimated precision for major elements is ± 1% for SiO_2, $A1_2O_3$, Fe_2O_3, MgO, CaO, K_2O and TiO_2; ± 2% for MnO, Na_2O, P_2O_5 and S and ± 10% for Rb. Precision for trace elements is ± 15%. Minimum detectable concentrations is: Be 3 ppm; Yb 4 ppm; Ag, Ba and Cr 5 ppm; Cu 7 ppm; Ni, Co and Sr 10 ppm; V and Zr 20 ppm; Y 40 ppm; Mn, B and Mo 50 ppm; Ti and La 100 ppm; Ce, Zn and Sn 200 ppm; Sb 500 ppm; Pb ;700 ppm and As 2000 ppm. Ag, As, Be, Ce, La, Mo, Pb, Sb, Sn and Yb were below detectable limits in all samples analyzed. Only three samples showed detectable B.

Rock types sampled

The letter in sample numbers indicates rocks samples:

A — Kutcho Formation, Cry Lake map area

B — basic schist, Kutcho Formation, Cry Lake map area

C — Kutcho Formation in the Eaglehead area

D — rocks north of the Kutcho Fault, Cry Lake map area

E — Inklin Formation, Cry Lake map area

F — Stuhini Formation and unnamed Upper Triassic volcanic rocks, Cry Lake and Dease Lake map areas

G — Cache Creek Group, Cry Lake map area.

Abbreviations used in Appendix

Q — Quartz	WO — Wollastonite	CM — Chromite
C — Corundum	CPX — Clinopyroxene	HM — Hematite
OR — Orthoclase	OPX — Orthopyroxene	IL — Ilmenite
AB — Albite	FO — Forsterite	SP — Sphene
AN — Anorthite	FA — Fayalite	RU — Rutile
NE — Nepheline	MT — Magneite	AP — Apatite

Sample Number	A.1	A.2	A.3	A.4	A.5	A.6	A.7	A.8	A.9
SiO_2	50.60	78.90	50.00	45.60	47.60	51.40	74.10	48.80	72.10
Al_2O_3	18.60	11.60	19.70	12.40	14.90	13.80	12.60	16.40	10.00
Fe_2O_3	3.30	.80	5.40	2.20	2.30	4.90	-	2.70	.70
FeO	4.10	.10	3.00	8.10	7.40	5.60	3.30	6.70	.60
MgO	3.42	.14	3.96	13.60	6.56	4.03	2.13	9.30	.44
CaO	9.31	.06	8.81	8.35	7.25	10.70	.33	6.62	5.00
Na_2O	3.60	6.00	3.10	1.90	3.30	2.40	4.30	3.20	3.40
K_2O	.54	.10	1.89	-	.03	.10	.33	.01	1.51
TiO_2	1.08	.12	.74	1.17	1.66	1.62	.47	1.03	.18
P_2O_5	.28	-	.11	.10	.12	.18	.05	.08	.01
MnO	.21	.01	.19	.21	.25	.18	.07	.24	.03
CO_2	1.80	.10	.90	1.80	3.00	1.60	-	.50	3.80
H_2O	2.90	.70	2.90	3.80	4.70	2.50	2.40	4.60	1.00
Total	99.74	98.63	100.70	99.23	99.47	99.01	100.08	100.18	98.77
Ba	354	39.8	673	12.1	216	29.5	99.9	16.7	940
Co	13.1	<10	23.6	45.5	23.4	31.1	<10	39.8	10
Cr	<5	< 5	34	734	105	<5.1	<5	235	<5
Ni	<10	<10	<10	28.6	39.5	20.4	<10	89.2	<10
Cu	23.7	21.9	22.4	30.4	50.9	39.3	<7	<7	13
Zn	40	40	40	40	80	50	-	50	-
Rb	-	-	20	-	-	-	-	-	-
Sr	576	51.2	532	63.4	128	264	50.7	122	205
V	147	<20	310	190	324	347	32.3	331	26.4
Y	45	40.2	<40	<40	43.1	51.8	56.8	43	<40
Zr	117	204	86.9	60.2	64.4	89.2	114	69.8	46.5
F	400	200	400	300	300	300	300	600	200
Cl	200	200	100	200	100	100	200	100	100
S	-	-	-	-	4100	-	-	-	-
Q	4.46	44.24	2.14	.00	1.55	12.99	42.61	.00	41.28
C	.00	1.55	.00	.00	.00	.00	4.80	.00	.00
OR	3.36	.60	11.53	.00	.19	.62	2.00	.06	9.50
AB	32.05	51.89	27.07	17.16	29.97	21.40	37.25	28.47	30.62
AN	34.71	.30	35.34	27.00	27.63	28.00	1.34	31.91	8.05
NE	.00	.00	.00	.00	.00	.00	.00	.00	.00
WO	.00	.00	.00	.00	.00	.00	.00	.00	6.02
CPX	9.62	.00	7.03	13.23	8.20	21.45	.00	1.66	3.08
OPX	7.92	.36	7.10	22.27	22.76	4.36	10.97	28.08	.00
FO	.00	.00	.00	10.35	.00	.00	.00	2.41	.00
FA	.00	.00	.00	3.86	.00	.00	.00	1.01	.00
MT	5.03	.01	8.08	3.40	3.58	7.49	.00	4.12	1.08
CM	.00	.00	.00	.11	.02	.00	.00	.03	.00
HM	.00	.81	.00	.00	.00	.00	.00	.00	.00
IL	2.16	.23	1.45	2.37	3.38	3.24	.91	2.06	.36
SP	.00	.00	.00	.00	.00	.00	.00	.00	.00
RU	.00	.00	.00	.00	.00	.00	.00	.00	.00
AP	.69	.00	.26	.25	.30	.44	.12	.20	.02

Sample Number	A.10	A.11	A.12	A.13	A.14	A.15	A.16	A.17	A.18
SiO_2	64.00	63.30	69.00	68.40	52.90	59.50	52.10	74.00	46.90
Al_2O_3	13.00	14.90	13.50	12.90	15.00	16.10	14.30	13.10	16.40
Fe_2O_3	.10	.60	1.50	1.00	1.30	.50	1.30	2.90	1.50
FeO	5.10	3.90	2.20	3.30	3.90	2.60	4.50	.80	7.90
MgO	2.63	2.69	2.37	3.15	2.01	2.94	4.62	.14	8.55
CaO	2.13	4.06	4.61	1.54	6.89	3.37	9.91	.03	10.20
Na_2O	.80	2.40	1.90	2.40	1.90	.50	2.90	7.20	2.80
K_2O	3.42	2.10	1.01	.79	2.63	3.46	.44	.10	-
TiO_2	.48	.57	.32	.39	.33	.41	.47	.50	1.13
P_2O_5	.03	.07	.02	.03	.03	.05	.11	.05	.07
MnO	.07	.08	.04	.04	.32	.10	.45	.07	.14
CO_2	5.50	3.10	.30	1.40	10.40	6.60	5.70	.10	.10
$H_2O\pm$	2.30	2.70	2.20	3.90	2.40	2.70	3.40	.40	3.20
Total	99.56	100.47	98.97	99.24	100.01	98.83	100.20	99.39	98.89

Ba	848	705	292	128	713	230	115	31.2	29.3
Co	<10	11.8	24.2	<10	<10	<10	17.3	<10	27.8
Cr	<5	15.4	127	<5	140	<5	43	14.4	230
Ni	<10	10.1	427	<10	<10	<10	<10	<10	78.3
Cu	18.1	26.3	264	12.2	<7	<7	38.7	8.1	53.7
Zn	110	60	50	30	50	120	30	30	30
Rb	30	20	40	-	20	20	-	97	-
Sr	13.9	139	273	24.8	85.7	215	110	35.8	29
V	59.7	121	231	33.9	78.5	100	160	<20	247
Y	<40	42.8	<40	<40	<40	51.2	<40	<40	<40
Zr	1000	157	68.7	130	84.9	140	66.3	180	53.8
F	400	600	900	400	500	900	700	300	400
Cl	100	100	500	100	300	400	100	200	300
S	7500	500	-	-	-	700	-	-	-

Q	36.41	27.57	41.07	44.05	15.29	33.61	8.31	31.89	.00
C	4.40	1.54	.98	5.72	.00	6.15	.00	1.16	.00
OR	21.25	13.08	6.18	4.97	17.82	22.76	2.85	.60	.00
AB	7.12	21.40	16.66	21.62	18.43	4.71	26.94	61.62	24.78
AN	10.90	20.74	23.55	7.92	28.23	18.24	27.11	.00	33.65
NE	.00	.00	.00	.00	.00	.00	.00	.00	.00
WO	.00	.00	.00	.00	.00	.00	.00	.00	.00
CPX	.00	.00	.00	.00	8.93	.00	21.24	.00	15.25
OPX	14.32	13.14	8.61	13.32	8.31	12.30	10.23	.35	7.14
FO	.00	.00	.00	.00	.00	.00	.00	.00	9.02
FA	.00	.00	.00	.00	.00	.00	.00	.00	5.44
MT	.15	.92	2.25	1.54	2.16	.81	2.07	1.37	2.27
CM	.00	.00	.02	.00	.02	.00	.00	.00	.03
HM	.00	.00	.00	.00	.00	.00	.00	1.99	.00
IL	.96	1.14	.63	.79	.72	.87	.98	.96	2.24
SP	.00	.00	.00	.00	.00	.00	.00	.00	.00
RU	.00	.00	.00	.00	.00	.00	.00	.00	.00
AP	.07	.17	.05	.07	.08	.13	.28	.05	.17

Sample Number	A.19	A.20	A.21	A.22	A.23	A.24	A.25	A.26	A.27
SiO_2	49.10	53.60	41.80	58.60	87.10	92.30	48.50	42.90	72.20
Al_2O_3	13.80	18.80	17.80	12.00	.70	3.00	14.70	14.50	13.50
Fe_2O_3	1.20	5.10	3.20	.50	10.30	-	2.00	1.30	1.40
FeO	11.50	3.00	12.90	1.10	1.30	-	6.30	9.50	1.40
MgO	6.80	3.20	6.04	.87	.30	-	7.25	6.79	1.13
CaO	4.39	7.62	5.49	11.60	.05	3.39	8.04	7.59	2.33
Na_2O	1.30	4.00	3.20	4.60	-	-	3.00	3.10	5.10
K_2O	.45	1.14	.02	1.08	-	-	1.15	1.36	.47
TiO_2	2.23	.86	3.17	.24	-	-	1.41	3.14	.41
P_2O_5	.24	.17	.26	.07	.01	.01	.13	.44	.05
MnO	.22	.16	.25	.05	.01	-	.22	.21	.12
CO_2	1.50	-	-	9.00	-	2.70	1.60	3.50	.40
$H_2O\pm$	6.70	3.00	5.70	.30	.10	2.50	4.40	5.40	1.30
Total	99.43	100.65	99.83	100.01	99.87	103.90	98.70	99.73	99.81
Ba	269		43	40	190	190	137	379	90.2
Co	47.3		47.9	<10	<10	<10	30.2	26.4	<10
Cr	93.3		13.1	<5	<5	<5	66	79.4	<5
Ni	75		40.1	<10	<10	<10	72.7	12.4	<10
Cu	287		25.2	7.8	16.3	<7	75.2	15	<7
Zn	70		110	-	-	<200	60	90	<10
Rb	-		-	-	-	-	20	10	-
Sr	37.8		163	48.9	-	<10	151	359	167
V	429		582	34.8	<20	<20	260	250	35.6
Y	56.9		54.2	<40	<40	<40	<40	<40	<40
Zr	115		181	109	46.5	20	30.5	125	26.1
F	300		400	400	100	400	200	400	300
Cl	200		300	300	500	100	400	600	100
S	-		300	-	-	-	-	-	-
Q	14.55	6.89	.00	12.76	86.77	88.06	.00	.00	34.42
C	4.13	.00	3.35	.00	.63	.00	.00	.00	.49
OR	2.91	6.90	.13	7.04	.00	.00	7.33	8.85	2.83
AB	12.05	34.66	28.72	42.91	.00	.00	27.38	24.96	43.98
AN	22.14	30.69	27.08	9.81	.18	8.29	25.07	23.81	11.44
NE	.00	.00	.00	.00	.00	.00	.00	2.12	.00
WO	.00	.00	.00	18.15	.00	3.62	.00	.00	.00
CPX	.00	5.37	.00	7.85	.00	.00	13.74	11.82	.00
OPX	37.04	5.84	15.74	.00	.75	.00	16.61	.00	3.85
FO	.00	.00	5.87	.00	.00	.00	2.36	10.64	.00
FA	.00	.00	6.98	.00	.00	.00	1.15	8.02	.00
MT	1.91	7.57	4.92	.80	4.23	.00	3.13	2.07	2.07
CM	.02	.00	.00	.00	.00	.00	.02	.02	.00
HM	.00	.00	.00	.00	7.40	.00	.00	.00	.00
IL	4.64	1.67	6.39	.50	.00	.00	2.89	6.56	.79
SP	.00	.00	.00	.00	.00	.00	.00	.00	.00
RU	.00	.00	.00	.00	.00	.00	.00	.00	.00
AP	.61	.41	.64	.18	.02	.02	.33	1.13	.12

Sample Number	A.28	A.29	A.30	A.31	A.32	A.33	A.34	A.35	A.36
SiO_2	61.10	36.80	71.60	47.20	68.50	82.50	50.10	45.50	78.00
Al_2O_3	15.70	14.80	14.20	15.50	13.50	10.10	14.80	18.50	11.70
Fe_2O_3	1.50	1.30	.90	1.30	1.20	-	5.20	2.40	.20
FeO	2.50	7.70	2.30	9.90	3.80	.20	3.60	7.60	.70
MgO	1.97	6.90	.94	16.20	2.88	.34	5.51	9.26	.52
CaO	4.29	14.00	2.51	-	1.66	.01	12.80	7.45	-
Na_2O	4.00	3.50	5.70	-	3.90	5.20	1.80	3.00	6.30
K_2O	1.69	.06	.10	-	.28	.08	.02	.22	.03
TiO_2	.56	1.12	.42	1.10	.64	.17	.90	.90	.17
P_2O_5	.16	.10	.06	.08	.12	.01	.11	.08	.01
MnO	.09	.23	.03	.20	.19	-	.25	.20	.01
CO_2	3.20	9.10	-	.50	.60	-	2.20	-	-
$H_2O\pm$	2.90	4.60	1.10	8.40	2.60	.50	3.40	5.20	.70
Total	99.66	100.21	99.95	100.39	99.87	99.11	100.69	100.31	98.34
Ba	1690	316	316	8.4	343	38.8		30.4	18.8
Co	12.8	<10	<10	43.8	<10	<10		40.4	<10
Cr	14.8	<5	<5	32.9	<5	<5		146	<5
Ni	<10	<10	<10	117	<10	<10		69.7	<10
Cu	8.2	7.7	7.7	326	55.7	<7		178	<7
Zn	40	-	-	371	40	-		130	-
Rb	50	-	-	-	-	-		-	-
Sr	353	132	132	185	54.1	14.5		87.8	33.6
V	94.8	43.9	43.9	283	42.7	<20		353	<20
Y	<40	<40	<40	<40	<40	<40		<40	<40
Zr	135	<20	<20	385	498	<20		<20	49.7
F	400	200	200	200	300	200		300	200
Cl	200	100	100	800	300	200		200	200
S	-	900	900	400	-	-		-	-
Q	19.86	.00	30.50	17.42	36.03	52.13	10.76	.00	41.05
C	.00	.00	.30	16.92	4.19	1.48	.00	.00	1.34
OR	10.67	.00	.60	.00	1.71	.48	.12	1.37	.18
AB	36.18	.00	48.64	.00	34.14	44.62	16.02	26.69	54.60
AN	21.26	28.18	12.16	.00	7.70	.00	33.90	38.21	.00
NE	.00	18.46	.00	.00	.00	.00	.00	.00	.00
WO	.00	.00	.00	.00	.00	.00	.00	.00	.00
CPX	.30	29.69	.00	.00	.00	.00	25.24	.06	.00
OPX	7.87	.00	5.04	61.08	12.88	.95	3.96	8.01	2.21
FO	.00	7.76	.00	.00	.00	.00	.00	13.16	.00
FA	.00	5.70	.00	.00	.00	.00	.00	6.83	.00
MT	2.32	2.17	1.32	2.06	1.80	.00	7.93	3.66	.30
CM	.00	.00	.00	.00	.00	.00	.00	.02	.00
HM	.00	.00	.00	.00	.00	.00	.00	.00	.00
IL	1.14	2.45	.80	2.28	1.26	.33	1.80	1.80	.33
SP	.00	.00	.00	.00	.00	.00	.00	.00	.00
RU	.00	.00	.00	.00	.00	.00	.00	.00	.00
AP	.40	.27	.14	.00	.29	.02	.27	.20	.00

(*) Data from Panteleyev (pers. comm. 1977); trace element data not available

Sample Number	A.37	A.38	A.39	A.40	A.41*	A.42*	A.43*	A.44*	A.45*
SiO_2	53.30	71.20	49.80	45.20	69.22	68.79	70.96	76.54	52.08
Al_2O_3	14.50	12.30	15.70	12.30	13.83	12.56	12.86	12.47	15.69
Fe_2O_3	4.60	1.10	2.30	1.50	1.65	1.78	1.02	.16	6.02
FeO	8.50	3.00	6.50	8.40	2.40	2.70	3.34	.97	5.50
MgO	6.55	2.15	7.95	14.70	2.15	2.18	2.42	1.41	3.98
CaO	5.89	1.05	8.77	8.59	2.83	1.99	.91	.16	9.16
Na_2O	.30	4.00	3.80	1.60	2.83	3.19	3.78	6.37	.82
K_2O	.04	.66	.04	.58	1.57	2.28	1.07	.13	.36
TiO_2	.59	.56	1.15	1.05	.38	.60	.58	.33	.66
P_2O_5	.02	.09	.06	.07	.32	.34	.15	.27	.57
MnO	.17	.13	.15	.20	.05	.15	.14	.03	.18
CO_2	-	.10	.10	.30	.23	.90	.06	.06	.16
$H_2O\pm$	4.40	2.00	3.50	5.80	2.42	2.00	1.67	.82	3.00
Total	98.86	98.34	99.82	100.29	99.88	99.46	98.96	99.72	98.18
Ba	24.5	60.7	40.1	42.7					
Co	52.5	<10	35.2	43.9					
Cr	19.2	<5	186	217					
Ni	28.6	<10	66	74.7					
Cu	10.5	17.6	89.2	102					
Zn	30	80	50	50					
Rb	-	-	-	10					
Sr	226	59.3	101	108					
V	348	26.5	276	307					
Y	63	<40	<40	<40					
Zr	<20	54.8	<20	29.2					
F	300	200	400	300					
Cl	200	200	200	100					
S	-	-	-	-					
Q	25.41	39.93	.00	.00	38.30	34.89	38.73	36.84	21.87
C	3.50	3.44	.00	.00	3.18	2.11	4.31	1.87	.00
OR	.25	4.05	.25	3.64	9.54	13.95	6.50	.78	2.24
AB	2.69	35.17	33.41	14.37	24.63	27.95	32.89	54.61	7.30
AN	30.79	4.80	26.66	26.17	12.28	7.92	3.63	.00	40.05
NE	.00	.00	.00	.00	.00	.00	.00	.00	.00
WO	.00	.00	.00	.00	.00	.00	.00	.00	.00
CPX	.00	.00	14.62	14.89	.00	.00	.00	.00	3.10
OPX	29.08	9.63	11.10	13.16	8.09	8.50	10.92	4.73	13.54
FO	.00	.00	5.50	16.69	.00	.00	.00	.00	.00
FA	.00	.00	2.57	6.44	.00	.00	.00	.00	.00
MT	7.06	1.66	3.46	2.31	2.46	2.67	1.52	.24	9.19
CM	.00	.00	.03	.03	.00	.00	.00	.00	.00
HM	.00	.00	.00	.00	.00	.00	.00	.00	.00
IL	1.19	1.11	2.27	2.12	.74	1.18	1.13	.63	1.32
SP	.00	.00	.00	.00	.00	.00	.00	.00	.00
RU	.00	.00	.00	.00	.00	.00	.00	.00	.00
AP	.05	.22	.15	.17	.77	.82	.36	.29	1.40

Sample Number	A.46*	A.47*	A.48*	A.49*	A.50*	A.51*	A.52*	A.53*	A.54*
SiO_2	79.86	73.64	50.87	73.90	73.85	72.57	67.38	75.70	65.28
Al_2O_3	11.41	13.33	14.02	12.26	11.40	12.20	11.30	12.05	14.75
Fe_2O_3	.25	.60	3.79	1.42	1.03	1.64	2.02	2.01	1.30
FeO	.63	2.39	8.73	.15	1.62	.86	1.31	.87	4.27
MgO	.31	1.23	5.79	.22	1.47	1.05	4.42	.83	2.41
CaO	.11	.52	6.83	2.53	1.48	2.26	1.57	4.59	2.85
Na_2O	6.20	5.79	4.00	4.25	2.90	3.13	1.25	3.26	5.56
K_2O	.09	.21	.09	1.42	1.52	1.45	.76	.39	.14
TiO_2	.19	.56	1.61	.31	.29	.33	.26	.25	.63
P_2O_5	.21	.25	.30	.25	.15	.15	.15	.17	.16
MnO	.01	.06	.22	.03	.05	.05	.09	.04	.10
CO_2	.06	.19	.26	2.37	1.42	3.21	6.37	.40	.70
$H_2O\pm$	.64	1.58	.88	.55	1.91	1.93	2.09	.82	2.31
Total	99.97	100.35	97.39	99.66	99.09	100.83	98.97	101.38	100.46
Q	43.06	36.03	2.66	40.17	47.45	44.76	52.43	45.57	21.00
C	1.12	3.28	.00	.00	2.77	1.81	6.55	.00	.67
OR	.54	1.26	.55	8.67	9.38	8.95	4.96	2.30	.85
AB	52.91	49.69	35.16	37.17	25.62	27.68	11.69	27.54	48.28
AN	.00	.96	20.81	10.52	6.64	10.69	7.52	17.06	13.43
NE	.00	.00	.00	.00	.00	.00	.00	.00	.00
WO	.00	.00	.00	.00	.00	.00	.00	.00	.00
CPX	.00	.00	10.12	.29	.00	.00	.00	3.55	.00
OPX	1.44	6.23	21.09	.43	5.64	2.73	12.69	.42	12.23
FO	.00	.00	.00	.00	.00	.00	.00	.00	.00
FA	.00	.00	.00	.00	.00	.00	.00	.00	.00
MT	.37	.88	5.71	.00	1.56	2.07	3.24	2.21	1.93
CM	.00	.00	.00	.00	.00	.00	.00	.00	.00
HM	.00	.00	.00	1.47	.00	.29	.00	.49	.00
IL	.36	1.08	3.18	.39	.58	.65	.55	.47	1.23
SP	.00	.00	.00	.28	.00	.00	.00	.00	.00
RU	.00	.00	.00	.00	.00	.00	.00	.00	.00
AP	.20	.59	.73	.60	.37	.37	.39	.40	.38

Sample Number	A.55*	A.56*	B.1	B.2	B.3	B.4	B.5
SiO_2	61.38	65.12	49.20	51.20	48.30	47.20	51.60
Al_2O_3	15.88	14.80	13.70	14.70	16.40	14.80	17.60
Fe_2O_3	1.42	2.06	2.10	3.70	3.50	2.50	1.80
FeO	4.89	2.99	5.80	4.80	5.10	6.40	6.10
MgO	3.72	2.97	5.23	5.15	5.49	6.50	3.50
CaO	4.32	3.76	7.50	7.83	4.22	6.65	4.78
Na_2O	1.89	4.29	2.80	3.00	2.40	2.60	3.60
K_2O	1.53	.11	2.72	1.96	3.54	1.48	3.51
TiO_2	.65	.40	.60	.62	.71	.72	.69
P_2O_5	.15	.15	.79	.82	.86	.90	.64
MnO	.10	.21	.17	.17	.12	.19	.22
CO_2	.40	.22	5.00	3.10	3.80	4.30	2.40
$H_2O\pm$	3.82	2.57	3.70	3.50	4.30	5.30	4.00
Total	100.15	99.65	99.31	100.55	98.74	99.54	100.44
Ba			700	170	560	241	875
Co			28	<10	16.7	24.9	18.7
Cr			98.8	<5	78.4	96.3	<5
Ni			40.6	<10	27.2	90.3	<10
Cu			159	16.5	307	268	206
Zn			70	10	70	90	80
Rb			50	0	70	-	60
Sr			312	228	195	321	292
V			209	37.9	234	229	179
Y			<40	51.8	<40	<40	<40
Zr			82.3	136	66.4	81.4	96.3
F			500	600	800	900	600
Cl			200	400	300	200	400
S			-	-	-	-	-
Q	28.15	26.93	.46	4.83	3.84	1.76	.00
C	3.77	1.18	.00	.00	3.32	.00	.77
OR	9.43	.67	17.74	12.33	23.08	9.72	22.06
AB	16.67	37.48	26.14	27.02	22.40	24.45	32.39
AN	21.31	18.24	18.51	22.19	16.89	27.05	20.76
NE	.00	.00	.00	.00	.00	.00	.00
WO	.00	.00	.00	.00	.00	.00	.00
CPX	.00	.00	13.73	10.81	.00	2.50	.00
OPX	16.87	11.27	16.76	13.82	21.16	26.63	16.74
FO	.00	.00	.00	.00	.00	.00	.72
FA	.00	.00	.00	.00	.00	.00	.81
MT	2.15	3.08	3.36	5.71	5.60	4.03	2.77
CM	.00	.00	.02	.00	.02	.02	.00
HM	.00	.00	.00	.00	.00	.00	.00
IL	1.29	.78	1.26	1.25	1.49	1.52	1.39
SP	.00	.00	.00	.00	.00	.00	.00
RU	.00	.00	.00	.00	.00	.00	.00
AP	.36	.36	2.03	2.03	2.21	2.33	1.59

Sample Number	B.6	B.7	B.8	B.9	B.10*	B.11	B.12	B.13	B.14
SiO_2	46.00	48.50	53.50	50.60	53.00	50.20	50.80	51.10	48.50
Al_2O_3	15.20	13.70	17.80	16.30	17.30	16.30	15.60	17.50	14.00
Fe_2O_3	1.50	.90	2.00	3.50	2.80	3.20	2.10	3.80	2.80
FeO	7.20	6.80	4.20	4.50	4.50	6.70	6.00	4.40	7.50
MgO	5.45	4.77	2.84	3.09	3.66	5.04	4.78	3.31	6.44
CaO	7.31	7.01	3.79	8.04	5.55	8.05	6.67	6.81	7.97
Na_2O	1.20	2.50	2.60	3.40	4.50	2.20	2.90	2.80	1.60
K_2O	3.57	3.51	5.32	3.00	2.96	3.58	3.80	3.91	4.30
TiO_2	.71	.64	.59	.61	.62	.69	.64	.64	.73
P_2O_5	.65	.79	.69	.82	.79	.68	.64	.87	.87
MnO	.18	.18	.08	.18	.17	.16	.16	.15	.19
CO_2	7.40	8.80	2.60	2.40	2.40	.60	3.40	1.20	2.00
H_2O+	4.20	2.50	3.10	2.20	2.30	2.90	3.00	2.30	2.90
Total	100.60	100.60	99.11	98.87	100.55	100.30	100.49	98.79	99.80
Ba	608	559	893	556	536	491	462	890	679
Co	28.1	19.8	<10	22.4	11.9	29.1	27.2	25.2	28.6
Cr	56.9	82.7	<5	13.9	9.5	48	38.9	23	92.7
Ni	17.1	16.8	<10	10.5	<10	24.9	14.6	12.8	16
Cu	318	282	15.7	273	346	157	175	400	171
Zn	60	110	80	50	70	80	60	120	70
Rb	-	100	50	40	50	90	110	100	90
Sr	341	445	368	1160	727	618	620	757	469
V	264	164	116	197	117	246	209	205	267
Y	<40	<40	<40	<40	<40	<40	<40	<40	<40
Zr	20	20	60.9	104	61.5	224	24.1	46	20
F	400	600	700	600	300	800	700	700	200
Cl	200	100	200	100	700	100	300	200	600
S	300	300	-	1300	-	-	-	-	-
Q	.00	.00	5.60	.83	.00	.00	.00	1.94	.00
C	.00	.00	2.70	.00	.00	.00	.00	.00	.00
OR	23.67	23.65	33.65	18.71	18.25	21.85	23.87	24.25	26.77
AB	11.39	17.65	23.55	30.37	39.72	19.23	26.08	24.86	14.26
AN	28.65	17.65	15.30	21.48	19.05	24.81	19.47	24.79	19.29
NE	.00	.00	.00	.00	.00	.00	.00	.00	.00
WO	.00	.00	.00	.00	.00	.00	.00	.00	.00
CPX	5.97	12.75	.00	12.18	3.48	9.69	9.20	3.79	13.36
OPX	23.72	13.43	13.17	7.06	9.02	14.74	10.04	11.18	10.05
FO	.38	2.11	.00	.00	1.90	1.07	2.92	.00	4.85
FA	.35	2.15	.00	.00	1.20	.82	2.31	.00	3.53
MT	2.44	1.46	3.10	5.36	4.23	4.79	3.24	5.78	4.28
CM	.02	.02	.00	.00	.00	.00	.00	.00	.02
HM	.00	.00	.00	.00	.00	.00	.00	.00	.00
IL	1.51	1.36	1.20	1.22	1.23	1.35	1.29	1.28	1.46
SP	.00	.00	.00	.00	.00	.00	.00	.00	.00
RU	.00	.00	.00	.00	.00	.00	.00	.00	.00
AP	1.70	2.06	1.72	2.02	1.92	1.48	1.59	2.13	2.14

Sample Number	B.15*	B.16*	B.17	B.18	C.1	C.2	C.3	C.4
SiO_2	50.95	52.03	46.10	54.50	70.30	61.60	50.20	51.60
Al_2O_3	13.16	13.58	14.10	16.20	16.50	16.50	16.40	16.30
Fe_2O_3	3.17	3.58	5.40	.40	1.00	1.80	1.70	1.60
FeO	6.21	5.22	4.70	5.70	.30	.20	6.00	6.30
MgO	6.30	5.93	5.41	4.17	.37	.46	6.85	4.50
CaO	5.12	7.05	1.20	2.70	2.39	12.30	7.62	4.90
Na_2O	3.23	3.52	-	2.50	5.90	2.30	3.20	4.70
K_2O	3.25	3.83	4.05	5.34	1.35	.45	1.33	.82
TiO_2	.73	.73	.78	.64	.15	.16	1.53	1.89
P_2O_5	.87	.85	.98	.69	.03	.05	.38	.45
MnO	.18	.21	.17	.07	.06	.05	.14	.13
CO_2	3.33	.06	6.50	4.20	.90	7.00	1.00	2.10
$H_2O\pm$	2.43	1.81	4.80	2.50	1.00	2.30	2.90	4.00
Total	98.93	98.40	94.19	99.61	100.25	105.17	99.25	99.29
Ba			1230	723	2020	1570	475	424
Co			46.3	11.7	<10	<10	22.8	24.8
Cr			232	41.7	<5	<5	17.5	23.4
Ni			808	23.9	<10	<10	73.4	41.9
Cu			238	95.6	9.0	<7	30.7	36.7
Zn			80	120	10	-	60	60
Rb			30	140	30	-	40	20
Sr			291	139	903	306	374	359
V			305	206	<20	44.2	138	153
Y			54.1	<40	<40	<40	<40	<40
Zr			85.1	34.7	67.7	<20	104	187
F			100	900	300	400	600	700
Cl			300	200	200	200	300	200
S			-	370	100	-	200	400
Q	.00	.00	25.35	5.71	25.64	26.60	.00	2.10
C	.00	.00	11.72	3.28	1.08	.00	.00	.00
OR	20.61	23.44	28.86	33.90	8.11	2.77	8.23	5.19
AB	29.33	30.85	.00	22.72	50.74	20.30	28.37	42.59
AN	12.67	10.30	.00	9.54	11.85	34.80	27.71	22.44
NE	.00	.00	.00	.00	.00	.00	.00	.00
WO	.00	.00	.00	.00	.00	10.52	.00	.00
CPX	6.87	16.23	.00	.00	.00	2.58	7.49	.36
OPX	21.71	2.06	20.25	20.96	.94	.00	20.48	19.63
FO	.14	5.76	.00	.00	.00	.00	.71	.00
FA	.08	2.50	.00	.00	.00	.00	.34	.00
MT	4.93	5.38	9.44	.62	.70	.36	2.58	2.48
CM	.00	.00	.04	.00	.00	.00	.00	.00
HM	.00	.00	.00	.00	.53	1.63	.00	.00
IL	1.49	1.44	1.79	1.31	.29	.32	3.04	3.84
SP	.00	.00	.00	.00	.00	.00	.00	.00
RU	.00	.00	.00	.00	.00	.00	.00	.00
AP	2.18	2.05	2.56	1.73	.07	.12	.93	1.12

Sample Number	C.5	C.6	D.1	D.2	D.3	D.4	D.5	D.6
SiO_2	65.10	66.10	81.00	65.00	81.20	69.30	64.20	74.40
Al_2O_3	13.90	15.50	2.40	13.00	1.90	16.50	15.20	14.90
Fe_2O_3	.30	.80	.80	2.00	.60	1.00	1.60	.60
FeO	1.10	1.50	2.68	2.00	.10	.90	1.50	.20
MgO	.73	.76	2.68	2.00	.84	.75	1.18	.15
CaO	6.12	2.55	5.77	2.00	7.25	.61	3.95	.52
Na_2O	5.70	.41	-	2.00	-	4.00	2.90	4.20
K_2O	1.09	2.70	.13	.20	.51	3.43	3.56	3.13
TiO_2	.26	.27	.10	.50	.08	.26	.39	.03
P_2O_5	.09	.08	-	.10	-	.07	.11	-
MnO	.03	.04	.23	.10	.19	.03	.05	.08
CO_2	4.10	2.80	4.70	-	6.40	.50	2.60	.30
$H_2O\pm$	.90	1.60	1.40	2.40	1.00	1.50	2.00	.80
Total	98.61	95.11	101.89	91.30	100.07	98.85	99.24	99.31
Ba	654	1800	577	1150	1310	1250	1490	262
Co	<10	<10	<10	<10	<10	<10	<10	<10
Cr	<5	<5	<5	<5	<5	<5	<5	<5
Ni	<10	<10	<10	<10	10.7	<10	<10	<10
Cu	9.2	19.9	119	50.3	41.9	9.0	7.8	12.1
Zn	-	20	10	-	-	30	60	20
Rb	-	90	-	-	-	130	130	250
Sr	459	383	187	134	183	310	563	92.1
V	313	40.1	<20	121	<20	38.9	91.8	<20
Y	<40	<40	<40	<40	<40	<40	<40	<40
Zr	109	39	56	166	51.1	146	212	46.6
F	200	400	200	300	300	600	600	500
Cl	100	400	100	100	200	200	100	100
S	-	-	-	-	-	-	-	-
Q	18.70	50.96	69.88	50.61	74.93	31.47	24.93	37.32
C	.00	8.22	.00	6.86	.00	5.44	.00	3.72
OR	6.82	17.59	.80	1.33	3.25	20.93	22.23	18.83
AB	51.08	3.82	.00	19.04	.00	34.95	25.93	36.18
AN	9.66	13.37	6.43	10.42	3.97	2.65	18.95	2.63
NE	.00	.00	.00	.00	.00	.00	.00	.00
WO	5.60	.00	.00	.00	11.94	.00	.00	.00
CPX	6.94	.00	19.15	.00	4.87	.00	.79	.00
OPX	.00	3.99	2.32	7.16	.00	2.40	3.66	.38
FO	.00	.00	.00	.00	.00	.00	.00	.00
FA	.00	.00	.00	.00	.00	.00	.00	.00
MT	.46	1.28	1.21	3.26	.77	1.50	2.45	.83
CM	.00	.00	.00	.00	.00	.00	.00	.00
HM	.00	.00	.00	.00	.12	.00	.00	.04
IL	.52	.57	.20	1.07	.16	.51	.78	.06
SP	.00	.00	.00	.00	.00	.00	.00	.00
RU	.00	.00	.00	.00	.00	.00	.00	.00
AP	.22	.21	.00	.26	.00	.17	.27	.00

Sample Number	D.7	D.8	D.9	D.10	E.1	E.2
SiO_2	81.50	68.50	70.10	76.70	78.20	60.30
Al_2O_3	4.30	16.50	16.30	13.20	12.90	16.40
Fe_2O_3	.60	1.40	1.60	.60	.30	4.10
FeO	1.00	1.00	2.00	-	-	2.60
MgO	.38	.10	.30	.03	.43	2.73
CaO	5.01	2.48	1.09	-	.02	5.49
Na_2O	.10	5.00	5.80	5.50	5.00	2.80
K_2O	1.20	1.27	1.67	1.14	1.52	1.95
TiO_2	.47	.30	.25	.02	.06	.74
P_2O_5	.08	.09	.05	-	-	.19
MnO	.04	.16	.05	.05	.01	.14
CO_2	4.40	.20	.70	-	-	.10
$H_2O\pm$	1.10	1.20	1.20	.09	1.60	2.50
Total	100.18	98.20	101.11	97.33	100.04	100.04
Ba	311	1470	1260	172	682	742
Co	<10	<10	<10	<10	<10	<10
Cr	11.5	<5	<5	<5	<5	<5
Ni	<10	<10	<10	<10	<10	<10
Cu	11.2	20.4	<7	<7	<7	34
Zn	0	50	20	60	-	50
Rb	200	20	20	90	-	30
Sr	282	807	608	132	457	521
V	20	43.1	29.8	<20	24.5	143
Y	<40	<40	<40	<40	<40	<40
Zr	150	90	92.7	<20	48.7	114
F	300	400	400	200	200	700
Cl	200	100	200	200	400	200
S	600	-	-	200	-	-
Q	72.25	30.09	26.62	41.41	43.29	21.62
C	.00	2.69	3.11	3.00	3.04	.16
OR	7.47	7.75	9.95	6.92	9.12	11.83
AB	.89	43.71	49.47	47.81	42.98	24.32
AN	8.15	12.10	5.12	.00	.10	26.67
NE	.00	.00	.00	.00	.00	.00
WO	5.66	.00	.00	.00	.00	.00
CPX	3.17	.00	.00	.00	.00	.00
OPX	.00	.76	2.80	.08	1.09	7.41
FO	.00	.00	.00	.00	.00	.00
FA	.00	.00	.00	.00	.00	.00
MT	.92	2.10	2.34	.03	.00	6.10
CM	.00	.00	.00	.00	.00	.00
HM	.00	.00	.00	.59	.30	.00
IL	.94	.59	.48	.04	.02	1.44
SP	.00	.00	.00	.00	.00	.00
RU	.00	.00	.00	.00	.05	.00
AP	.20	.22	.12	.00	.00	.45

Sample Number	F.1	F.2	F.3	F.4	F.5	F.6
SiO_2	47.80	49.80	55.80	53.00	49.50	47.40
Al_2O_3	12.50	17.80	17.40	15.00	18.00	11.50
Fe_2O_3	1.30	1.70	1.10	1.00	3.80	1.90
FeO	6.80	6.40	5.50	6.90	6.30	9.20
MgO	13.30	3.90	.38	5.00	4.34	12.90
CaO	12.00	13.40	6.60	5.00	8.50	8.12
Na_2O	.80	1.80	5.40	3.00	2.80	1.10
K_2O	.74	.17	.76	.60	1.16	3.69
TiO_2	.61	.98	.83	.90	1.17	.52
P_2O_5	.08	.14	.13	.10	.26	.49
MnO	.15	.19	.14	.20	.19	.19
CO_2	-	-	-	.50	-	-
$H_2O\pm$	4.00	3.00	2.40	3.40	3.00	2.60
Total	100.08	99.28	96.44	94.60	99.02	99.62

Ba	357	112	254	337	347	622
Co	436	13.1	13.6	<10	21.9	70.2
Cr	1110	130	<5	170	5.5	9.7
Ni	246	42.7	<10	80.7	<10	25.6
Cu	61.7	8.6	38.7	<7	54.1	17.1
Zn	20	60	30	0	90	110
Rb	-	-	-	-	-	80
Sr	267	228	504	460	518	236
V	254	328	240	173	256	241
Y	<40	<40	<40	<40	<40	<40
Zr	72.9	86.1	75.7	93.2	<20	<20
F	400	300	300	200	300	1300
Cl	200	100	200	200	400	300
S	-	-	1500	-	-	100

Q	.00	6.17	6.29	11.56	3.43	.00
C	.00	.00	.00	.62	.00	.00
OR	4.55	1.04	4.74	3.91	7.14	22.47
AB	7.04	15.82	48.24	27.98	24.67	9.59
AN	29.44	41.52	22.16	26.61	34.48	16.01
NE	.00	.00	.00	.00	.00	.00
WO	.00	.00	.00	.00	.00	.00
CPX	25.53	21.93	10.08	.00	6.24	17.92
OPX	22.11	8.68	3.93	25.55	15.35	.78
FO	6.28	.00	.00	.00	.00	18.67
FA	2.22	.00	.00	.00	.00	9.48
MT	1.96	2.56	1.68	1.60	5.74	2.84
CM	.17	.02	.00	.03	.00	.00
HM	.00	.00	.00	.00	.00	.00
IL	1.20	1.93	1.66	1.88	2.31	1.02
SP	.00	.00	.00	.00	.00	.00
RU	.00	.00	.00	.00	.00	.00
AP	.19	.34	.32	.26	.63	1.18

Sample Number	G.1	G.2	G.3	G.4	G.5	G.6	G.7	G.8
SiO_2	51.00	49.30	57.10	55.40	54.30	53.50	54.20	48.60
Al_2O_3	13.00	15.80	14.90	13.00	12.80	13.50	16.60	14.90
Fe_2O_3	2.00	4.50	3.50	1.60	.80	3.30	1.50	1.70
FeO	7.90	5.90	5.50	5.20	6.90	4.40	5.10	7.90
MgO	12.00	5.72	5.47	8.83	8.92	5.22	6.40	9.06
CaO	4.00	10.60	7.39	10.80	6.39	10.90	5.07	9.76
Na_2O	2.00	1.50	2.60	.90	4.70	1.40	5.90	1.60
K_2O	-	.32	.04	.06	.02	.40	.03	1.67
TiO_2	.30	2.19	.49	.48	1.40	.38	.50	.38
P_2O_5	.05	.25	.02	.01	.08	.04	.02	-
MnO	.02	.13	.09	.11	.18	.12	.15	.18
CO_2	-	-	-	-	-	4.20	.40	.90
$H_2O\pm$	5.60	3.80	2.30	3.40	2.60	3.40	3.30	4.20
Total	97.87	100.01	99.40	99.79	99.09	100.76	99.17	100.85

Ba	14.7	118	292	241	13.3	198	6.9	304
Co	37.3	374	30.8	17.3	36.9	18.5	23.4	53.3
Cr	726	708	70.4	210	115	286	51	272
Ni	282	90.3	52.9	98.8	80	75.5	5.9	111
Cu	461	43	15.6	21.5	60.4	43.2	7.3	110
Zn	-	90	-	-	70	26	-	50
Rb	-	-	-	-	-	-	-	50
Sr	41.3	321	56.1	35	25.5	246	41.6	791
V	276	251	339	205	233	189	181	234
Y	<40	55.2	<40	<40	<40	<40	<40	<40
Zr	54	159	64.6	34	141	44.3	41.8	20
F	200	300	100	100	300	200	200	200
Cl	100	200	200	200	200	500	200	100
S	-	-	-	-	-	-	-	-

Q	8.02	10.89	17.05	15.55	.00	16.99	.00	.00
C	2.77	.00	.00	.00	.00	.00	.00	.00
OR	.00	1.96	.24	.37	.12	2.54	.19	10.30
AB	18.32	13.18	22.65	7.90	41.21	12.71	52.29	14.13
AN	21.12	36.79	29.72	32.41	14.26	31.51	19.60	29.79
NE	.00	.00	.00	.00	.00	.00	.00	.00
WO	.00	.00	.00	.00	.00	.00	.00	.00
CPX	.00	12.85	6.38	18.52	14.56	21.08	5.33	16.86
OPX	45.77	12.52	17.71	21.85	23.82	9.12	11.95	17.08
FO	.00	.00	.00	.00	1.24	.00	4.80	5.21
FA	.00	.00	.00	.00	.62	.00	2.51	3.26
MT	3.14	6.78	5.23	2.41	1.20	5.13	2.28	2.57
CM	.11	.11	.02	.03	.02	.05	.02	.05
HM	.00	.00	.00	.00	.00	.00	.00	.00
IL	.62	4.32	.96	.95	2.75	.77	.99	.75
SP	.00	.00	.00	.00	.00	.00	.00	.00
RU	.00	.00	.00	.00	.00	.00	.00	.00
AP	.13	.61	.05	.02	.19	.10	.05	.00

APPENDIX 2

Location, Stratigraphic Unit, Field Name and Irvine-Barager Name (classification after Irvine and Baragar, 1971) for rocks from north-central British Columbia

Letters in sample numbers indicate rocks sampled and are as described in Appendix 1.

Sample Number	Lat.(N.)/ Long.(W.)	Stratigraphic Rock Unit	Field Name	Irvine-Baragar Name
A.1	58° 13'/ 129° 07'	Tuff and Argillite	Chlorite-feldspar schist	Calc-alkaline Basalt, High Al
A.2	58° 14'/ 129° 00'	Silicic Schist	Quartz-eye-sericite schist	Calc-alkaline Rhyolite, K-poor
A.3	58° 11'/ 128° 50'	Tuff and Argillite	Chlorite-feldspar-epidote schist	Calc-alkaline Basalt, K-rich, High Al
A.4	58° 11'/ 128° 50'	Tuff and Argillite	Chlorite-feldspar-epidote schist	Tholeiitic Basalt, K-poor
A.5	58° 07'/ 128° 20'	Tuff and Argillite	Calcareous tuff	Tholeiitic Andesite, K-poor
A.6	58° 09'/ 128° 23'	Basic to Intermediate Tuff-Breccia	Chlorite-feldspar-epidote schist	Tholeiitic Basalt
A.7	58° 07'/ 128° 20'	Silicic Shist	Quartz-eye-feldspar-chlorite-sericite schist	Calc-alkaline Rhyolite, K-poor
A.8	58° 14'/ 129° 00'	Silicic Schist	Chlorite-feldspar schist with epidote clots	Calc-alkaline Basalt, K-poor, High Al
A.9	58° 23'/ 129° 30'	Conglomerate	Matrix of conglomerate quartz-feldspar-sericite schist	Calc-alkaline Basalt, K-poor
A.10	58° 12'/ 128° 24'	Silicic Schist	Quartz-eye-sericite schist	Calc-alkaline Rhyolite, K-rich
A.11	58° 12'/ 128° 24'	Silicic Schist	Quartz-feldspar-chlorite-sericite schist	Calc-alkaline Rhyolite, K-poor
A.12	58° 11'/ 128° 20"	Silicic Schist	Feldspar-quartz-eye-sericite-chlorite schist	Tholeiitic Andesite, K-rich
A.13	58° 12'/ 128° 24'	Silicic Schist	Quartz-eye-feldspar-sericite schist	Calc-alkaline Rhyolite, K-poor
A.14	58° 11'/ 128° 20'	Silicic Schist	Quartz-eye-sericite schist	Calc-alkaline Rhyolite
A.15	58° 11'/ 128° 20'	Silicic Schist	Quartz-eye-sericite schist	Calc-alkaline Rhyolite, K-rich
A.16	58° 11'/ 128° 20'	Breccia	Feldspar-chlorite-sericite schist	Calc-alkaline Andesite, K-poor, High Al
A.17	58° 11'/ 128° 20'	Tuff and Argillite	Silicic tuff	Tholeiitic Rhyolite
A.18	58° 11'/ 128° 20'	Tuff and Argillite	Chlorite Schist	Calc-alkaline Basalt, K-poor, High Al
A.19	58° 12'/ 129° 13'	Tuff and Argillite	Feldspar-chlorite-sericite schist	Tholeiitic Basalt
A.20	58° 14'/ 129° 02'	Tuff and Argillite	Feldspar-chlorite schist	Calc-alkaline Andesite, High Al

Sample Number	Lat.(N.)/ Long.(W.)	Stratigraphic Rock Unit	Field Name	Irvine-Baragar Name
A.21	58° 08'/ 128° 27'	Basic to inter- mediate Tuff- Breccia	Chlorite-feldspar- epidote schist	Calc-alkaline Basalt, K-poor, High Al
A.22	58° 25'/ 129° 44'	Tuff anf Argil- lite	Calcareous sandstone	Calc-alkaline Rhyolite, K-poor
A.23	58° 11'/ 128° 30'	Silicic schist	Ferruginous chert	----------
A.24	58° 24'/ 129° 49'	Tuff and Argil- lite	Poorly banded chert	----------
A.25	58° 24'/ 129° 49'	Tuff and Argil- lite	Feldspar-augite- chlorite schist	Tholeiitic Basalt
A.26	58° 24'/ 129° 49'	Tuff and Argil- lite	Chlorite-feldspar- epidote schist	Tholeiitic Basalt, K-rich
A.27	58° 10'/ 128° 15'	Tuff and Argil- lite	Quartz-feldspar- Chlorite-epidote	Calc-alkaline Dacite, K-poor
A.28	58° 10'/ 128° 15'	Silicic Schist	Quartz-feldspar- sericite schist	Calc-alkaline Rhyolite, K-poor
A.29	58° 11'/ 128° 20'	Basic to Inter mediate Tuff- Breccia	Chlorite-feldspar schist	Calc-alkaline Andesite, K-poor, High Al
A.30	58° 09'/ 128° 32'	Tuff-Argillite	Silicic tuff	Calc-alkaline Dacite, K-poor
A.31	58° 13'/ 128° 24'	Chlorite schist	Chlorite-Sericite schist	Tholeiitic Andesite, K-poor
A.32	58° 13'/ 128° 24'	Silicic Schist	Quartz-eye-feldspar- chlorite-sericite schist	Calc-alkaline Dacite, K-poor
A.33	58° 11'/ 128° 22'	Silicic Schist	Quartz-eye-feldspar- sericite schist	Calc-alkaline Rhyolite, K-poor
A.34	58° 11'/ 128° 21'	Basic to Inter- mediate Tuff- Breccia	Chlorite-feldspar- epidote schist	Tholeiitic Basalt, K-poor
A.35	58° 11'/ 128° 21'	Basic to Inter- mediate Tuff Breccia	Chlorite-epidote- feldspar schist	Calc-alkaline Basalt, K-poor, High Al.
A.36	58° 11'/ 128° 21'	Silicic Schist	Quartz-eye-feldspar- sericite schist	Calc-alkaline Rhyolite, K-poor
A.37	58° 12' 128° 21'	Chlorite Schist	Chlorite-feldspar schist	Tholeiitic Basalt, K-poor
A.38	58° 10' 128° 35'	Silicic Schist	Epidote-chlorite- feldspar-sericite schist	Calc-alkaline Dacite, K-poor
A.39	58° 10'/ 128° 35'	Basic to Inter mediate Tuff- Breccia	Feldspar-chlorite- epidote schist	Calc-alkaline Basalt, K-poor, High Al
A.40	58° 09'/ 128° 35'	Basic to Inter- mediate Tuff- Breccia	Chlorite-epidote- tremolite- actinolite schist	Tholeiitic Basalt, K-poor

Sample Number	Lat.(N.)/ Long.(W.)	Stratigraphic Rock Unit	Field Name	Irvine-Baragar Name
A.41	58° 11'/ 128° 23'	Silicic Schist	Quartz-eye-feldspar-sericite schist	Hanging Wall Unit*
A.42	58° 11'/ 128° 18'	Basic to Intermediate Tuff Breccia	Chlorite-sericite schist	Rare quartz and feldspar, carbonate* metacrysts
A.43	58°10'30" /128° 18'	Basic to Intermediate Tuff-Breccia	Feldspathic chlorite schist	Very fine feldspar crystals*
A.44	58°10'20" /128°18'	Tuff Argillite	Siliceous tuff	Layered*
A.45	58°10'10" 128°18'	Basic to Intermediate Tuff-Breccia	Chlorite-epidote schist	Altered basalt*
A.46	58°10'05" /128°18'	Silicic Schist	Rhyolite dike or sill	*
A.47	58° 10'/ 128° 20'	Silicic Schist	Quartz-feldspar chlorite-sericite schist	"trondhjemite"*
A.48	58°10'05" /128°21'	Basic to Intermediate Tuff-Breccia	Chlorite Schist	Basalt flow*
A.49	58° 12'/ 128° 20'	Silicic Schist	Quartz-eye-sericite schist	*
A.50	58° 12'/ 128° 20'	Silicic Schist	Quartz-eye-feldspar sericite schist	*
A.51	58° 12'/ 128° 20'	Silicic Schist	Quartz-eye-sericite schist	Dolomitic, Hanging wall*
A.52	58° 12'/ 128° 20'	Silicic Schist	Siliceous sericite schist	No quartz eyes*
A.53	58°12'30" /128°23'	Silicic Schist	Quartz-feldspar-sericite schist	Clast from hanging Wall fragmental*
A.54	58° 11'/ 128° 23'	Basic to Intermediate Tuff-Breccia	Chlorite schist	
A.55	58° 11'/ 128° 24'	Basic to Intermediate Tuff Breccia	Feldspathic chlorite schist	
A.56	58° 11' 128° 16'	Silicic Schist	Quartz-feldspar sericite schist	very coarse grained*

* Indicates data from A. Panteleyev (personal communication, 1977)

Sample Number	Lat.(N.)/ Long.(W.)	Field Name	Irvine-Baragar Name	Comments
B.1	58° 12'/ 128° 24'	Feldspar-chlorite-sericite schist	Calc-alkaline Dacite*	Abundant car bonate parti
B.2	53° 11'/ 128° 20'	Coarse bladed plagioclase-chlorite-biotite-epidote schist	Calc-alkaline Andesite, High Al	
B.3	58° 11'/ 128° 20	Chlorite-sericite schist	Calc-alkaline Dacite*	Carbonate rh abundant
B.4	58° 12'/ 128° 24'	Feldspar-chlorite schist	Calc-alkaline Andesite, K-poor, High Al	Well layered
B.5	58° 11'/ 128° 21'	Feldspar-chlorite sericite schist	Calc-alkaline Dacite*	
B.6	58° 13'/ 128° 23'	Medium grained, bladed feldspar-chlorite schist	Calc-alkaline Dacite*	
B.7	58° 13'/ 128° 23'	Coarse bladed plagioclase-chlorite schist	Tholeiitic Basalt	
B.8	58° 11'/ 128° 20'	Coarse bladed plagioclase-chlorite-sericite schist	Calc-alkaline Rhyolite*	
B.9	58° 11'/ 128° 24'	Coarse bladed plagioclase-chlorite-biotite schist	Calc-alkaline Andesite, K-rich, High Al	
B.10	58° 10'/ 128° 18'	Coarse bladed plagioclase-chlorite-biotite schist	Calc-alkaline Dacite, average	
B.11	58° 13' 128° 24'	Plagioclase-chlorite-biotite-tremolite-actinolite schist	Calc-alkaline Dacite, average	
B.12	58° 13' 128° 24'	Plagioclase-chlorite-biotite schist	Calc-alkaline Andesite, High Al	Very fine grained
B.13	58° 12'/ 128° 24'	Plagioclase-biotite-epidote schist	Calc-alkaline Andesite, K-rich, High Al	
B.14	58° 13'/ 128° 24'	Plagioclase-tremolite-actinolite-biotite schist	Tholeiitic Basalt, K-rich	
B.15	58° 13'/ 128° 23'	Chlorite-biotite tremolite-actinolite schist	Not Available	Hornblendite
B.16	58° 13'/ 128° 23'	Chlorite-biotite tremolite-actinolite schist	Not Available	Hornblendite
B.17	58° 11' 128° 20'	Chlorite-sericite carbonate schist	Calc-alkaline Rhyolite, K-rich	
B.18	58° 13'/ 128° 24'	Sericite-biotite-feldspar schist	Calc-alkaline Rhyolite	Very fine grained

* Indicates data from A. Panteleyev (Personal communication, 1977)

ample umber	Lat.(N.)/Long.(W.)	Field Name	Irvine-Baragar Name
.1	58° 29'/129° 08'	Quartz-feldspar-sericite schist	Calc-alkaline Rhyolite, K-poor
.2	58° 30'/129° 09'	Feldspar-quartz-sericite schist	Calc alkaline Dacite
.3	58° 30'/129° 10'	Feldspar-augite-epidote schist	Calc-alkaline Basalt
.4	58° 30'/129° 10'	Fine feldspar epidote-chlorite schist	Calc-alkaline Andesite, K-poor, High Al
.5	58° 28'/129° 44'	Quartz-eye-feldspar sericite schist	Calc-alkaline Rhyolite, K-poor
.6	58° 30'/129° 09'	Quartz-feldspar-sericite schist	Calc-alkaline Rhyolite, K-rich
.1	58° 15'/128° 26'	Banded chert or fine grained sandstone	Not applicable
.2	58° 24'/128° 42"	Quartz-eye-plagioclase crystal tuff	Calc-alkaline Andesite, K-poor, High Al
.3	58° 24'/128° 24'	Interlayered chlorite and feldspar-chlorite-carbonate schist	Not applicable
.4	58° 25'/128° 45'	Coarse quartz-eye-feldspar-sericite schist	Calc-alkaline Rhyolite, K-poor
.5	58° 24'/128° 44'	Feldspar-quartz-eye-chlorite-sericite schist	Calc-alkaline Rhyolite
.6	58° 25'/128° 45'	Quartz-eye rhyolite	Calc-alkaline Rhyolite, K-poor
.7	58° 25'/128° 45'	Quartz Arenite to Quartz Wacke	Not applicable
.8	58° 23'/128° 35'	Quartz-feldspar porphyry	Calc-alkaline Dacite, K-poor
.9	58° 26'/128° 44'	Quartz-eye-feldspar-chlorite-sericite schist	Tholeiitic Rhyolite, K-poor
.10	58° 25'/128° 43'	Fine quartzitic sandstone	Not applicable
.1	58° 13'/129° 10'	Arkose	Not applicable
.2	58° 13'/129° 10'	Greywacke	Not applicable
.1	58° 24'/128° 32'	Augite-feldspar crystal tuff	Tholeiitic Basalt, K-rich
.2	58° 11'/128° 45'	Feldspar-epidote chlorite tuff	Tholeiitic Andesite, K-poor
.3	58° 24'/128° 44'	Well layered intermediate tuff	Tholeiitic andesite, K-poor
.4	58° 24'/128° 42'	Augite-feldspar crystal tuff	Calc-alkaline, Basalt, K-rich, High Al
.5	58° 24'/130° 05'	Augite-Plagioclase crystal tuff and breccia	Calc-alkaline Basalt, K-rich, High Al
.6	58° 11'/129° 52'	Sheared Augite porphyry	Tholeiitic Picrite Basalt, K-rich
.1	58° 20'/128° 43'	Greenstone	Tholeiitic Basalt, K-poor
.2	58° 20'/128° 43'	Feldspar-chlorite-epidote schist	Tholeiitic Basalt, K-rich
.3	58° 20'/128° 26'	Greenstone	Tholeiitic Basalt, K-poor
.4	58° 20'/128° 26'	Greenstone with chlorite clots	Tholeiitic Basalt, K-rich
.5	58° 24'/129° 02'	Feldspar-chlorite-sericite schist	Calc-alkaline, Andesite, K-poor, High Al
.6	58° 20'/128° 45'	Feldspar-chlorite-epidote schist	Tholeiitic Basalt, K-rich
.7	58° 20'/128° 45'	Epidotized feldspar-chlorite schist	Calc-alkaline andesite, K-poor
.8	58° 08'/128° 25'	Chlorite-feldspar schist	Tholeiitic Basalt, K-rich

Energy, Mines and Resources Canada
Énergie, Mines et Ressources Canada